

# Solid-State Fermentation

---

Modelling Fungal Growth and Activity

J.P. Smits

Promotor: dr. ir. J. Tramper  
hoogleraar in de bioprocestechnologie

Copromotoren: dr. ir. A. Rinzema  
universitair docent bij de sectie Proceskunde  
dr. ir. H.M. van Sonsbeek  
onderzoeker bij TNO Voeding

J.P. Smits

Solid-State Fermentation,  
Modelling Fungal Growth and Activity

Proefschrift  
ter verkrijging van de graad van doctor  
op gezag van de rector magnificus  
van de Landbouww Universiteit Wageningen,  
dr. C.M. Karssen,  
in het openbaar te verdedigen  
op maandag 26 januari 1998  
des namiddags te 16.00 uur in de Aula.

ISBN 90-5485-805-2

**BIBLIOTHEEK  
LANDBOUWUNIVERSITEIT  
WAGENINGEN**

- 1 Het door Staron beschreven detoxificerende effect tijdens de fermentatie van raapzaadschroot wordt door hem ten onrechte toegeschreven aan de toegevoegde entcultures.  
Staron, T. (1974) La détoxification des tourteaux de colza par voie biologique. *l'Alim et la Vie* 62 165 - 179  
Llanos Palop, M., Smits, J.P., Ten Brink, B. (1995) Degradation of sinigrin by *Lactobacillus agilis* strain R16  
*Int. J. Food Microbiol.* 26 219 - 229
- 2 De door de regering voorgestelde flexibilisering van de arbeid leidt tot sociale onrust op individueel niveau en zal op korte en lange termijn zwaar drukken op de financiële uitgaven van de ministeries van, respectievelijk, Verkeer en Waterstaat en van Volksgezondheid, Welzijn en Sport.
- 3 Complementair zijn is een goede basis voor succesvol samenwerken.
- 4 In het artikel van Soccol *et al.* wordt getracht een wetenschappelijk onjuiste benadering te staven door het aanwenden van statistiek.  
Soccol, C., Leon, J.R., Marin, B., Roussos, S., Raimbault, M. (1993) *Biotech. Tech.* 8 563 - 568
- 5 Waar het gaat om het bestrijden van files verdient een tijdgebonden snelheidsbeperking de voorkeur boven een plaatsgebonden snelheidsbeperking.
- 6 Vaste-stof fermentatie biedt het perspectief de kinetiek van schimmelgroei en de correlatie hiervan met respiratieactiviteit op te helderen.  
Dit proefschrift
- 7 Tijdens vaste-stof fermentatie in een niet-isotherme schotelbed kan een hogere biomassa opbrengst worden verkregen door de aanvangstemperatuur in het bed lager te kiezen dan de temperatuur waarbij de hoogste waarde voor de maximale specifieke-groeisnelheid wordt waargenomen.  
Dit proefschrift
- 8 Evenals een kunstenaar heeft een creatieve wetenschapper een 'piano van Veldijk'.
- 9 Geweld verbroedert.  
Leeuwarden, 19 september 1997, 23:00 uur
- 10 Een voordeel van een niet gemengde vaste-stof fermentatie is dat infectie onder deze omstandigheden geen Booleaanse variabele is.
- 11 Voor het uitvoeren van vaste-stof fermentaties op grote schaal biedt de intensieve varkenshouderij mogelijkheden voor wat betreft outillage en technologie.
- 12 Wie hard fietst krijgt de wind tegen.

Stellingen behorend bij het proefschrift  
*Solid-State Fermentation, Modelling Fungal Growth and Activity*

J.P. Smits  
Wageningen, 26 januari 1998

# Contents

---

Chapter 1	
General Introduction .....	7
Chapter 2	
Description of Solid-State Fermentation System .....	29
Chapter 3	
Solid-State Fermentation of Wheat Bran by <i>Trichoderma reesei</i> QM9414 .....	43
Chapter 4	
Influence of Temperature on Solid-State Fermentation .....	59
Chapter 5	
Modelling of Solid-state Fermentation .....	75
Chapter 6	
General Discussion:	
Modelling Biomass Growth and Activity in Fungal Solid-State Fermentation .....	101
Summary .....	119
Samenvatting .....	121
Curriculum Vitae .....	123
Nawoord .....	125
Bibliography .....	127

# Chapter I

---

## General Introduction

Submitted for publication as  
Smits, J.P., Van Sonsbeek, H.M., Rinzema, A., Tramper, J., Knol, W.  
Solid-state fermentation - a mini review  
Agro Food Industry Hi-tech

## Summary

The increasing interests in biotechnology for the application of fungi on the one hand, and for cheap agricultural products on the other, can be combined in so-called solid-state fermentation (SSF). SSF resembles a close to natural habitat for filamentous microorganisms and can be applied to insoluble substrates. Many applications are described in the literature, ranking from animal feed to production of fine chemicals. The substrates used are, with the exception of synthetic media, cheap agricultural end- and by-products. The fermentation itself can be executed very simply. Several static and dynamic fermenters are described in the literature. Despite the wide applicability and apparent simplicity, fungal SSFs contain complex intrinsic difficulties. Therefore, biological and physical processes in SSF are difficult to control. This chapter gives an overview of the applications and intrinsic difficulties of SSF.

## Fungi in biotechnology

Mushrooms, truffles, moulds, puffballs, smut, morels, rusts and yeasts belong to the group of fungi, of which more than 70,000 are known (1). The world's largest fungus originating from one single fertilized spore registered is the underground fungus *Armillaria ostoyae* covering some 600 ha in the forests of Washington state, USA. The heaviest fungus reported is *Armillaria bulbosa*, covering about 15 ha and calculated to weigh 100 tonnes, which is of the order of magnitude of a blue whale (2). Other species, such as some yeast-type ascomycetes, are small enough to have their natural habitat in the gut of cigar beetles where they detoxify plant material consumed by the host.

Most people associate fungi with deterioration of food, with wood or with black spots on bathroom tiles and moist walls. On the other hand, connoisseurs associate fungi with production of delicacies, not only edible mushrooms and blue cheeses but also truffles, beers, breads and wines.

Although fungi belong to a large diverse group of organisms, the mechanism behind the deterioration and the production of comestibles is in fact the same. All fungi metabolize substrates, most of them consume oxygen and produce and secrete enzymes and organic and inorganic compounds simultaneously.

A target in biotechnology is to explore these features and use them for food production, environmental applications and health care. To do so, fermentation processes are being developed in which fungi are brought in contact with substrates and, if necessary, oxygen under defined conditions. While the fungus consumes substrates, it grows in size and number of organisms and produces the desired products. It depends on what product is wanted whether the mixture of fungus, substrate and products is further treated to obtain purified enzymes (as for bread making, jeans bleaching and addition to washing powders) and organic compounds (antibiotics, ethanol, lactic acid, citric acid), or sold as such (blue cheeses, tempeh, beer, koji).

## Types of fermentations

In most commercial fermentation processes for production of enzymes and organic compounds, all substrate components are dissolved in excess of water. Such a fermentation is



called liquid-state fermentation (LSF) and is usually conducted in a stirred-tank reactor or bubble column.

Stirred-tank reactors, however, are less practical, or may even be useless, when the fermentation concerns a large quantity of water-insoluble substrates. If this fermentation contains excess of water, it manifests itself as a mixture of insoluble particles in water or a slurry. These will be referred to below as submerged fermentation (SmF).

A fermentation in which water availability is restricted, as evidenced by the absence of free-flowing water, is called solid-state fermentation (SSF). In most SSFs, the water content varies between 30 and 75% (3), dependent on the water-absorbing capacity of the substrate and the minimum water activity required for microbial growth (4).

The classification of fermentations into LSF, SmF and SSF relies on visual observations. No measurable parameter makes objective classification possible (5). Figure 1 gives a schematic presentation of the two extremes, LSF and SSF, and the twilight zone of SmF, in relation to the visual presence of water and solids.

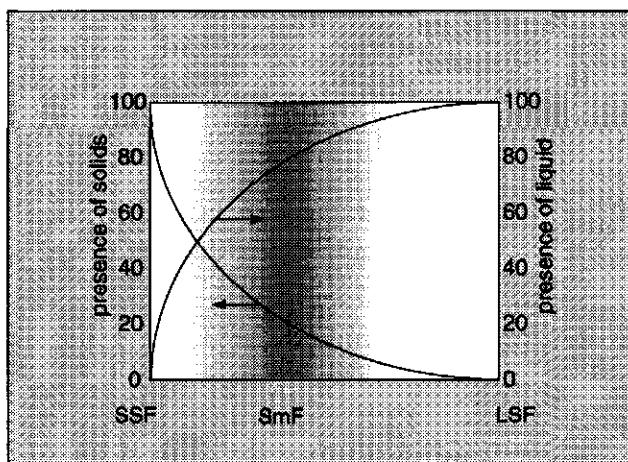


**Figure 1:** Schematic presentation of solid-state (SSF, white area on the left), submerged (SmF, grey area) and liquid-state fermentation (LSF, white area on the right) as classified according to the visual presence of solids and liquid (solid lines) in arbitrary units.

### The role of water

In LSFs, water is the continuous phase, making it easy to mix and to obtain a homogeneous system. Added water-soluble substrates, nutrients and oxygen are directly and homogeneously mixed with the substrates already present. In this way, water functions as a mass-transfer medium.

Besides mass, the water phase also transfers heat. Heat is produced during growth and maintenance activity of microorganisms. This is most clearly shown during SSFs, such as composting, storage of wet hay and ensilage, where microbial activity can result in

temperatures above 50 °C (5).

In an LSF, the water phase is the transfer medium of heat within the fermenter. Heat is exchanged between the fermentation broth and the environment of the fermenter. By controlling the temperature of the environment and by creating sufficient exchange surface, the temperature in the broth can be kept largely constant. In SSF, heat transfer to the environment is more difficult due to the absence of a continuous phase with a large heat capacity. Here, the most effective contribution of water to heat removal seems to be evaporation (6).

The presence of large amounts of water (90-99 % of total mass) in LSF may be a disadvantage when the desired fermentation product needs further purification. Then, water needs to be separated from the product by energy-consuming techniques such as centrifugation, evaporation or filtration. From this point of view, SSF might have an economic advantage over LSF (5).

A certain amount of water will always remain necessary in SSF for the fungus to remain alive. Water is needed for intracellular transport of mass, as a substrate, for physical protection against turgor forces, and as a solvent for nutrients. There is a pronounced distinction among species with respect to the minimum amount of free water necessary for growth. Therefore, restricted water availability can prevent the outgrowth of undesired microorganisms in nonsterile fermentations, especially in combination with extreme pH, thus reducing the need for sterilization (7). This has been mentioned as an advantage of SSF over LSF (4). On the other hand, the number of species that can be applied in low-water-content SSF is restricted (8). Thus, because of the low water content, SSF can have advantages over LSF, which are enumerated by Lonsane *et al.* (3): superior productivity, simple technique, low capital investment, reduced energy requirement, low waste water output, improved product recovery, and elimination of foam problems.

### **Applications of SSF**

Many articles have been published on SSF. Table 1 gives an overview of those published in the scientific literature. It presents examples of the wide application potential of SSF regarding substrates, (fungal) species and product formation but does not pretend to be complete. Noticeably, agricultural raw products and by-products (cereal grains, wheat bran, wheat straw) are frequently applied as substrates for SSF. The use of these cheap substrates is an advantage of SSF over LSF.

Most agricultural products are rich carbon and nitrogen sources and contain a variety of other nutrients encapsulated in biopolymer structures such as cellulose and protein, which are largely water-insoluble. Often no additions have to be made. Usually, pretreatment of the agricultural product can be restricted to chopping, cutting or grinding, sterilization or pasteurization. However, chemical pretreatment or addition of extra nutrients may increase product yields significantly (9, 10,11) or increase accessibility towards enzymatic digestibility (12).

Complex agricultural products may have the additional advantage of high buffer capacity, which may allow omission of pH control. On the other hand, when, for instance, ammonium salts are used as extra nutrients, pH may drop significantly (7), requiring pH control.

**Table 1:** Examples of applications of SSF.

target	product	substrate	microorganism	system	ref.
increase digestibility	animal feed	cassava peel	<i>Manihot esculenta</i>		(49)
		orange peel	<i>Pleurotus ostreatus</i> <i>Agrocybe aegerita</i> <i>Armillariella mellea</i>	bags	(50)
increase nutritional value	animal feed	wheat straw	<i>Chaetomium cellulolyticum</i> <i>Trichoderma reesei</i> <i>Candida lipolytica</i>	mixed system	(51)
		coffee pulp	<i>Aspergillus niger</i>	packed bed	(52)
		rape-seed meal	<i>Aspergillus clavatus</i> <i>Fusarium oxysporum</i>	packed bed Petri dishes	(53)
		sago starch	<i>Rhizopus oligosporus</i>	packed bed	(54)
	single-cell protein	sugar beet pulp	<i>Trichoderma reesei</i> <i>Talaromyces emersonii</i>		(55)
		sugar beet pulp	<i>Trichoderma viride</i>	box kiln pilot scale	(56)
		manure	<i>Chaetomium cellulolyticum</i>	jar	(57)
	tempeh	soy beans	<i>Rhizopus oligosporus</i>	tray rotating drum	(17)
	protein	sawdust	<i>Chaetomium cellulolyticum</i>	tray rotating drum	(58)
		lignocellulosic substrates	<i>Chaetomium cellulolyticum</i>	flasks	(59)
		cassava starch	<i>Rhizopus oligosporus</i>	inert carrier	(60)
		banana wastes	<i>Aspergillus niger</i>	stirred tank pilot scale	(61)
		citrus peel	<i>Aspergillus niger</i>	packed bed	(62)
	protein + ethanol	fodder beets	<i>Saccharomyces cerevisiae</i>	mixed system pilot scale continuous system	(20)
		maize	<i>Aspergillus niger</i> <i>Saccharomyces sake</i>	flasks	(63)
		bagasse	<i>Schwanniomyces castelli</i>	column	(64)
enzyme production	amylase	wheat bran rice bran	<i>Aspergillus niger</i>	flasks	(65)
	amylase	synthetic medium	<i>Aspergillus oryzae</i>	flasks	(66)

target	product	substrate	microorganism	system	ref.
enzyme production (cont.)	amylase + protease	rice	<i>Aspergillus oryzae</i>	koji fermentation	(67)
	arabino- furanosidase	sugar beet pulp	<i>Trichoderma reesei</i>		(68)
	galactosidase	wheat bran	<i>Aspergillus oryzae</i>	flasks	(69)
	cellulase	barley straw	<i>Trichoderma</i> sp.	Petri dishes	(70)
		leached beet pulp	<i>Trichoderma aeroviride</i>	packed bed	(71)
		wheat straw	mixture of thermophilic methanogenic microorganisms	mixed reactor anaerobic	(72)
		wheat bran	<i>Trichoderma reesei</i> <i>Sporotrichum cellulophilum</i>	tray	(35)
		wheat bran	<i>Talaromyces</i> sp.	flasks	(73)
		lignocellulosic substrates	<i>Trichoderma</i> sp.		(9)
			<i>Pestalotiopsis versicolor</i>	flask	(74)
		sorghum	<i>Trichoderma reesei</i> <i>Aspergillus niger</i>	jar	(75)
	cellulase + amylase + xylanase + protease	wheat bran	<i>Trichoderma reesei</i>	Petri-dishes	(45)
	cellulase + glucosidase + xylanase + arabinase + pectinase + galacturonidase	beet pulp wheat bran apple pomace potato pulp	<i>Penicillium</i> sp. <i>Aspergillus</i> sp. <i>Talaromyces</i> sp.	tray rotating drum	(76)
	$\beta$ -glucosidase	sugar beet pulp	<i>Aspergillus phoenicis</i>	column	(77)
	$\beta$ -glucosidase + endoglucanase + exoglucanase	sugar cane bagasse wheat bran wheat straw rice bran groundnut shells	<i>Aspergillus ellipticus</i> <i>Aspergillus fumigatus</i>	flasks	(78)
	hydrolase	orange peel	<i>Aspergillus niger</i>	rotating drum	(79)
	pectinesterase polygalacturonase	apple pomace	<i>Aspergillus niger</i>	rotating drum	(80)
	lipase	wheat bran	<i>Penicillium</i> sp. <i>Aspergillus niger</i> <i>Rhizopus</i> sp. <i>Mucor miehei</i>	flasks	(81)

target	product	substrate	microorganism	system	ref.
enzyme production (cont.)	lipase (cont.)	rice	<i>Candida rugosa</i>	Petri dishes	(82)
	nuclease P1	synthetic medium	<i>Penicillium citrinum</i>	inert carrier	(83)
	protease	wheat bran	<i>Aspergillus flavus</i>	tray	(84)
		wheat bran	<i>Aspergillus oryzae</i>	flasks	(85)
		wheat bran	<i>Pseudomonas</i> sp.	flasks	(86)
		rice bran	<i>Rhizopus oligosporus</i>	flasks	(87)
		synthetic medium	<i>Aspergillus oryzae</i>	inert carrier repeated batch	(88)
	L-glutaminase	synthetic medium	<i>Vibrio costicola</i>	inert carrier	(89)
	tannase	wheat bran	<i>Rhizopus oryzae</i>	Petri dishes	(90)
	phytase	canola meal	<i>Aspergillus carbonarius</i>	flasks	(11)
production of organic compounds	alkaloids	bagasse	<i>Claviceps purpurea</i>	packed bed	(91)
	citric acid	coffee husk	<i>Aspergillus niger</i>	flasks	(92)
		beet pulp cane pulp	<i>Aspergillus niger</i>	tray non sterile	(93)
	ethanol	maize	<i>Saccharomyces sake</i>	packed bed pilot scale	(94)
	gibberellic acid	cassava flour sugar cane bagasse pith synthetic medium	<i>Gibberella fujikuroi</i>	column	(95)
		bagasse	<i>Brevibacterium</i> sp.		(96)
	lactic acid	sugar cane pressmud	<i>Lactobacillus casei</i> <i>L. helveticus</i> <i>Streptococcus thermophilus</i>	flasks	(97)
		bagasse	<i>Rhizopus oryzae</i>	packed bed	(98)
	chitosan	wheat straw	<i>Lentinus edodes</i>		(99)
	ochratoxin A	wheat	<i>Aspergillus ochraceus</i>	rotating drum	(100)
	pigment food colour	cassava	<i>Monascus</i> sp.	flasks	(101)

target	product	substrate	microorganism	system	ref.
production of antibiotics	iturin	okara	<i>Bacillus subtilis</i>	flasks lab and pilot scale	(46)
		wheat bran	<i>Bacillus subtilis</i>	flasks	(102)
	oxytetracycline	potato residues	<i>Streptomyces rimosus</i>	packed bed	(103)
		bagasse	<i>Penicillium chrysogenum</i>	packed bed	(104)
production of fungal biomass	spores	rice	<i>Aspergillus flavus</i> <i>Aspergillus oryzae</i>	plastic bags	(105)
		buckwheat seed	<i>Penicillium roqueforti</i>		(106)
	mushrooms	compost	<i>Agaricus bisporus</i>	pile	(107)
biocontrol	bioinsecticide	enriched clay	<i>Beauveria bassiana</i>	flasks packed bed	(109)
	biofungicide	wheat bran	<i>Stilbella aciculosa</i>	flasks	(110)
	bioherbicide	vermiculite rice hulls	<i>Colletotrichum truncatum</i>	flasks dishes	(111)

### Fermenter types

The applications of SSF described in the literature can be classified as commercial or as research. Examples of commercial applications are composting, and enzyme, koji and tempeh production. The target of research applications is often the acquisition of knowledge, the search for new applications, optimization and scale-up. Therefore, different fermenter types are used in research and commercial applications.

Several fermenter types, mentioned in Table 1, will be briefly discussed here.

**Flasks and Petri dishes.** Some research applications are done in flasks and Petri dishes. The use of flasks originates from LSF and is usually satisfactory for preliminary experiments. Since a flask can be considered as a semi-closed system, environmental conditions are hard to control. Flasks are only applicable for fermentation of small amounts of solids. For scale-up and control studies, other systems have to be chosen.

Petri dishes may allow exchange of air with the (conditioned) environment when the lid does not cover the dish airtight. In case of high surface volume ratios of the substrate, a good heat and mass exchange between substrate and environment is possible.

Flasks and Petri dishes may be considered as down-scaled tray fermenters.

**Tray fermenter.** The simplest static SSF system for commercial production is the tray fermenter. It consists of a (perforated) tray into which the moistened and inoculated substrate is poured. The tray is incubated in an environment of a certain temperature and (high) relative humidity for a couple of days. Scale-up of a tray fermentation can be done by increasing the number of trays, but results in a production process which is more labour-intensive (3). Examples of commercially applied tray fermenters can be found for production of tempeh, cheeses and enzymes (cellulases and proteases).

The advantage of a tray system is in its simplicity. During fermentation, no handling is needed other than controlling the ambient temperature, relative humidity and gas composition. The disadvantage of a tray is the inefficiency of substrate use. Due to elevated temperature, lack of oxygen or high carbon-dioxide concentrations, inhibition of microbial growth and activity can occur. Temperature increase, low oxygen and high carbon dioxide concentration occur faster in the core of the fermenter bed than in the outer layers, and thus inhibition effects differ among locations in the bed (13). This results in inhomogeneity of the substrate layer. Experiments have shown that enzyme production takes place only in the outer layer of about 5 cm (14).

**Aerated systems.** To improve heat removal and oxygen supply in a static bed, aeration of the fermenter bed with (moistened) air is applied. These so-called packed-bed systems are used in production and on a laboratory scale for research purposes. An example of the latter is the frequently used column system of Raimbault and Alazard (7). Advantages are the possibilities for obtaining a nearly constant temperature and sufficient oxygen supply throughout the fermentation bed. By increasing the air flow through the bed, however, not only heat may be removed but also water vapour. Besides channelling in the bed, a disadvantage of a large-scale packed bed is the enlarged risk of desiccation of the substrate (15).

**Mixed systems.** The difficulty of obtaining a homogeneous system, and thus to avoid heat build-up, can partly be overcome by mixing the substrate bed. This can be done continuously or intermittently in a drum-type fermenter (16, 17) or by using augers. The latter is done during the commercial production of koji (4). Similar devices are known in the malting industry.

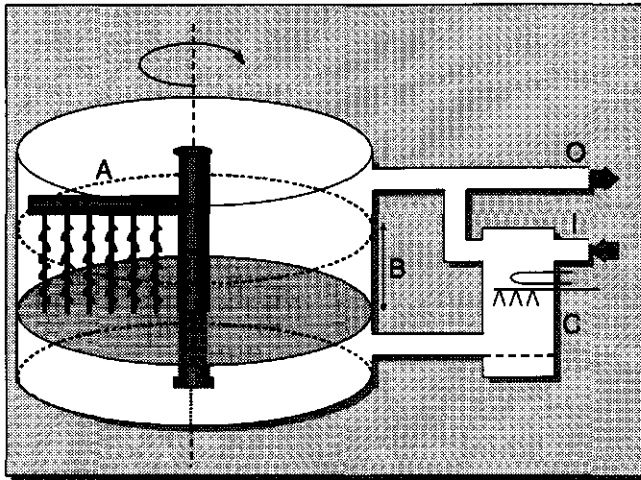


**Figure 2:** Schematic presentation of koji production equipment (adapted from Fujiwara Engineering Co., Ltd, Japan). Shown are a mixing device with 6 augers (A), the fermenter bed (B), the air conditioner (C) with humidifier and heater and the inlet (I) and outlet (O) of air.

The disadvantages are damage of fungal biomass during mixing in case of filamentous microorganisms (18), aggregation of substrate particles into balls in large-scale fermenters (3), the large void volume and the energy input needed in large-scale systems.

**Combined aerated and mixed systems.** Probably most effective are fermentation systems in which aeration and mixing can be done simultaneously. The already mentioned fermenter for koji production is an example in which mixing and aeration are combined in a large-scale system (see Figure 2).

**Fluidized beds.** In fluidized beds, mixing is attained by forced aeration with a large air flow. A fluidized bed forms a homogeneous mixed substrate bed (19), but puts high demands regarding uniformity of substrate particles and fermenter devices.

**Continuous systems.** A continuous SSF system is described by Gibbons et al. (20). It consists of a tube in which the substrate, a solid slurry of beets, is slowly conveyed and mixed by an auger. The retention time of the substrate in the tube is equal to the fermentation time.

### **The intrinsic difficulties of the SSF process**

In an SSF bed, three phases can be distinguished: solid, liquid and gas phase. In an ideal system, these three phases are homogeneously distributed in the fermenter on a macroscopic scale. The fungus uses the solid as a support, metabolizes the nutrients from the solid or those dissolved in the liquid phase, and consumes oxygen from the gas phase. Meanwhile, it may produce metabolites, carbon dioxide, enzymes, newly formed biomass, water and heat, which are excreted into the system.

In any SSF process, biomass increase, biomass activity, heat production and transfer, water production and evaporation, water vapour transfer, oxygen diffusion and consumption and substrate consumption play more or less important roles. In a static system, the rates of these processes vary in time, but also in place. This is caused by the differences in conditions existing between the fermentation bed and its surroundings, which result in transport of mass (e.g. oxygen, carbon dioxide, water vapour) and heat. Besides, transport rates between the surface of the bed and its surroundings are different from those within the bed, which results in increased inhomogeneity of the fermentation bed.

A target in research on modelling SSF is to predict the course of the inhomogeneity in time by describing the changes of variables involved in time and place.

### **Interaction of parameters**

Besides the variation of variables in time and place, a mutual interaction exists between them. For instance, the increase in temperature results in a change in biomass growth rate and (respiration) activity, and thus in a change in heat production, oxygen and substrate consumption, carbon dioxide and water production. The temperature changes differ locally and therefore have locally different effects on biomass growth and activity. Only if heat transfer is sufficient, local differences in temperature can be avoided. In a small system, for example, heat exchange might be sufficient to allow the fungus to grow unrestrictedly. This will continue until another parameter becomes restrictive. Oxygen exhaustion has been measured in a small fermenter chamber (13). This was also predicted to occur in an isothermal system (21).



An example of a mutual relation exists in the relation between oxygen consumption and heat production. The correlation between both can be described as a constant relationship (22), but there is an opposite effect between both in SSF: high oxygen consumption rates result in high temperatures, and high temperatures inhibit oxygen consumption.

If a decrease in oxygen concentration occurs, approximately a similar increase in carbon dioxide concentration will take place (13). Heat production can therefore also be coupled to carbon dioxide production (15). Similar mutual relations can be found between water and nutrient availability on the one hand, and biomass growth and (respiration) rate on the other (23).

The interactions determine the complexity of an SSF process and make it difficult to predict the course of the inhomogeneity in time without the help of mathematical models. Therefore, large-scale SSFs are difficult to control. The inhomogeneity complicates drawing of representative samples for analysis and the use of results for process control. On-line measurements, such as those of oxygen and carbon dioxide concentration in the air, provide overall information on the fermentation process but do not give insight into extreme values.

### Complexity of fungal growth

Many fungi can use biopolymers from agricultural products as substrates. Besides, the capacity to grow at lower water activity and the capacity to migrate over the substrate surface by forming mycelium make filamentous fungi ideal species for SSF. In fact, growth under SSF conditions is most natural for fungi (7).

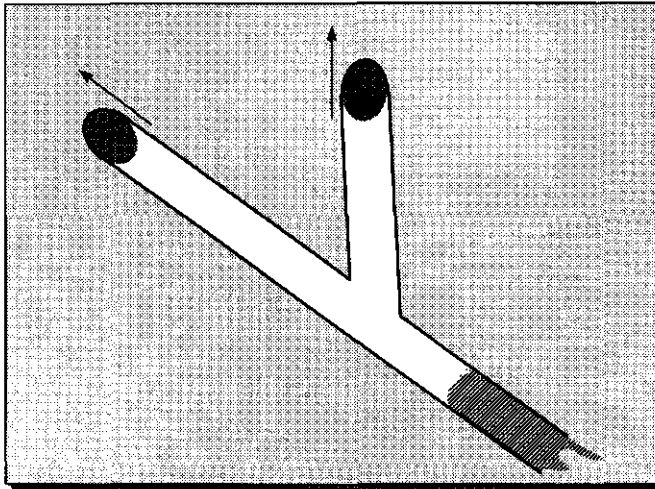


**Figure 3:** Schematic presentation of a filamentous fungus showing one branch with two tips elongating in the direction of the arrows.

Filamentous fungi grow by elongating and branching of the hyphae (see Figure 3). Early reports by Trinci (24, 25) on fungi growing on agar plates describe the combined exponential

increase of number of tips and linear elongation of the hyphae during the first hours of growth, resulting in an exponential increase of total hyphal length. These observations form the basis of later studies on modelling of fungal growth (26, 27).

The elongation rate and branching frequency, i.e. the morphology, depend on environmental circumstances, such as substrate availability, temperature, pH, oxygen tension and water activity (28, 108). The inhomogeneity in an SSF system may thus strongly influence fungal growth.

All physical changes in a fungal SSF described above start with the growth of the fungus. By describing the growth of the fungus as a function of physical parameters it should be possible to predict the evolution of inhomogeneity in SSF. A major problem, however, is to quantify the fungal biomass dry weight in the system (29). The fungus is attached to the substrate, which makes quantitative separation impossible. Alternatives, such as the amount of fungal protein (30), DNA (31), ATP (32), ergosterol (33, 34) and glucosamine (15, 35), are available and give an indication of the amount of biomass.

One of the most promising parameter is the glucosamine content of fermented substrates. Glucosamine is the monomer of cell-wall chitin. Its increase during fermentation is correlated with the increase in total amount of fungal biomass present, but it cannot be used to distinguish between living and dead, active and inactive fungal biomass. Moreover, there might be no constant relationship between glucosamine and biomass dry weight (29, 33). The use of glucosamine as the biomass indicator has, as far as we know, not yet been used directly in modelling of SSF, except in our group.

### Modelling SSF

A mathematical model can be a powerful tool to predict the result of a fermentation and may be very useful in, for instance, process design and control.

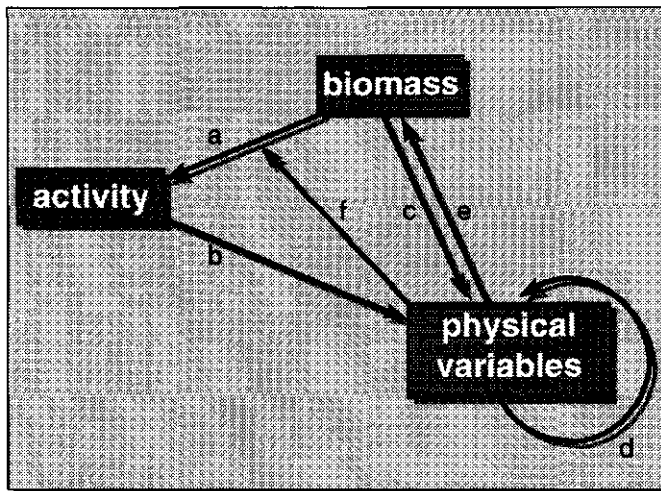


**Figure 4:** Schematic presentation of modelling steps. Arrows a to f refer to the interactions described in the text.

**Model construction.** To construct such a model, several variables and their interactions have to be described. First there is a certain amount of biomass growing with a specific-growth rate, which has a corresponding amount of activity (arrow *a* in Figure 4). In SSF literature, the logistic equation and the linear-growth model of Pirt (36) are often used to describe the correlation between biomass, its growth rate and activity (16, 35, 37, 38, 39, 40, 44). Figure 5 gives the equations which are used to calculate the specific activity of fungal biomass. A second relation (arrow *b* in Figure 4) describes the effect of any activity on physical variables. The correlation between measured carbon dioxide production rate and increase in water content, as given by Narahara et al. (15), and the correlation between oxygen consumption rate (22) or carbon dioxide production rate (37) and heat production are three examples.

Because biomass occupies a certain volume in the system, it can influence physical variables not only through activity, but also directly (arrow *c*). A change of void volume, for example, may alter diffusion, convection, heat conduction and, in a packed-bed system, pressure drop (41). The fourth correlation concerns mutual effects of physical variables and processes (arrow *d* in Figure 4). Examples of these are the effects of temperature on water evaporation, water evaporation on water concentration, water concentration on enthalpy, and heat production on temperature.

Each physical variable may have a more or less significant effect on biomass growth. The effect of temperature is often described (39, 42, 43). Temperature also affects the correlation between biomass and activity (44). These correlations are represented by arrows *e* and *f*, respectively.

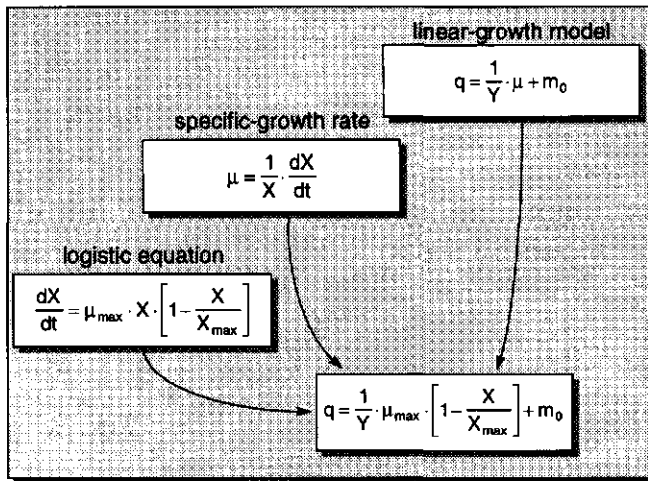


**Figure 5:** Logistic equation, specific-growth rate and linear-growth model used to calculate the specific activity  $q$ .  $\mu$  is the specific-growth rate,  $\mu_{\max}$  is the maximum specific-growth rate,  $X$  is the amount of biomass present,  $X_{\max}$  is the maximum attainable amount of biomass,  $Y$  is the yield factor and  $m_0$  is the maintenance coefficient.

- Bioeng. **35** 802-808
- 40 Gutiérrez-Rojas, M., Auria, R., Benet, J.C., Revah, S. (1995) A mathematical model for solid-state fermentation of mycelial fungi on inert support. *Chem. Engin. J.* **60** 189-198
- 41 Auria, R., Morales, M., Villegas, E., Revah, S. (1993) Influence of mold growth on pressure drop in aerated solid-state fermentors. *Biotechnol. Bioeng.* **47** 1007-1013
- 42 Sangsurasak, P., Mitchell, D.A. (1995) The investigation of transient multidimensional heat transfer in solid-state fermentation. *Chem. Engin. J.* **60** 199-204
- 43 Rajagopalan, S., Modak, J.M. (1994) Heat and mass transfer simulation studies for solid-state fermentation processes. *Chem. Engin. Sci.* **49** 2187-2193
- 44 Szewczyk, K.W., Myszka, L. (1994) The effect of temperature on the growth of *A. Niger* in solid-state fermentation. *Bioprocess Engin.* **10** 123-126
- 45 Smits, J.P., Rinzema, A., Tramper, J., Sonsbeek, H.M. van, Knol, W. (1996) Solid-state fermentation of wheat bran by *Trichoderma reesei* QM9414: substrate composition changes, C-balance, enzyme production, growth and kinetics. *Appl. Microbiol. Biotechnol.* **46** 489-496
- 46 Ohno, A., Ano, T., Shoda, M. (1993) Production of the antifungal peptide antibiotic, iturin by *Bacillus subtilis* NB22 in solid-state fermentation. *J. Ferment. Bioengin.* **75** 23-27
- 47 Rajagopalan, S., Modak, J.M. (1995) Modelling of heat and mass transfer for solid-state fermentation process in tray bioreactor. *Bioprocess Engin.* **13** 161-169
- 48 Lonsane, B.K., Saucedo-Castañeda, G., Raimbault, M., Roussos, S., Viniegra-Gonzalez, G., Ghildyal, N.P., Ramakrishna, M., Krishnaiah, M.M. (1992) Scale-up strategies for solid-state fermentation systems. *Process Biochem.* **27** 259-273
- 49 Ofuya, C.O., Obilor, S.N. (1994) The effects of solid-state fermentation on the toxic components of cassava peel. *Process Biochem.* **29** 25-28
- 50 Nicolini L., Volpe, C., Pezzotti, A., Carilli, A. (1993) Changes in in-vitro digestibility of orange peels and distillery grape stalks after solid-state fermentation by higher fungi. *Bioresources Technol.* **45** 17-20
- 51 Viesturs, U.E., Apsite, A.F., Laukevics, J.J., Ose, V.P., Bekers, M.J., Tengerdy, R.P. (1981) Solid-state fermentation of wheat straw with *Chaetomium cellulolyticum* and *Trichoderma lignorum*. *Biotechnol. Bioeng. Symp.* **11** 359-369
- 52 Peñaloza, W., Molina, M.R., Brenes, R.G., Bressani, R. (1985) Solid-state fermentation: an alternative to improve the nutritive value of coffee pulp. *Appl. Environ. Microbiol.* **49** 388-393
- 53 Smits, J.P., Knol, W., Bol, J. (1992) Glucosinolate degradation by *Aspergillus clavatus* and *Fusarium oxysporum* in liquid and solid state fermentation. *Appl. Microbiol. Biotechnol.* **38** 696-701
- 54 Gumbira-Sa'id, E., Mitchell, D.A., Greenfield, P.F., Doelle, H.W. (1992) A packed bed solid-state cultivation system for the production of animal feed: cultivation, drying and product quality. *Biotechnol. Letters* **14** 623-628
- 55 Considine, P.J., Mehra, R.K., Hackett, T.J., O'Rorke, A., Comerford, F.R., Coughlan, M.P. (1986) Upgrading the value of agricultural residues. *Ann. New York Acad. Sci.* **469** 304-311
- 56 Durand, A., Chereau, D. (1988) A new pilot reactor for solid-state fermentation: application to the protein enrichment of sugar beet pulp. *Biotechnol. Bioeng.* **31** 476-486
- 57 Ulmer, D.C., Tengerdy, R.P., Murphy, V.G., Linden, J.C. (1980) Solid-state fermentation of manure fibres for SCP production. In: *Developments in industrial microbiology*, vol. 21, 425-434, Underkofler, L.A. and Wulf, M.L. (ed.), Soc. Indus. Microbiol., Arlington USA.
- 58 Pamment, N., Robinson, C.W., Hilton, J., Moo-Young, M. (1978) Solid-state cultivation of *Chaetomium cellulolyticum* on alkali-pretreated sawdust. *Biotechnol. Bioeng.* **20** 1735-1744
- 59 Chahal, D.S., Vlach, D., Moo-Young, M. (1980) Upgrading the protein feed value of lignocellulosic materials using *Chaetomium cellulolyticum* in solid-state fermentation. In: *Advances in biotechnology*. Vol. 2 pp 327-332 Ed: Moo-Young, M., Robinson, C.W., Pergamon press, Toronto
- 60 Mitchell, D.A., Greenfield, P.F., Doelle, H.W. (1986) A model substrate for solid-state

- fermentation. *Biotechnol. Letters* **8** 827-832
- 61 Baldensperger, J., Le Mer, J., Hannibal, L., Quinto, P.J. (1985) Solid-state fermentation of banana wastes. *Biotechnol. Letters* **7** 743-748
  - 62 Rodríguez, J.A., Echevarría, J., Rodríguez, F.J., Sierra, N., Daniel, A., Martínez, O. (1985) Solid-state fermentation of dried citrus peel by *Aspergillus niger*. *Biotechnol. Letters* **7** 577-580
  - 63 Han, I.Y., Steinberg, M.P. (1986) Solid-state yeast fermentation of raw corn with simultaneous koji hydrolysis. *Biotechnol. Bioeng. Symp.* **17** 449-462
  - 64 Saucedo-Castañeda, G., Lonsane, B.K., Navarro, J.M., Roussos, S., Raimbault, M. (1992) Potential of using a single fermenter for biomass build-up, starch hydrolysis and ethanol production. *Appl. Biochem. Biotechnol.* **36** 47-61
  - 65 Pandey, A., Radhakrishnan, S. (1993) The production of glucoamylase by *Aspergillus niger* NCIM 1245. *Process Biochem.* **28** 305-309
  - 66 Murado, M.A., González, M.P., Torrado, A., Pastrana, L.M. (1997) Amylase production by solid-state culture of *Aspergillus oryzae* on polyurethane foams: some mechanistic approaches from an empirical model. *Process biochem.* **32** 35-42
  - 67 Fukushima, D. (1982) Koji as an important source of enzymes in the orient and its unique composite systems of proteinases and peptidases. In: *Use of enzymes in food technology*, Dupuy, D. (ed.), 381-388, Technique et Documentation, Lavoisier, Paris.
  - 68 Roche, N., Berna, P., Desgranges, C., Durand, A. (1995) Substrate use and production of alpha-L-arabinofuranosidase during solid-state culture of *Trichoderma reesei* on sugar beet pulp. *Enzyme Microb. Technol.* **17** 935-941
  - 69 Annunziato, M.E., Mahoney, R.R., Mudgett, R.E. (1986) Production of  $\alpha$ -galactosidase from *Aspergillus oryzae* grown in solid-state culture. *J. Food Sci.* **51** 1370-1371
  - 70 Mukhopadhyay, A. K., Sikyta, B. (1981) Solid fermentation of barley straw. *Zbl. Bakt. II. Abt.* **136** 644-647
  - 71 Illanes, A., Aroca, G., Cabello, L., Acevedo, F. (1992) Solid substrate fermentation of leached beet pulp with *Trichoderma aureoviride*. *World J. Microbiol. Biotechnol.* **8** 488-493
  - 72 Vandevoorde, L., Verstraete, W. (1987) Anaerobic solid-state fermentation of cellulosic substrates with possible application to cellulase production. *Appl. Microbiol. Biotechnol.* **26** 479-484
  - 73 Nishio, N., Kurisu, H., Nagai, S. (1981) Thermophilic cellulase production by *Talaromyces* sp. in solid-state cultivation. *J. Ferment. Technol.* **59** 407-410
  - 74 Rao, M.N.A., Mithal, B.M., Thakur, R.N., Sastry, K.S.M. (1983) Solid-state fermentation for cellulase production by *Pestalotiopsis versicolor*. *Bioetchnol. Bioeng.* **25** 869-872
  - 75 Castillo, M.R., Gutierrez-Correa, M., Linden, J.C., Tengerdy, R.P. (1994) Mixed culture solid-substrate fermentation for cellulolytic enzyme production. *Biotechnol. Lett.* **16** 967-972
  - 76 Considine, P.J., Coughlan, M.P. (1989) Production of carbohydrate-hydrolyzing enzyme blends by solid-state fermentation. in: *Enzyme systems for lignocellulose degradation*. Coughlan, M.P. (ed.) Elsevier Appl. Sci., London
  - 77 Deschamps, F., Huet, M.C. (1984)  $\beta$ -Glucosidase production by *Aspergillus phoenicis* in solid-state fermentation. *Biotechnol. Letters* **6** 55-60
  - 78 Gupte, A., Madamwar, D. (1997) Solid-state fermentation of lignocellulosic waste for cellulase and  $\beta$ -glucosidase production by cocultivation of *Aspergillus ellipticus* and *Aspergillus fumigatus*. *Biotechnol. Prog.* **13** 166-169
  - 79 Nishio, N., Tai, K., Nagai, S. (1979) Hydrolase production by *Aspergillus niger* in solid-state cultivation. *European J. Appl. Microbiol. Bioetchnol.* **8** 263-270
  - 80 Berovič, M., Ostroveršnik, H. (1997) Production of *Aspergillus niger* pectolytic enzymes by solid-state bioprocessing of apple pomace. *J. Biotechnol.* **53** 47-53
  - 81 Rivera-Muñoz, G., Tinoco-Valencia, J.R., Sánchez, S., Farrés, A. (1991) Production of microbial lipases in a solid-state fermentation system. *Biotechnol. Letters* **13** 277-280
  - 82 Rao, P.V., Jayaraman, K., Lakshmanan, C.M. (1993) Production of lipase by *Candida rugosa* in solid state fermentation: Determination of significant process variables.

concentration and increases in CO<sub>2</sub> concentration were measured as volume percentages (% v/v) and recorded simultaneously for at least 20 min. OCR and CPR were calculated from the change in O<sub>2</sub> and CO<sub>2</sub> concentration per second ( $\Delta\%/ \Delta t$ ), respectively. The gas volume in the system ( $V \text{ m}^3$ ), atmospheric pressure ( $p \text{ N}\cdot\text{m}^{-2}$ , as registered by the Koninklijk Nederlands Meteorologisch Instituut, De Bilt, Netherlands), the gas constant ( $R = 8.314 \text{ J}\cdot\text{mol}^{-1}\cdot\text{K}^{-1}$ ), temperature ( $T = 299 \text{ K}$ ) and the amount of fermented wheat bran per measurement ( $W \text{ kg}$ ) were taken into account:

$$r = \frac{\Delta\%}{\Delta t} \cdot \frac{1}{100} \cdot \frac{V \cdot p}{R \cdot T} \cdot \frac{1}{W} \quad \text{mol}\cdot\text{s}^{-1}\cdot\text{kg}^{-1} \quad (1)$$

The gas volume was corrected for the volume occupied by the Petri-dishes and wheat bran. The density of inoculated wheat bran was 0.92 g per ml, estimated by measuring the volume of hand-pressed wheat bran. During the time of a single measurement  $p$  was assumed to be constant.

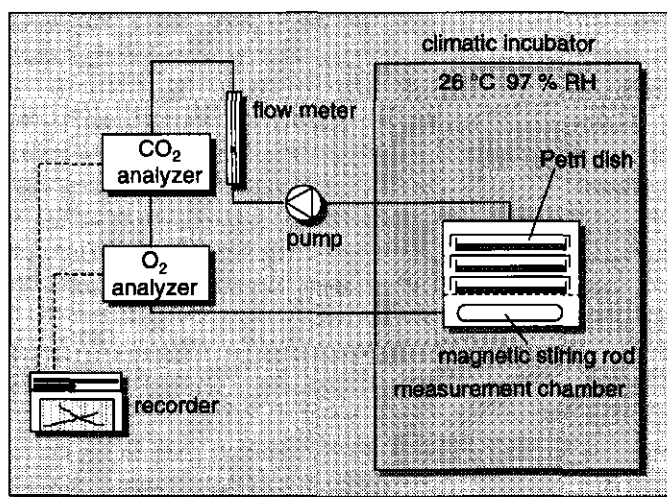


**Figure 1:** Set-up for measurement of carbon-dioxide production rate (CPR) and oxygen consumption rate (OCR).

**ATP.** From the fermented bran, 0.4 g was extracted by adding 4.0 ml 200 g per l trichloroacetic acid (TCA) in 4 mM EDTA and mixing for 30 s on a Vortex. The extract was diluted to at least 1:5000 with filter-sterilized HEPES buffer (2.5 mM EDTA in 25 mM HEPES, pH 7.75). The ATP level was measured with the Lumac Biocounter M 2500 (Lumac, Landgraaf, Netherlands), which method is based on the light generating with luciferin and firefly luciferase. Solutions of 100, 500 and 5000 nM ATP (Boehringer Mannheim, Germany) in HEPES buffer were used for calibration.

**Glucosamine.** For hydrolysis of the samples for glucosamine analyses, the method described by Lin and Cousin (12) was modified. Approximately 0.1 g fermented bran was hydrolysed with

2.5 ml 4 M HCl for 3 h at 100 °C in a sealed tube. The hydrolysate was diluted to 10 ml with distilled water after cooling. The concentration of sugars was then measured by HPLC ion-exchange chromatography (CarboPac PA-1 column with guard column, Dionex, Sunnyvale, CA) with pulse amperometric detection, at 25 °C, using D(+)-glucosamine hydrochloride (Sigma, St. Louis, MO) as reference solution. As eluent 18 mM NaOH was used.

**CMC-ase.** Considine *et al.* (2) and Chahal (13) have reported an extraction efficiency between 90 and 93 % of the total amount of recoverable cellulolytic enzyme activity from several lignocellulose substrates within 2 h of extraction with 20 mM sodium-acetate buffer pH 5 or 0.1 % Tween 80. The procedure followed in this chapter was based on both reports. Samples of 1 g fermented wheat bran were extracted twice in 10 ml 1 g per l Tween-80 for 1 h at 4 °C. The two supernatants per sample, obtained after centrifugation (10 min, 4000-g), were pooled and dialysed in a 10 kDa cut-off cellulose-acetate dialysis tube against 2000 ml 50 mM citric acid (pH 4.8) for 4 h at 4 °C to reduce the influence of the free sugars originating from the fermented bran on the measurement. The dialysed extracts obtained were stored at -20 °C prior to further analysis. CMC-ase activity was measured in undiluted dialysed extracts according to the method described by Wood and Bhat (14), with dinitrosalicylic acid solution (DNS) as colouring agent of reduced sugars. A 20 g·l<sup>-1</sup> suspension of carboxymethyl cellulose (CMC, Aldrich, Brussels, Belgium) in 50 mM citric-acid pH 4.8 was used as substrate. The undiluted dialysed extracts were incubated (1:1) with the CMC suspension for 30 min at 50 °C. The reaction was stopped by adding DNS. After 5 min in a boiling water bath and after dilution with water, the absorbance at 540 nm was measured in a spectrophotometer. Activities of CMC-ase were corrected for blanks, which were incubations with citric acid buffer instead of substrate. A calibration curve was made using glucose solutions in citric acid buffer. All activities are expressed as units (U) per actual gram fermented wheat bran. 1 U releases 1 µmol glucose per minute from the substrate.

**Carbon balance:** A fermentation was executed and analysed for CPR, weight changes and elemental and chemical composition to set up a carbon balance. Data on changes in dry matter weight and composition of fermented wheat bran were used to calculate the CO<sub>2</sub> production, using the C-based elemental composition of cellulose (CH<sub>1.67</sub>O<sub>0.83</sub>), starch (CH<sub>1.67</sub>O<sub>0.83</sub>), free sugars (CH<sub>2</sub>O), fat (CH<sub>1.84</sub>O<sub>0.114</sub>) and wheat bran protein (CH<sub>1.94</sub>O<sub>0.56</sub>N<sub>0.27</sub>) (15). The results were compared with CO<sub>2</sub> production estimated by integration of the curve fit through the CPR results. Samples were taken every 8 h and analysed for CPR and weight changes. Samples taken at 0 and 72 h of fermentation were analysed for chemical and elemental composition using the following methods for food- and feed-composition analysis. Protein was measured by the Kjeldahl method (N-6.25). Fat was measured after acid hydrolysis according to the method described by Schormüller (16). Ash was measured after heating to 550 °C. Total carbohydrate content was measured as reduced sugars after boiling in water, digestion with pancreatin and acid hydrolysis according to the method of Van de Kamer (17). Free sugars were analysed by using HPLC with RI detector (18). Starch content was calculated from the total carbohydrate content minus the free-sugar content. Fibre content was determined by colorimetry using the Englyst Fiberzym Kit (Novo Nordisk Bioindustries U.K. Ltd., Farnham, U.K.). The methods used cover statistically approximately 94 % of the total material analysed. Elemental analysis was done, using GC.

**Statistics and curve fit.** For calculating the standard deviation  $s$ , a set of data independent of time is obligatory. These were only obtained for wet and dry matter weight, ATP and CMC-ase activity. Due to the method of sampling and measurement, results of OCR, CPR and glucosamine were not obtained at the same time since the measurements of OCR and CPR took at least 20 minutes. To exclude a time-dependent change, the next procedure was followed. The results measured were plotted against time, and a curve was fitted through these results, using the method of least squares. The standard error of fit,  $s_e$ , was calculated using the method described in the appendix. To calculate the standard deviation within a time fragment  $\tau$  around  $t$ , in which samples were taken, formula (2) was used.

$$s_{\tau} = \sqrt{\frac{\sum (y_i - \bar{y})^2}{n_{\tau} - m}} \quad \text{with } i \in \tau \quad (2)$$

The denominator in (2) represents the degree of freedom, with  $n_{\tau}$  being the number of samples, and  $m$  being the number of coefficients of the curve fit in fragment  $\tau$ . The results obtained at around  $t_{25}$ ,  $t_{45}$  and  $t_{70}$  were not obtained completely independent of each other since, although in random order, the same 10 sets of Petri-dishes were used at each measurement time.

Curve fits and statistical calculations were done with the computer software SlideWrite for Windows V3.00 (Advanced Graphics Software, Carlsbad, CA).

## Results and Discussion

**Wet and dry-matter weight.** An incubation, consisting of 60 Petri-dishes, each containing approximately 5 g wheat bran, divided over the three racks in the incubator, was done to measure the standard deviation ( $s$ ) in wet and dry-matter weight after 72 h of fermentation. In Figure 2 wet and dry-matter weight are shown, expressed per g initial weight of inoculated wheat bran to facilitate statistical calculations and comparisons. Mean value ( $\bar{x}$ ) and  $s$  are given in Table 1. Of both wet and dry-matter weight,  $s$  was less than 5.0 % of the mean values. There was an influence of the location of the Petri-dish in the incubator on the weight. Wet

**Table 1:** Mean value  $\bar{x}$  and  $s$  of wet and dry-matter weight after 72 h of fermentation, expressed per g initial weight.

	wet weight $\bar{x} \pm s$ (g)	dry matter weight $\bar{x} \pm s$ (g)
rack 1	0.828 $\pm$ 0.041	0.408 $\pm$ 0.020
rack 2	0.895 $\pm$ 0.028	0.400 $\pm$ 0.009
rack 3	0.806 $\pm$ 0.040	0.409 $\pm$ 0.012



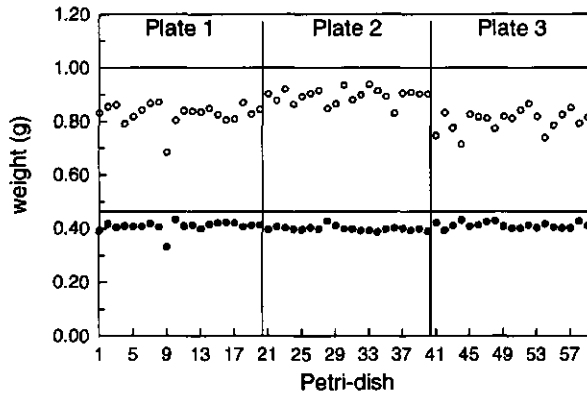


**Figure 2:** Wet (O) and dry-matter (●) weight after 72 h of fermentation, expressed per g initial weight of inoculated wheat bran. The horizontal lines represent the initial values.

weights of Petri dishes located on Rack 2 were higher than those on Racks 1 and 3. In contrast, results of dry matter weight measurements did not differ significantly. The differences in wet weight found on Rack 2 could be explained by differences in accumulation of water droplets, which were seen at the inside of the cover of the Petri-dishes. This formation of condensate droplets might be caused by small differences in air currents, and therefore by small differences in temperature and diffusion. The influence of these condensate droplets seems to be negligible. To check the influence of the amount of inoculated wheat bran per Petri-dish on the dry matter weight changes, 56 Petri-dishes, initially containing between 1.5 and 11.5 g wheat bran, were incubated for 72 h. The results are shown in Figure 3. The horizontal line represents initial dry matter weight per g wheat bran, calculated from the dry matter content of the wheat bran and the amount of water added to it during substrate preparation and inoculation. The results showed that below approximately 4 g initial weight scatter increased slightly. The  $s$  in dry matter weight appeared to be less than 3.5 % of the mean value in Petri-dishes initially containing more than 4 g of wheat bran. Thus, high initial weights up to 11.5 g have no significant effect on the change of dry matter weight during fermentation. Throughout the rest of the experiments between 4 and 8 g of wheat bran per Petri-dish was used.

**OCR and CPR.** The respiration activities, OCR and CPR, were measured in 10 sets of 3 Petri-dishes after about 25, 45 and 70 h of fermentation. One single measurement with three Petri-dishes was done shortly after  $t = 0$ . The order of Petri-dishes in the measurement chamber did not influence the results of the measurement (data not shown). The change in concentration of oxygen and carbon dioxide,  $\Delta\%/\Delta t$ , was nearly linear throughout the measurement time of 20 min. Results of OCR measurements, presented as dots, and a fitted curve through the sets of measured OCR values are presented in Figure 4. Based on the arbitrary choice of the logistic

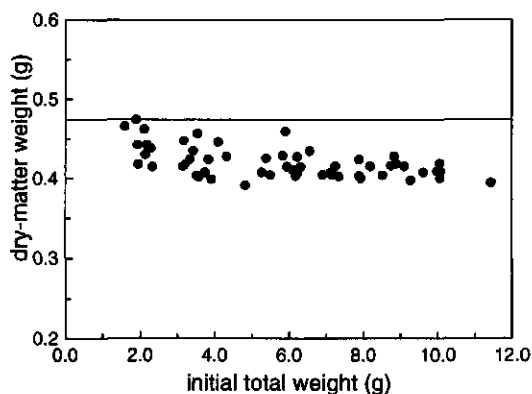


**Figure 3:** Influence of the initial amount of wheat bran per Petri-dish on dry matter weight after 72 h of fermentation, expressed per g initial weight of inoculated wheat bran. The horizontal line represents the initial value.

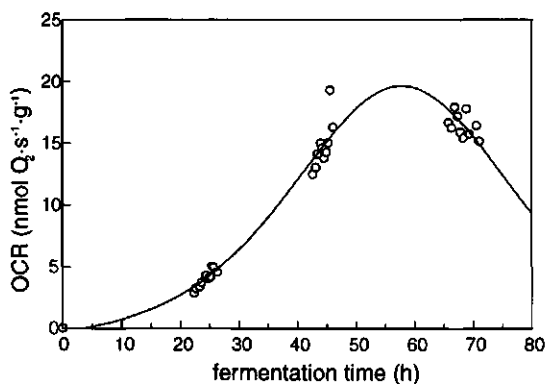


**Figure 4:** OCR measured after  $t = 0, 25, 45$  and  $70$  h of fermentation (○), and the curve fit (solid line).

curve to describe the growth of fungi in SSF (9), the differential of the logistic curve was used as curve-fit equation. The  $s_p$  of the OCR measurement showed to be  $1.05 \cdot 10^{-6}$  mol O<sub>2</sub> per s per kg, equal to 6.8 % of the predicted OCR value at 70 h of fermentation. The  $s_p$  of the CPR showed to be  $0.77 \cdot 10^{-6}$  mol CO<sub>2</sub> per s per kg, which is 5.6 % of the predicted CPR value at 70

h of fermentation. Table 2 gives, besides the  $s_e$ , the standard deviation  $s_r$  of the sets of data around  $t = 25, 45$  and  $70$  h of fermentation. The values of  $s_r$  are presented as a percentage of the OCR and CPR values predicted by the curve fit at  $t = 25, 45$  and  $70$  h of fermentation,

**Table 2:** Estimated standard error of curve fit,  $s_e$ , presented as a percentage of values of OCR and CPR predicted by curve-fits at  $t_{70}$ , and standard deviation,  $s_r$ , presented as a percentage of values of OCR and CPR predicted by curve-fits at  $t_{25}$ ,  $t_{45}$  and  $t_{70}$ .

	OCR			CPR		
$s_e$ (% of predicted rate)	6.8			5.6		
fermentation time $t$ (h)	25	45	70	25	45	70
$s_r$ (% of predicted rate)	9.8	12.5	7.6	4.8	6.1	9.4

respectively. The fact that the  $s_r$ 's appear to be larger than the overall  $s_e$  is caused by the difference in degrees of freedom and the fact that values are presented as relative values.  $s_e$  gave the standard error of curve fit, over a period of a little more than  $70$  h of fermentation. The values of  $s_e$  might give the wrong idea that the scatter in OCR and CPR was constant over time. In fact, it fluctuated in time as can be seen by the values of the  $s_r$ 's. Time dependence of  $s_r$  was improbable, but it could not be concluded whether or not the scatter in OCR and CPR depended on the magnitude of OCR and CPR. The increase in scatter, visible during the increase of biological activity, might be caused by the influence of the cultivation method used, or by the natural variation in growth of fungi (19) due to the complexity of the substrate, or due to genetic determination.

**Glucosamine.** Samples used for OCR and CPR measurements at around  $t = 70$  h were used for determination of the accuracy in glucosamine measurements. Results of the glucosamine measurement depend therefore also on time of sampling. Figure 5 shows the results of the glucosamine measurement in which the time dependence is visible. The time dependence has, like in OCR and CPR measurements, to be excluded before accuracy could be determined. However, in this case an overall curve could not be fit to calculate  $s_e$  since data were available only around  $t_{70}$ . The course of glucosamine in time was expected to be a sigmoidal curve (6). Fragments of this curve could be described by the second-order polynomial equation (3), which replaced the sigmoidal fit within each fragment. Figure 5 shows the second-order polynomial fit through the measured glucosamine values.

$$y = a_0 + a_1 \cdot x + a_2 \cdot x^2 \quad (3)$$

The  $s_{t=70}$  calculated using equation (3) is  $0.194 \text{ mg} \cdot \text{g}^{-1}$  ( $n = 10$ ,  $m = 3$ ), which was  $4.5 \%$  of the glucosamine content at  $t_{70}$ , predicted by equation (3).

**ATP.** Measurement of ATP was done in 8 samples taken from one Petri-dish and in 10 samples of wheat bran taken from 10 Petri dishes after  $70$  h fermentation. The correlation coefficient of the calibration curve was  $0.999$ . The  $s$  in the ATP content of the 8 samples

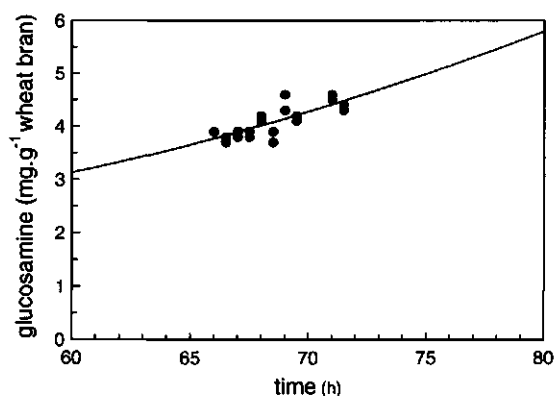


**Figure 5:** Results of glucosamine measurement at  $t_{70}$  (●) and the second-order polynomial fit (solid line).

appeared to be 5.2 %, and of the 10 independent samples 9.9 %, of the mean ATP level. This last figure was significantly higher than the  $s$  for weight measurement, the  $s$  for OCR and CPR, and the  $s_{t=70}$  for glucosamine measurements.

Contrary to glucosamine, ATP is a measure of biological activity. It, therefore, seems to have a high potential for use in SSF control. The amount of ATP is described as a useful parameter for kinetic modelling (20) and production control (21), but the amount present in microbial cells depends strongly on the physiological status of the cells, and hence on the available substrate and sample treatment. In a complex substrate, like wheat bran, large variation in ATP is therefore not unlikely.

The measurement of ATP is fast but demands practical skilfulness. In our research, we observed extremely high inaccuracies in the ATP measurement in samples of fermented wheat bran taken during the course of the fermentation, which forced us to reject the ATP measurement as a tool in our SSF research.

**CMC-ase.** Measurement of activity of cellulolytic-enzymes activity with DNS as colouring agent is widely used in a broad range of research disciplines (22, 23, 24, 25). The DNS method has, however, a large spread (24). The spread in the measurement of CMC-ase activity was, in our experience, caused by the interaction between substrate and product since the presence of CMC largely increased the spread of standard glucose solutions (results not shown). The spread in CMC-ase activity measurement in dialysed extracts was 14 % ( $n=10$ ) of the measured activity level of 7 U per gram wheat bran.

**C-balance:** The amount of  $\text{CO}_2$  produced during 72 h of fermentation could be predicted using the elemental composition of the dry matter, and the change in dry matter weight, calculated as C-mol substrate.

$\text{CO}_2$  production could also be predicted based on the changes in chemical composition of the bran, that is, changes in amount of starch, free sugars, fibre and fat, and their elemental

composition. Components originating from biomass (cellular substances and enzymes) are present in the fermented bran and are therefore included in these components unless they belong to the missing 6 % of the total weight which could not be determined.

Both predictions can be compared with the CO<sub>2</sub> production as calculated from the integral of the curve fit through the CPR values.

The predicted and the calculated CO<sub>2</sub> productions are given in Table 3. The elemental and chemical composition of wheat bran at 0 and 72 h are also given in Table 3.

**Table 3:** Chemical and elemental composition of fermented wheat bran after 0 and 72 h of fermentation, and predicted and calculated CO<sub>2</sub> productions. Values are expressed per g initial dry matter.

		composition		CO <sub>2</sub> production
		t = 0 h	t = 72 h	
chemical composition				
starch + fibres +				
free sugars	(g)	0.58	0.43	
protein	(g)	0.18	0.18	
fat	(g)	0.05	0.04	
ash	(g)	0.07	0.07	
rest	(g)	0.12	0.15	
total	(g)	1.00	0.86	
	(C-mol)	31.4·10 <sup>-3</sup>	24.7·10 <sup>-3</sup>	
predicted CO <sub>2</sub> production	(mol)			6.7·10 <sup>-3</sup>
elemental composition				
elemental formula		CH <sub>1.747</sub> O <sub>0.680</sub> N <sub>0.053</sub>	CH <sub>1.750</sub> O <sub>0.643</sub> N <sub>0.063</sub>	
dry matter	(g)	1.00	0.86	
predicted CO <sub>2</sub> production	(mol)			4.9·10 <sup>-3</sup>
CPR				
calculated CO <sub>2</sub> production	(mol)			5.2·10 <sup>-3</sup>

## Conclusion

The presented system, in which Petri-dishes containing inoculated wheat bran were incubated in a incubator at constant temperature and humidity, showed to be accurate. By taking ten samples, an overall *s* could be obtained which was less than 7 % of the mean measured value of wet weight, dry matter weight, OCR, CPR and glucosamine. Thus, within the same experimental circumstances, there was a certainty of more than 95 % that the real value of a measured parameter *A* is  $A \pm 15$  %. For the purpose of modelling in our SSF research this is an acceptable range.

Measurement of the ATP level is less accurate. Besides, the application of ATP measurement has another drawback: the level of ATP depends largely on the physiological state of the microorganism and is thus related to the complexity of the substrate and handling of the

samples. Wheat bran might be too complex a substrate for accurate measurement of ATP. CMC-ase measurements are even more inaccurate. The high  $s$  is mainly caused by the combination of CMC and glucose within the DNS method.

Measurements of standard deviations of OCR, CPR and glucosamine were obstructed by time-dependent changes. These changes could be excluded by a curve fit through the sets of measured values. The calculated  $s_0$  can be used as an estimation of the actual time-independent standard deviation.

The results of CPR measurement showed to be in good agreement with those of elemental and chemical composition of fermented wheat bran, indicating a good reliability of the results of measurements.

### Acknowledgement

This research was financially supported by TNO Nutrition and Food Research Institute, Bavaria BV, Gist brocades, Unilever Research Laboratorium and Quest International. The authors wish to thank Eric Schoen and Henk van Sonsbeek for their comments on this chapter, Cees Verbeek for glucosamine analysis, members of the Organic Chemistry Department of the Agricultural University Wageningen, Netherlands, for executing elemental analyses, and members of the Division of Analytical Sciences of TNO Nutrition and Food Research Institute for composition analysis. Elemental analysis for oxygen was executed by Ets Gordinne & Co N.V., Rotterdam, Netherlands.

### References

- 1 Pandey, A. (1992) Recent process developments in solid-state fermentation. *Process Biochem.* **27** 109-117
- 2 Considine, P.J., Mehra, R.K., Hackett, T.J., O'Rorke, A., Comerford, F.R., Coughlan, M.P. (1986) Upgrading the value of agricultural residues. *Ann. New York Acad. Sci.* **469** 304-311
- 3 Paredes-López, O., Alpuche-Solís, A. (1992) Solid substrate fermentation - A biotechnological approach to bioconversion of wastes. In: *Bioconversion of waste materials to industrial products*, A.M.Martin (Ed.). Elsevier Scientific Publishers, London 117-145
- 4 Trejo Hernández, M.R., Lonsane, B.K., Raimbault, M., Roussos, S. (1993) Spectra of ergot alkaloids produced by *Claviceps purpurea* 1029c in solid-state fermentation system: influence of the composition of liquid medium used for impregnating sugar-cane pith bagasse. *Process Biochem.* **28** 23-27
- 5 Fukushima, D. (1982) Koji as an important source of enzymes in the orient and its unique composite systems of proteinases and peptidases. In: *Use of enzymes in food technology*. P. Dupuy (Ed.), Technique et documentation Lavoisier, Paris 281-388
- 6 Kim, J.H., Hosobuchi, M., Kishimoto, M., Yoshida, T., Taguchi, H., Ryu, D.D.Y. (1985) Cellulase production by a solid-state culture systems. *Biotechnol. Bioeng.* **27** 1445-1450
- 7 Raimbault, M., Alazard, D. (1980) Culture method to study fungal growth in solid fermentation. *European. J. Appl. Microbiol. Biotechnol.* **9** 199-209
- 8 Silman, R. (1980) Enzyme formation during solid-substrate fermentation in rotating vessels. *Biotechnol. Bioeng.* **22** 411-420
- 9 Mitchell, D.A., Do, D.D., Greenfield, P.F., Doelle, H.W. (1991) A semimechanistic mathematical model for growth of *Rhizopus oligosporus* in a model solid-state fermentation system. *Biotechnol. Bioeng.* **38** 353-362

- 10 Smits, J.P., Janssens, R.J.J., Knol, W., Bol, J. (1994) Modelling of the glucosinolate content in solid-state fermentation of rapeseed meal with fuzzy logic. *J. Ferment. Bioeng.* **77** 579-581
- 11 Young, J.F., (1967) Humidity control in the laboratory using salt solutions - a review., *J. Appl. Chem.* **17** 241-245
- 12 Lin, H.H., Cousin, M.A. (1985) Detection of mold in processed foods by high performance liquid chromatography., *J. Food Protection* **48** 671-678
- 13 Chahal, D.S. (1991) Production of *Trichoderma reesei* cellulase system with high hydrolytic potential by solid-state fermentation. In: ACS Symposium Series, J. Comstock (Ed.), American Chemical Society, Washington DC 111-122
- 14 Wood, T.M., Bhat, K. M. (1988) Methods for measuring cellulase activities. In *Methods in Enzymology*. ed. W.A. Wood, S.T. Kellogg, S.T., Academic Press Inc., San Diego 100-102
- 15 Pomeranz, Y., Shellenberger, J.A. (1971) In *Bread science and technology*. Y. Pomeranz (Ed.), and J.A. Shellenberger, AVI Publishing Company Inc., Westport 224-245.
- 16 Schormüller, J. (1969) In: *Handbuch der Lebensmittelchemie band IV*, Springer Verlag 423-425
- 17 Kamer, J.H. van de (1941) *Chemisch Weekblad* **38** 286-288
- 18 Richter, K and Woelk, H.U. (1977) *Die Stärke* **29** 273-277
- 19 Lonsane, B.K., Saucedo-Castaneda, G., Rimbault, M., Roussos, S., Viniestra-Gonzalez, G., Ghildyal, N.P., Ramakrishna, M., Krishnaiah, M.M. (1992) Scale-up strategies for solid-state fermentation systems. *Process Biochem.* **27** 259-273.
- 20 Wang, H-H., Wu, T-Z., Hsu, J-P., Tsai, Y-S. (1991) A kinetic analysis of sorghum brewing - A typical solid-state fermentation. *Nippon Shokuhin Kogyo Gakkaishi* **38** 716-721
- 21 Cochet, N., Tyagi, R.D., Ghose, T.K., Lebeault, J.M. (1984) ATP measurement for cellulase production control. *Biotechnol. Lett.* **6** 155-160
- 22 Sinha, S.N., Ghosh, B.L., Ghose, S.N. (1981) Detection of cellulase inhibitor in the wheat bran culture of *Aspergillus terreus*. *Can. J. Microbiol.* **27** 1334-1340
- 23 Sim, T.S., Oh, J.C.S. (1990) Spent brewery grains as substrate for the production of cellulases by *Trichoderma reesei* QM9414. *J. Industrial Microbiol.* **5** 153-158
- 24 Bailey, M.J., Biely, P., Poutanen, K. (1992) Interlaboratory testing of methods for assay of xylanase activity., *J. Biotechnol.* **23** 257-270
- 25 Olama, Z.A., Hamza, M.A., El-Sayed, M.M., Abdel-Fattah, M. (1993) Purification, properties and factors affecting the activity of *Trichoderma viride* cellulase., *Food Chem.* **47** 221-226

### -Appendix-

The value of a measured dependent variable  $y$  is determined by the relationship between  $y$  and the independent variable  $x$  in combination with a random error  $\epsilon$ . A curve fit describes this relationship by approach. If, for instance, the real relationship is

$$y = \beta_0 + \beta_1 x + \epsilon \quad , \quad (a1)$$

in which  $\beta_0$  and  $\beta_1$  are the coefficients describing the relation between  $x$  and  $y$ , and in which  $\epsilon$  is the random error, then the curve fit approaches this relationship by the linear equation

$$\hat{y} = a_0 + a_1 x \quad (a2)$$

Here  $\hat{y}$  can be seen as the approximated mean value of  $y$  dependent on  $x$ . The coefficients  $a_0$  and  $a_1$  are the estimated values of  $\beta_0$  and  $\beta_1$ . These coefficients are calculated such that

$$SSE = \sum (y_i - \hat{y}_i)^2 \quad (a3)$$

is as small as possible (method of least squares). In fact equation (a3) is the sum of squares of the deviation of  $y$  from  $\hat{y}$ . The corresponding standard deviation,  $s_e$ , is the standard error of the curve fit.

$$s_e = \sqrt{\frac{\sum (y_i - \hat{y}_i)^2}{n - m}} \quad (a4)$$

$s_e$  is an estimation of  $\epsilon$ , the random error. Here, the number of degrees of freedom ( $n-m$ ) is determined by the number of samples ( $n$ ) and the number of coefficients in the curve fit ( $m$ ). In case of a linear fit, the number of coefficients  $m = 2$ .

The curve fit describes the variation in  $y$  due to variations in  $x$ , while  $s_e$  describes the variation of  $y$  occurring independent of variations in  $x$ . By calculating  $s_e$ , the standard deviation of a set of data, which cannot be sampled independent of variable  $x$ , is obtained.



# Chapter 3

---

## Solid-State Fermentation of Wheat Bran by *Trichoderma reesei* QM9414

Published as

Smits, J.P., Rinzema, A. Tramper, J., Van Sonsbeek, H.M., Knol, W.

Solid-state fermentation of wheat bran by *Trichoderma reesei* QM9414: substrate composition changes, C-balance, enzyme production, growth and kinetics.

Appl. Microbiol. Biotechnol. **46** 489-496 (1996)

## Summary

A description is given of the solid-state fermentation (SSF) of wheat bran by *Trichoderma reesei* QM9414 at constant temperature and relative humidity. Glucosamine, oxygen consumption rate (OCR), carbon dioxide production rate (CPR), changes in wheat bran composition and production of four enzymes were measured during 125 h of fermentation. A C-balance was set up between CO<sub>2</sub> production based on CPR measurements, CO<sub>2</sub> production as expected on the basis of substrate composition changes and substrate elemental composition in combination with dry matter weight loss.

Glucosamine was used as the measure of biomass. The results indicate that the glucosamine content of fungi in liquid culture cannot be used to estimate the biomass content in SSF. Using glucosamine, correlations between fungal growth and respiration kinetics could only partly be described with the linear-growth model of Pirt.

A decline in OCR and CPR started at the moment the glucosamine level was 50 % of its maximum value ( $G_{max}$ ). After the glucosamine level had reached  $G_{max}$ , OCR and CPR continued to decline.

The activities of xylanase and protease are linearly related to the glucosamine level. No clear correlations between glucosamine and carboxymethyl-cellulose-hydrolyzing enzyme (CMC-ase) activity and amylase activity were found.

## Introduction

As a result of their inhomogeneity, scale-up and optimization of solid-state fermentation (SSF) processes, necessary for commercial production, demand intensive research. Temperature evolution is generally seen as causing the main problems in scale-up of the fermentation process. Modelling is an indispensable tool to predict growth and activity of biomass, and thus to predict temperature evolution.

In our research on modelling of SSF, we use the production of carboxymethyl-cellulose-hydrolyzing enzyme (CMC-ase) activity by *Trichoderma reesei* QM9414 as a model fermentation. Commercial production of cellulases by *Trichoderma* sp. is carried out in both liquid and solid-state fermentation (1, 2). Wheat bran is one of the substrates yielding highest activities in SSF (3). Reports on production of cellulase by *Trichoderma* sp. in SSF (4, 5, 6, 7, 8) cannot be compared because different strains or mutants, substrates and culture conditions have been used.

We started our research with determining the accuracy of measurements of variables involved (9). The second step in our approach is to characterize the fermentation process under constant environmental conditions. The third step will be to determine the influence of environmental conditions on growth, respiration kinetics and product formation. The last step is to combine physical and kinetic parameters into a mathematical model, which has then to be validated.

The aim of the work reported in this chapter concerns the second step: description of growth, respiration kinetics, product formation and stoichiometry under constant environmental conditions. Glucosamine is used here as the fungal-biomass parameter. Correlations between glucosamine, oxygen consumption rate (OCR), carbon dioxide production rate (CPR) and enzyme production by the fungi are given. The results of the CPR measurements are also

used to set up a C-balance.

The correlation between glucosamine, OCR and CPR has been described before (4, 10, 11) using the linear-growth model, first described for growing bacteria by Pirt (12). Our results show that the correlation between specific-growth rate and specific activity deviates from the relation described by the linear-growth model.

## Material and Methods

**Microorganism.** *Trichoderma reesei* QM9414 (ATCC 26921) was used throughout the experiments. A spore suspension was obtained by growing the fungus in Roux bottles on malt extract agar (50 g per l, pH 5.4, Oxoid CM 59, Unipath, Basingstoke, UK) for 1 week at 28 °C, and harvesting the spores with 1 g per l Tween-80 in water. The spore suspension thus obtained was frozen (-80 °C) after adding 100 µl glycerol per ml spore suspension as cryo-protectant. The final suspension contained  $(3.1 \pm 1.2) \cdot 10^7$  viable spores per ml after thawing, counted as colony-forming units on plate-count agar, potato dextrose agar and glucose-yeast agar (n=12).

**Substrate, inoculation and incubation.** From a single batch of well-mixed wheat bran, containing 9 % w/w moisture, 90 g was taken and added to 62 ml water in a 1 l bottle with screw cap (Duran, Scott, Germany). After sterilization for 20 min at 121 °C and cooling to 26 °C, 4.5 ml spore suspension, suspended in 18.0 ml sterile 9 g per l NaCl, was aseptically sprayed over the bran and mixed thoroughly. The inoculated wheat bran thus obtained contained  $8.0 \cdot 10^5$  spores per gram wet weight. This procedure was executed in fourfold to obtain a sufficient amount of inoculated bran. The dry matter content of the inoculated wheat bran amounted to 466 mg per g, which corresponds with a water activity of 0.97 (results of measurements not shown). In total, 80 pre-weighed Petri dishes were filled with 5 - 7 g inoculated wheat bran, weighed again and placed in an incubator (VEA-Instruments, Houten, Netherlands) in which the temperature was kept at  $26.0 \pm 0.3$  °C and the relative humidity at  $97 \pm 1$  % throughout the fermentation.

**Sampling.** Sampling was done at regular intervals by taking Petri dishes out of the incubator. Remaining weight of the bran was determined and substrate loss was calculated by combining the results with the dry matter content measurements. Dry matter content was assayed by measuring the weight change of ca. 0.4 g fermented bran after 16 h drying at 106 °C. OCR and CPR were determined in three Petri dishes immediately after sampling. The remaining sample material of these three Petri dishes was combined and frozen at -80 °C for CMC-ase, xylanase, amylase, glucosamine and composition analysis.

**OCR and CPR.** OCR and CPR were calculated from the changes in volume fraction of O<sub>2</sub> and CO<sub>2</sub> in time, respectively, using the set up described before (9). This set up contained a cell in which three Petri dishes were placed and in which O<sub>2</sub> and CO<sub>2</sub> concentrations were measured by pumping the air in the cell through a paramagnetic O<sub>2</sub> analyser (Servomex Series 1100, Servomex, Zoetermeer, Netherlands) and an infrared CO<sub>2</sub> analyser (Servomex Series 1400). The changes in O<sub>2</sub> and CO<sub>2</sub> concentrations were followed in time, and OCR and CPR were calculated as described before (9). OCR and CPR were plotted against fermentation time, and curves through them were described by equation (1). This equation was chosen from a set of equations based on the results of the method of least squares.

$$r(t) = a_0 + a_1 \cdot e^{-0.5 \left( \frac{\ln \frac{t}{a_2}}{a_3} \right)^2} \quad (1)$$

Here,  $r(t)$  is either OCR(t) or CPR(t) in nmol per s per g bran and  $t$  is the fermentation time in h. The coefficients  $a_0$  to  $a_3$  are unspecified fit parameters.

**Glucosamine.** The glucosamine content of fermented wheat bran was assayed as described previously (9), using HPLC ion-exchange chromatography (CarboPac PA-1 column with guard column, Dionex, Sunnyvale, CA) with pulse amperometric detection, at 25 °C. As eluent 18 mM NaOH was used.

#### Enzyme activities

**CMC-ase.** The activity of CMC-ase in extracts of fermented wheat bran was assayed in dialysed and non-dialysed extracts as described before (9). Activity is expressed in Units (U), 1 U releasing 1  $\mu$ mol glucose per minute.

**Amylase.** To determine the contribution of amylase activity to the glucose measured in the CMC-ase activity assay, the following analysis was done. About 1 g of fermented bran was extracted for 1 h at 4 °C with 20 ml 0.1 % w/v Tween-80 in water. After centrifugation (5 min, 4000xg, Labofuge GL, Heraeus-Christ, Osterode) the supernatant was frozen (-20 °C) until the activity measurement was carried out. The measurement was done by incubating 0.5 ml 0.2 g per liter soluble starch in 50 mM citric acid buffer pH 4.5 for 20 min with 0.5 ml extract at 50 °C. The reaction was stopped by adding dinitrosalysilic acid solution (DNS) and further treated according to the method described by Wood and Bhat (13). Activities were calculated against glucose standard and corrected for activities found in blanks without substrate and blanks without enzyme. Activity is expressed in Units (U), 1 U releasing 1  $\mu$ mol glucose per minute.

**Xylanase.** Extracts used for the amylase assay were also used in a five-fold dilution to determine xylan-hydrolyzing enzyme activity according to the method of Bailey et al. (14). A 0.1 g per liter xylan suspension was made by suspending 1 g xylan from birchwood (Sigma, St. Louis, MO) in 80 ml 50 mM citric acid buffer pH 5.3 of 60 °C and heating until boiling. The suspension was mixed overnight, brought to a volume of 100 ml and stored in small portions at -20 °C until use. From the suspension 1.8 ml was taken which was pre-heated at 50 °C and incubated for exactly 10 min with 0.2 ml of the diluted extract. The reaction was stopped by adding DNS, and xylanase activity was calculated according to the method described by Wood and Bhat (13). Xylose was used as standard. Activity is expressed in Units (U), 1 U releasing 1  $\mu$ mol xylose per minute.

**Protease.** Extraction for protease activity measurement was done by adding 10 ml 100 mM phosphate buffer pH 7.0 to 1 g fermented bran and stirring the mixture for 30 min at 4 °C. After centrifugation the supernatant was frozen at -20 °C until further analyses. Protease activity was measured in duplicate with dimethyl casein (5 mg per ml in 20 mM phosphate buffer pH 7.0) as substrate using an autoanalyser. The release of alanine was measured and used as a basis for the expression of protease activity (1 U = 1  $\mu$ mol alanine per min per g).

**Composition.** Samples taken at 0, 24, 48, 72, 96, and 125 h of fermentation were analysed for composition, using standard methods for food and feed analysis as mentioned before (9).

Nitrogen was measured by the Kjeldahl method, and protein was calculated by multiplying the amount of organic nitrogen by 6.25. Ammonia content was measured by distillation. Fat was measured after acid hydrolysis. Ash was measured after heating at 550 °C. Total carbohydrate content was measured after digestion with pancreatin. The free sugars were analysed by ion-exchange chromatography (CarboPac PA-1 column with guard column, Dionex, Sunnyvale, CA) with pulse amperometric detection at 20 °C, using a three eluent system: deionized water, 100 mM sodium hydroxide and 100 mM sodium hydroxide in 500 mM sodium acetate. Starch content was calculated from the total carbohydrate content minus the free-sugar content. Fibre content was determined using the Englyst fiberzym kit (Novo Nordisk Bioindustries U.K., Surrey, UK). The results of these analyses are expressed per gram dry matter. Since dry matter content and weight loss are known, the results could also be calculated per gram initial weight.

pH was measured in a suspension of 1 g fermented bran in 15 ml water.

**Elemental composition.** Elemental analyses of fermented wheat bran were done by GC.

**Curve fit and mathematical calculations:** Curves were fitted using SlideWrite V6.0 (Advanced Graphics Software, Carlsbad, CA). Mathematical calculations (differentiations and numerical integrations) were done with Mathcad V6.0 Plus (Mathsoft, Cambridge, MA).

## Results

**Fermented-bran composition.** During 125 hours of fermentation a total decrease of 0.22 g per gram initial total weight of inoculated wheat bran was observed (Figure 1). This decrease is the result of both substrate utilization and changes in water content. The weight loss due to substrate utilization was 0.10 g per gram initial dry matter weight as calculated from the results of composition analyses.

Decrease in fibre content started after 24 h of fermentation. At this time starch content also

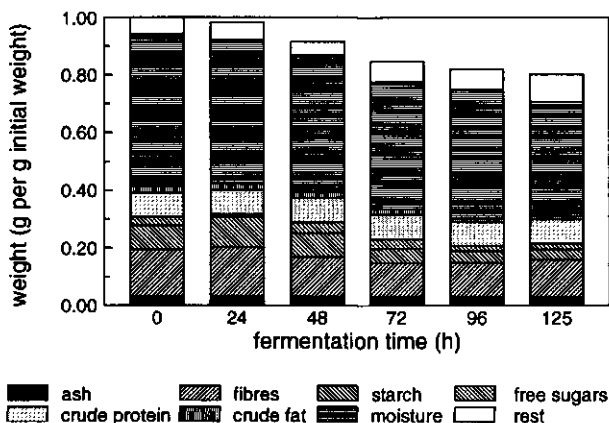


**Figure 1:** Changes in weight of wheat bran components during SSF with *Trichoderma reesei* QM9414.

decreased causing a temporary increase of total free sugar content in the next 24 h (Figure 1). The total amount of nitrogen (Kjeldahl) remained constant. The water content decreased during the whole fermentation probably as a result of a change of water-binding capacity of the fermented bran, since water activity was controlled during the whole fermentation period by keeping the relative humidity of the environment at  $97 \pm 1$  %. The amounts of fat and ash hardly change during fermentation.

The sum of the analysed components accounted for more than 94 % of dry matter weight. This recovery is in good agreement with the general recovery of agricultural products analysed with these methods.

**Glucosamine.** Based on the arbitrary choice of a logistic curve fit to describe the growth of fungi (15) the increase in biomass glucosamine ( $G(t)$ ), that is, the measured glucosamine content minus the background level of the wheat bran, is described with equation (2). Here,  $G_{\max}$  is the maximum amount of biomass glucosamine,  $G_0$  is the initial amount of biomass glucosamine, and  $\mu_{\max}$  is the maximum specific-growth rate.

$$G(t) = \frac{G_{\max}}{1 + \left( \frac{G_{\max}}{G_0} - 1 \right) \cdot e^{-\mu_{\max} \cdot t}} \quad (2)$$

The wheat bran itself contained 0.43 mg glucosamine per gram initial dry matter. The glucosamine content increased to a mean level of 4.6 mg per gram actual fermented bran as a result of fungal growth during the first 80 h of fermentation. Fit results, using equation (2), reveal that  $G_{\max}$  was 8.1 mg per gram initial dry matter,  $G_0$  was 0.02 mg per g and  $\mu_{\max}$  was  $0.123 \text{ h}^{-1}$ . Figure 2 shows the biomass glucosamine content of the fermented bran and the logistic curve.

**OCR and CPR.** The courses of OCR and CPR are presented in Figure 3a. Highest activities were found shortly after 53 h of fermentation. The curves fitted through OCR and CPR, using equation (1), were integrated to obtain the course of the cumulative oxygen consumption and carbon dioxide production (Figure 3b). During 125 h fermentation 8.8 mmol  $\text{O}_2$  per gram initial dry matter was consumed and 9.2 mmol  $\text{CO}_2$  per gram initial dry matter was produced.

**Enzyme production.** Activities of four enzymes were determined (Figure 4). CMC-ase activities in dialysed and non-dialysed extracts of fermented wheat bran were measured. Activities in dialysed extracts appeared to be ca. 25 % of the activities in non-dialysed extracts (results not shown), again demonstrating the significant influence of the dialysis-step on the final enzyme activity, as observed before (9). The contribution of glucose resulting from

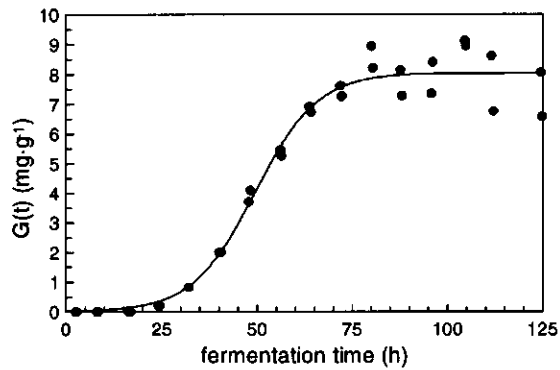


**Figure 2:** The experimentally determined biomass glucosamine  $G(t)$  (●), expressed as mg glucosamine per g initial dry matter, and the logistic curve (solid line).

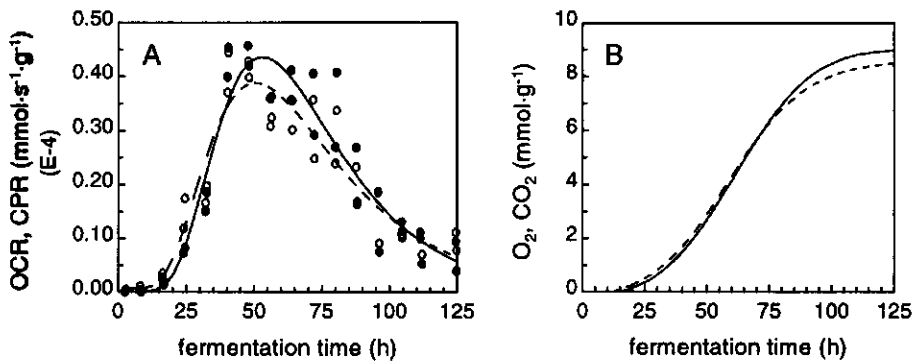


**Figure 3:** OCR (○) and CPR (●) with fitted curves (---and —, respectively) (A) and the accordingly consumed oxygen (---) and produced carbon dioxide (—) (B) based on the integration of the empirical curves of A. All results are expressed per g initial dry matter.

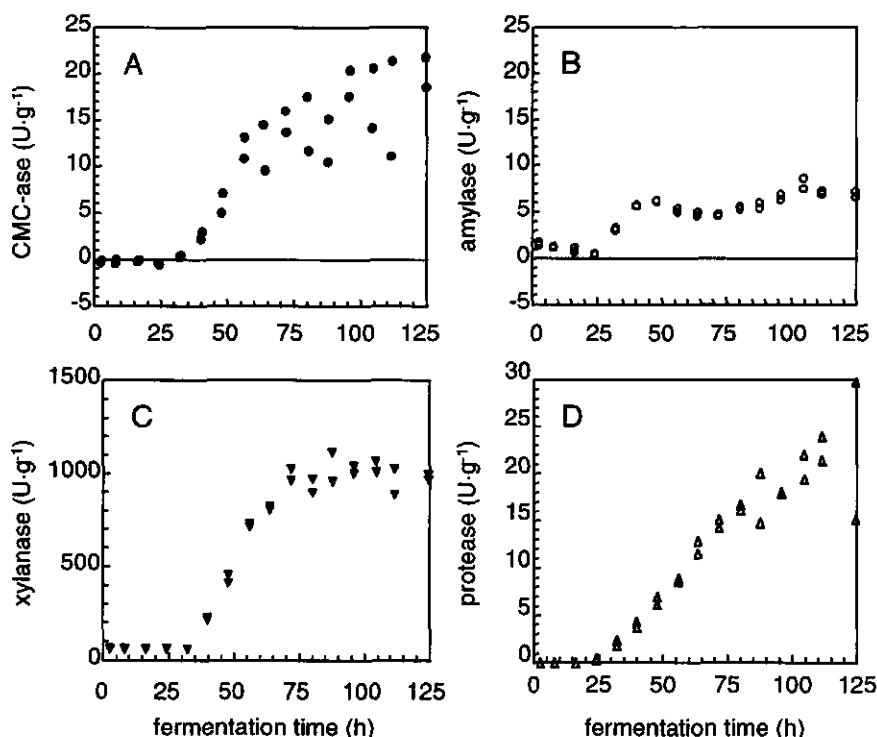


**Figure 4:** Enzyme production during SSF of wheat bran by *Trichoderma reesei* QM9414. Activities of CMC-ase (A), amylase (B), xylanase (C) and protease (D) in non-dialysed extracts are shown. All activities are expressed as Units per g initial dry matter.

amylase activity to the CMC-ase activity measured in non-dialysed extracts was low (Figure 4b). Xylanase activity was present in large amounts, even without additional supply of nutrients, although addition is reported to increase activity significantly (8). The course of the protease activity is shown in Figure 4d. Protease activity yielded only a small amount of ammonia: the amount measured in the bran remained below 7  $\mu\text{mol NH}_4$  per gram fermented bran during the 125 h of fermentation (results not shown). The pH remained between 6.45 and 6.86 throughout the whole fermentation.

## Discussion

**Correlation between glucosamine and biomass.** Due to the fact that biomass cannot be separated quantitatively from the substrate in SSF, glucosamine content of biomass growing in



liquid culture is often used to estimate the amount of biomass dry matter (4, 10, 11). An advantage of glucosamine is that it can be measured easily and accurately (9). However, the glucosamine content of biomass needs not to be constant and it might depend on the age and physiological state of the biomass. Kim et al. (4) used the amount of glucosamine per g *Trichoderma reesei* dry matter in liquid culture to calculate the amount of dry matter in SSF. According to Kim et al. (4) and Xiugong and Kechang (16), the amount in liquid culture is 21 mg per g biomass dry matter. With the maximum biomass glucosamine content of 8.1 mg glucosamine per g initial dry matter measured in our experiments, which is equal to 9.7 mg glucosamine per g actual dry matter, this would account for 0.46 g biomass dry matter per g fermented bran dry matter. This means that, based on the elemental composition of *Trichoderma reesei* QM9414 in submerged fermentation on a nutrient medium with cellulose, which is  $\text{CH}_{1.80}\text{O}_{0.710}\text{N}_{0.143}$  for  $D > 0.025 \text{ h}^{-1}$  (17), 2.4 mmol biomass-nitrogen per g fermented bran dry matter would be present. Kjeldahl analyses revealed 2.4 mmol N per g fermented bran dry matter, being nitrogen originating from biomass, wheat-bran protein and extra-cellular enzymes. Thus, the amount of biomass calculated with the figure of Kim et al. (4), appears to exceed the amount of biomass plus proteins based on Kjeldahl analyses.

These calculations indicate that the value of the glucosamine content of biomass from liquid culture is not applicable to biomass in SSF. In our research we therefore used the amount of glucosamine as the biomass parameter, without converting it into biomass dry matter.

**C-balance.** To determine the reliability of weight, composition and CPR measurements,  $\text{CO}_2$  production was calculated by integration of the curve through the CPR, and compared with the changes in weight, chemical composition and elemental composition. The correlation between dry matter weight loss and  $\text{CO}_2$  production was investigated. This correlation showed to be close to linear ( $r^2 = 0.892$ , see Figure 5). With this linear correlation the  $\text{CO}_2$  production based

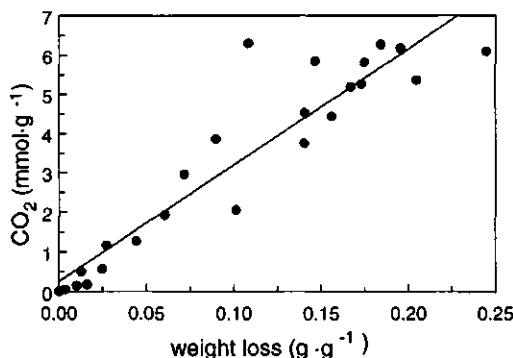


**Figure 5:** Correlation between dry matter weight loss, expressed as g per g initial dry matter, and  $\text{CO}_2$  production, calculated by integration of the CPR results, expressed in mmol per g initial dry matter.

**Table 1:** Equations describing the correlations between process variables and temperature, with their parameter values and dimensions.  $n$  is the number of data used to determine the parameters.

correlation	variables and parameters	value $\pm$ standard deviation
$u_{rad}(T) = (a_1 \cdot (T - T_{min}) \cdot (1 - \exp(a_2 \cdot (T - T_{max}))))^2$ <p>equation (1) (See Figure 1)</p>	$T$ $u_{rad}(T)$ $a_1$ $a_2$ $T_{min}$ $T_{max}$	  $(K)$ $(mm \cdot h^{-1})$ $(mm^{0.5} \cdot K^{-1} \cdot h^{0.5})$ $(K^{-1})$ $263 \pm 5$ $313.7 \pm 0.1$ $(K)$
$G_{max}(T) = (b_1 \cdot (T - b_2) \cdot (1 - \exp(b_3 \cdot (T - T_{max}))))^2$ <p>equation (8) (See Figure 3)</p>	$G_{max}(T)$ $b_1$ $b_2$ $b_3$	  $(mg \cdot g^{-1})$ $(mg^{0.8} \cdot K^{-1} \cdot g^{-0.5})$ $75 \pm 40$ $0.694 \pm 0.027$ $(K)$ $(K^{-1})$
$\mu_{max}(T) = (c_1 \cdot (T - T_{min}) \cdot (1 - \exp(c_2 \cdot (T - T_{max}))))^2$ <p>(See Figure 3)</p>	$\mu_{max}(T)$ $c_1$ $c_2$	  $(h^{-1})$ $(h^{0.5} \cdot K^{-1})$ $(K^{-1})$ $(9.14 \pm 0.37) \cdot 10^{-3}$ $0.544 \pm 0.099$
$Y_{G,O_2}(T) = d_1 + d_2 \cdot \exp(-0.5 \cdot [\frac{T - d_3}{d_4}]^2)$ <p>(See Figure 4A)</p>	$Y_{G,O_2}(T)$ $d_1$ $d_2$ $d_3$ $d_4$	    $(g \cdot mol^{-1})$ $(g \cdot mol^{-1})$ $(g \cdot mol^{-1})$ $(K)$ $(K)$ $1.187 \pm 1 \cdot 10^{-14}$ $1.97 \pm 1 \cdot 10^{-14}$ $301 \pm 2 \cdot 10^{-14}$ $3.67 \pm 5 \cdot 10^{-14}$
$m_d(T) = m_{d,0} + k_{md} \cdot \exp[-\frac{E_a}{R} \cdot (\frac{1}{T} - \frac{1}{T_{max}})]$ <p>equation (5) (See Figure 6)</p>	$m_d(T)$ $m_{d,0}$ $k_{md}$ $E_a$ $R$	    $(mmol \cdot h^{-2} \cdot g^{-1})$ $(mmol \cdot h^{-2} \cdot g^{-1})$ $(mmol \cdot h^{-2} \cdot g^{-1})$ $(J \cdot mol^{-1})$ $(J \cdot mol^{-1} \cdot K^{-1})$ $0.224 \pm 0.068$ $0.017 \pm 0.014$ $3.27 \cdot 10^5 \pm 0.47 \cdot 10^5$ $8.314$
	$n$	75
	$n$	5
	$n$	5
	$n$	4
	$n$	8

experimentally due to insufficient sensitivity of the glucosamine analysis method used here. Since there is no growth at temperatures higher than  $T_{max}$ ,  $\mu_{max}$  is assumed to approach zero and  $G_{max}$  is assumed approach  $G_0$  when  $T$  approaches  $T_{max}$ . These assumptions are used to describe the correlation between  $\mu_{max}$ ,  $G_{max}$  and  $T$ : the values  $\mu_{max}(314)=0$  and  $G_{max}(314)=G_0$  are used as additional data points.

There is a linear relationship between  $u_{\text{rad}}$  and  $\mu_{\text{max}}$  according to the work published by Trinci (14). This means that the Ratkowsky model should be able to describe the influence of temperature on  $\mu_{\text{max}}$  using the same values of  $T_{\text{min}}$  and  $T_{\text{max}}$ , and that a constant ratio exists between the two parameters of the Ratkowsky model applied to  $u_{\text{rad}}$  ( $a_1$  and  $a_2$ ) and the two parameters applied to  $\mu_{\text{max}}$  ( $c_1$  and  $c_2$ ; see equation (6)).

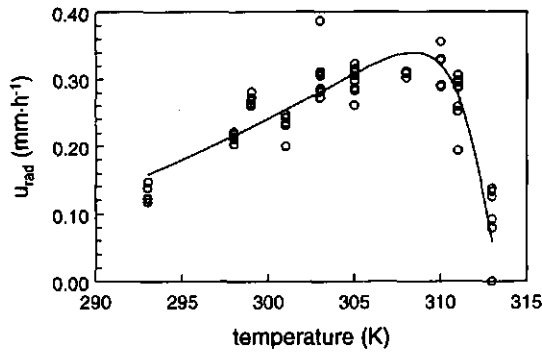


**Figure 1:** Ratkowsky fit (solid line) through the results of the  $u_{rad}$  measurements (O).

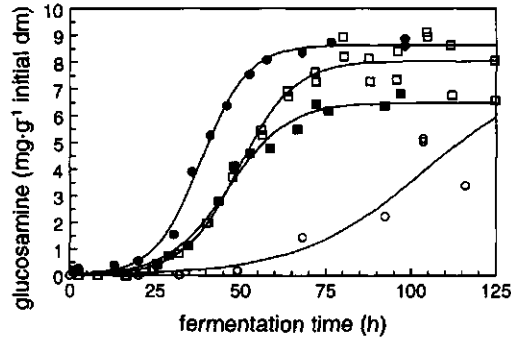


**Figure 2:** Glucosamine as function of time at 4 different temperatures: 293 (O), 299 (□), 305 (●) and 311 K (■). The solid lines represent the logistic curves (equation (2)) at each temperature.

$$\frac{a_1}{c_1} = \frac{a_2}{c_2} \quad (6)$$

For the purpose of describing the correlation between temperature and  $\mu_{\max}$  the model of Ratkowsky (equation (1)) appears to be applicable. The ratios between the Ratkowsky model parameters applied to  $\mu_{\max}$  and applied to  $G_{\max}$  (see Table 1) do not differ significantly, which supports the approach of Trinci (see equation (7)). The curve of the Ratkowsky model applied on the  $\mu_{\max}$  data is shown in Figure 3. Highest value of  $\mu_{\max}$  appears to be  $0.154 \text{ h}^{-1}$  at approximately 307 K.

$$\frac{a_1}{c_1} = 1.42 \pm 0.27 \quad (7)$$

$$\frac{a_2}{c_2} = 1.19 \pm 0.35$$

The course of  $G_{\max}$  against  $T$  is more horizontal than the course of  $\mu_{\max}$  against  $T$ . For describing this correlation, the Ratkowsky model had to be modified by making  $T_{\min}$  variable (equation (8)).

$$G_{\max}(T) = (b_1 \cdot (T - b_2) \cdot (1 - \exp(b_3 \cdot (T - T_{\max}))))^2 \quad (8)$$

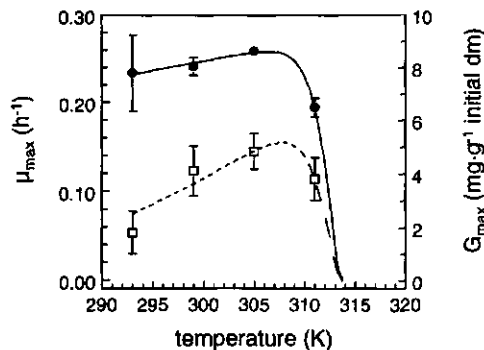


**Figure 3:** Correlation between the growth parameters  $\mu_{\max}$  ( $\square$ ) and  $G_{\max}$  ( $\bullet$ ), and temperature. The Ratkowsky fit, equation (1) (---), and the modified Ratkowsky fit, equation (8) (—), are shown. Error bars indicate the 95 % reliability limits of the individual data as were calculated by fitting the logistic equations through the glucosamine results presented in Figure 2.

With equation (8) it is possible to give a better description of the correlation between  $G_{\max}$  and  $T$  (Figure 3). The values of the coefficients resulting from the fit of equation (8) are given in Table 1. The statistical significance of coefficient  $b_2$  appeared to be low. Omitance of it in equation (8) simplifies the relationship without affecting the correlation coefficient ( $r^2$ ) which remains 0.999. Highest value of  $G_{\max}$  was found at approximately 307 K and appeared to be 8.7 mg per g initial dry matter.

Mukhopadhyay and Malik (15) describe an almost horizontal course of the maximum amount of biomass of *Trichoderma reesei* QM9414 against temperature. Although the temperature of their experiments, done in liquid cultures, did not exceed 307 K, our results are not in contradiction with these results.

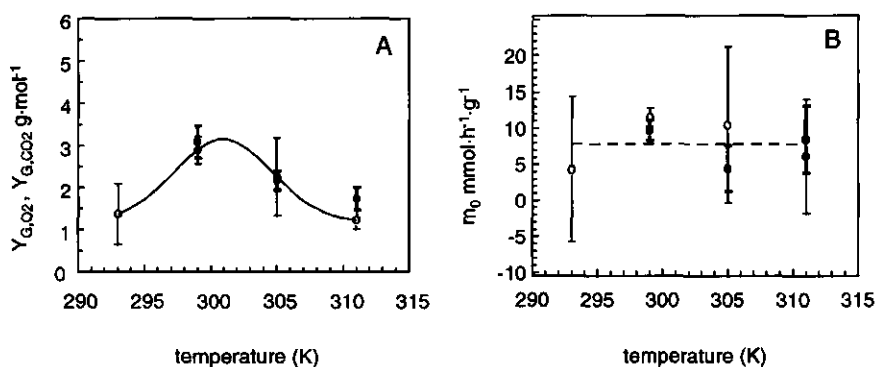


**Figure 4:** Correlation between the yield factors  $Y_{G,CO_2}$  (○, thin error bars) and  $Y_{G,CO_2}$  (●, thick error bars) in g glucosamine per  $\mu\text{mol}^{-1} \text{O}_2$  and  $\text{CO}_2$ , respectively (A), and the maintenance coefficients  $m_0$  (B) with temperature. The solid line in (A) represents the Gaussian curve. The dashed line in (B) represents the mean value for  $m_0$  of 7.848 mmol per h per g glucosamine. Error bars indicate 95 % reliability limits of the individual data.

**Specific activity.** The influence of temperature on the glucosamine-based yield factors ( $Y_{G,CO_2}$  and  $Y_{G,CO_2}$ ) and maintenance coefficient are shown in Figure 4. The reliability of these parameters depends largely on the number of measurements within each determination. The values at 299 K are therefore more reliable than those at 293, 305 or 311 K.

The courses of  $Y_{G,CO_2}$  and  $Y_{G,CO_2}$  can be described with a Gaussian curve (see Table 1 for description of  $Y_{G,CO_2}$ ). Highest values are found around 300 K. The spread in the determination of the maintenance coefficient,  $m_0$ , statistically allows it to be approached as a constant. The value of  $m_0$  is determined to be 7.85  $\mu\text{mol}$  per h per g glucosamine for  $\text{O}_2$  consumption as well as for  $\text{CO}_2$  production. Equal values were expected since the utilization of carbohydrates, with an elemental composition of approximately  $\text{C}_6\text{H}_{12}\text{O}_6$ , under non-growth circumstances is

expected to result in a respiration quotient ( $RQ = CPR/OCR$ ) of approximately 1.

The temperature dependence of the yield factor and the maintenance coefficient of *Aspergillus niger* growing on beet pulp has been described by Szweczyk and Myszka (2). Contrary to our findings, they report a constant value for the yield factor and a non-linear relation between maintenance coefficient and temperature. They base their findings solely on measurements of  $CO_2$  production and on the theoretical description of microbial growth with a logistic curve, and did not measure any other biomass-related parameter.

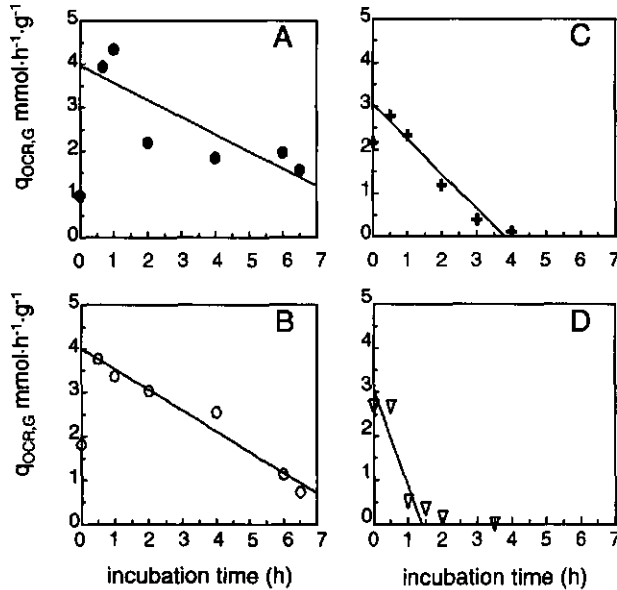


Figure 5: Decrease of  $q_{OCR,G}$  at four different temperatures: 313 (A), 318 (B), 323 (C) and 328 K (D). The solid lines represent equation (4) at each temperature.

**Decline of specific activity.** The decline of  $q_{OCR,G}$  as a function of time, determined at four temperatures below  $T_{max}$ , using data points at which  $\mu(t) < \mu_{max}/100$  is described with equation (4). The four obtained values of  $m_d$  lie within the 95 % reliability range of  $(0.256 \pm 0.204)$  mol per kg glucosamine per h<sup>2</sup>.

The decline rate in  $q_{OCR,G}$  measured during incubations at temperatures above  $T_{max}$  increases with increasing  $T$ . The course of  $q_{OCR,G}$  as a function of incubation time at four temperatures above  $T_{max}$  is shown in Figure 5.

For convenience sake, the results of  $m_d$  found below and above  $T_{max}$  are combined and described by the Arrhenius-type equation (5), although one should be aware that different mechanisms, such as substrate limitation and inactivation due to denaturation of proteins, might be responsible for the decline in specific activity above and below  $T_{max}$ . The course of  $m_d$

as a function of  $T$  is shown in Figure 6, and the values of the parameters are given in Table 1. Coefficient  $k_{md}$  significantly determines the course of the curve above  $T_{max}$ . The value of  $k_{md}$  depends strongly on the value of other coefficients. The large spread in  $k_{md}$  is therefore a cumulative result of the spread in the other coefficients. This is demonstrated by fitting equation (5) with the values of  $m_{d,0}$  and  $E_a$  fixed at 0.224 mmol per h<sup>2</sup> per g and  $3.27 \cdot 10^5$  J per mol, respectively. The so obtained standard deviation of  $k_{md}$  amounts only 0.0006 mmol per h<sup>2</sup> per g.

The results indicate the high sensitivity of the fungus to high temperatures. About 10 K above  $T_{max}$  the decline in specific activity will result in inactivation of the microorganism within a couple of hours, emphasizing the importance of temperature control during large-scale solid-state fermentation.

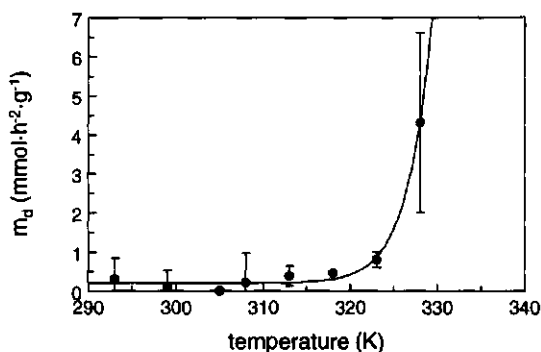


**Figure 6:** Correlation between temperature and specific-activity decline rate ( $m_d$ ) for oxygen consumption, expressed in mmol O<sub>2</sub> per h<sup>2</sup> per g initial dry matter weight. The calculated data (●) and equation (6) (solid line) are shown. Error bars indicate the 95% reliability limits of the individual data.

**Correlation between CO<sub>2</sub> production and dry matter weight loss.** The correlation between CO<sub>2</sub> production and dry matter weight loss at 299, 305 and 311 K is shown in Figure 7. The yield of CO<sub>2</sub> at 299 K has been previously shown to balance the loss of dry matter substrate (4). Theoretically, a weight loss of 1 kg dry matter can yield a maximum amount of ca. 40 mol CO<sub>2</sub> (the molecular weight on C-mol base of wheat bran is ca. 25 g per C-mol wheat bran (4)). CO<sub>2</sub> production at the three temperatures, being 31.1 (at 299 K), 35.2 (at 305 K) and 26.3 (at 311 K) mol CO<sub>2</sub> per kg dry matter weight loss respectively, is less than the theoretical maximum. During fermentation approximately 20 % of the initial dry matter weight is consumed (4), making these fluctuations represent less than 4.5 % of the total amount (C-mol) of substrate available. If the relationship between CO<sub>2</sub> production and dry matter weight loss is used in calculations that are based on amount of initial dry matter weight, these fluctuations

can be neglected and the correlation between dry matter weight loss and CO<sub>2</sub> production can be approached as being independent of temperature. The mean relationship can so be described by equation (9):

$$\Delta\text{CO}_2 = -30.66 \cdot \Delta\text{DM} \quad (9)$$

in which  $\Delta\text{CO}_2$  is the amount of CO<sub>2</sub> produced (mmol per g initial dry matter), and  $\Delta\text{DM}$  is the amount of weight loss (g per g initial dry matter). The standard deviation of the coefficient in equation (9) amounted 0.81 mmol CO<sub>2</sub> per g dry matter weight loss, and the correlation coefficient ( $r^2$ ) is 0.888.

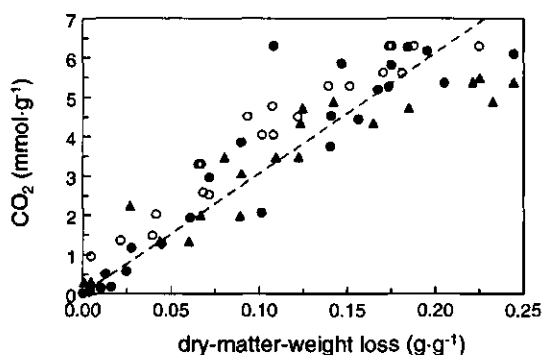


**Figure 7:** Correlation between CO<sub>2</sub> production (in mmol CO<sub>2</sub> per g initial dry matter) and dry matter weight loss (in g dry matter per g initial dry matter) at 299 (●), 305 (○) and 311 K (▲). The dashed line represents the correlation, given by equation (9).

**Effect of temperature on enzyme production.** As has been demonstrated before (4), the correlation of CMC-ase activity with glucosamine production during SSF at 299 K is not linear throughout the whole period of fermentation. These findings are confirmed by the results of the fermentations done at 305 and 311 K (Figure 8). The time at which a maximum specific-activity level is reached depends on the temperature of fermentation. Also the level of the maximum specific-activity depends on temperature. The negative values of specific CMC-ase activity, as shown in Figure 8, are caused by corrections with blanks during the period of the fermentation at which CMC-ase activity is low (2). These negative values are fortified by the division of it with low glucosamine values of the same period of fermentation.

A significantly lower specific activity is found at 311 K. Suh *et al.* (16) and Merivuori *et al.* (17) have demonstrated that *Trichoderma reesei* QM6A and QM9414 produce less cellulases at elevated temperatures in liquid cultures. Our results also confirm earlier findings that a clear constant relation between glucosamine and CMC-ase activity is absent (4), but also support



the notion that the physiology of the fungus changes with temperature.

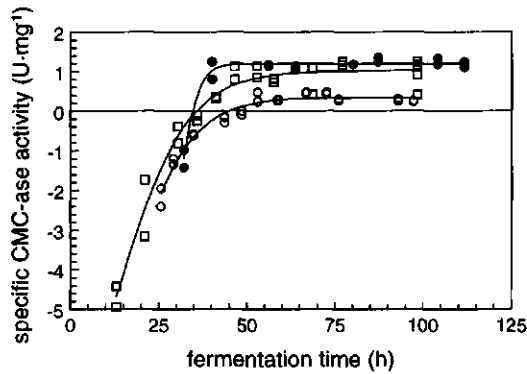


**Figure 8:** Specific activity of CMC-ase, expressed as U per mg glucosamine, at 299 (●), 305 (□) and 311 K (○). Solid lines, obtained by curve fitting using the method of least squares, indicate the differences in the course of enzyme activity in time at different temperatures. 1 U releases 1  $\mu\text{mol}$  glucose per minute from CMC.

## Conclusions

Temperature influences the kinetic parameters of *Trichoderma reesei* QM9414 in solid-state fermentation of wheat bran. The influence on growth of the fungus comes to expression in the temperature dependence of maximum specific-growth rate,  $\mu_{\max}$  and maximum glucosamine level,  $G_{\max}$ . Maximum temperature for growth can be determined by measuring the radial growth rates at different temperatures and can be described using Ratkowsky's equation.

Maximum temperature for growth,  $T_{\max}$  was 314 K.

Temperature also influences fungal respiration activity. Yield of glucosamine on  $\text{O}_2$  and  $\text{CO}_2$ ,  $Y_{\text{G},\text{O}_2}$  and  $Y_{\text{G},\text{CO}_2}$ , respectively, change by a factor of 2 when the temperature increases from 293 K to  $T_{\max}$ . No significant temperature dependence of the maintenance coefficient  $m_0$  is determined. The specific activity declines during growth of the microorganism at temperatures below  $T_{\max}$ . This decline becomes exponential when temperature increases above  $T_{\max}$ .

The physiology of *Trichoderma reesei* also changes with temperature. This is indicated by the change in specific CMC-ase activity with temperature.

The equations describing the correlation between temperature and the process variables will be used in the next step of our research, the development of a model describing the temperature evolution in a solid-state fermentation bed.

# Chapter 5

---

## Modelling of Solid-State Fermentation

To be published as

Smits, J.P., Geelhoed, W.S., Peeters, M.P.J., Van Sonsbeek, H.M., Rinzema, A., Tramper, J.,  
Knol, W.

Modelling fungal solid-state fermentation: the role of inactivation kinetics.

## Summary

The theoretical mathematical models described in this chapter are used to evaluate the effects of fungal biomass inactivation kinetics on a non-isothermal tray solid-state fermentation (SSF). The inactivation kinetics, derived from previously reported experiments done under isothermal conditions and using glucosamine content to represent the amount of biomass, are described in different ways leading to four models. The model predictions show only significant effects of inactivation kinetics on temperature and biomass patterns in the tray SSF after long fermentation periods.

The models in which inactivation is triggered by low specific-growth rates can predict restricted biomass evolution in combination with a fast temperature increase followed by a slower temperature decrease. Such inactivation might occur when substrate is limiting or products are formed in toxic concentrations.

Temperature is predicted to be the key parameter. Oxygen concentration is predicted to become limiting only at high heat conduction and low oxygen diffusion rates.

Desiccation of the substrate is predicted not to occur.

## Introduction

Solid-state fermentations (SSF) are applied for the production of, for example, enzymes, biopesticides, food, feed and fine chemicals. In SSF, microorganisms grow on a moist solid substrate without free-flowing water. The chemical reactions necessary for growth are exothermic and thus temperature control is necessary. It depends strongly on the type of fermenter system used (tray, packed bed, rotating drum) what the effect of heat production is on temperature in the fermenter bed and thus on the results of the fermentation. A typical temperature course during fermentation in a tray system shows a steep increase to 40 - 45 °C after a short lag phase, followed by a decline at a rate of 0.1 (1) to 0.5 °C (2) per hour, depending on the microorganism and type and size of system used.

Simulation models can provide insight into the complex interaction between microbial growth, oxygen consumption and concomitant heat production, and oxygen and heat transport. Ideally, these models should take into account the effects of growth, maintenance and decay on respiration activity, each as functions of, for instance, time, temperature, nutrient and water availability.

Several examples of models for fungal SSF processes can be found in the literature, describing different fermentation systems (3, 4, 5, 6, 7, 8). These reports focus on the biomass production phase of the fermentation and do not properly consider the period after growth has virtually stopped. Especially for secondary metabolites, the latter period may be very important. Besides, in most SSF systems fungal biomass is present growing at different rates, depending on combined effects of several parameters, such as temperature, water activity, and oxygen and carbon dioxide concentration. Thus, all biomass is not necessarily in the same growth phase. This emphasizes the need for

gradual decline in respiration activity is shown after the increase in glucosamine has stopped (9). Using results from isothermal incubation experiments, this inactivation was related to temperature by an Arrhenius-type equation and to time by zero-order kinetics (12).

The decline in respiration activity reduces the heat production rate, which is expected to have a strong effect on temperature patterns in SSF.

In this chapter, we describe the development of mathematical models for SSF in a tray system, using three different interpretations of the inactivation kinetics, previously reported for an isothermal SSF system with *Trichoderma reesei* on wheat bran (12). These interpretations represent likely responses of the fungus to the dynamic, non-isothermal conditions in larger-scale SSF, and are evaluated and discussed. A fourth model, which does not include inactivation, is used as a reference and to evaluate the importance of parameters that were not determined experimentally.

Since oxygen consumption and water production are incorporated in the models, the effects of biomass growth and activity on oxygen and water concentration could be predicted. These effects are also discussed.

### Model development

The tray system is chosen as the fermentation system because it is widely applied in SSF for production of enzymes, for example. The width of the tray is assumed to be infinite, allowing a one-dimensional mass and heat transfer approach in vertical direction (see Figure 1).

Substrate, water and air are assumed to be homogeneously divided in the tray. Heat and mass

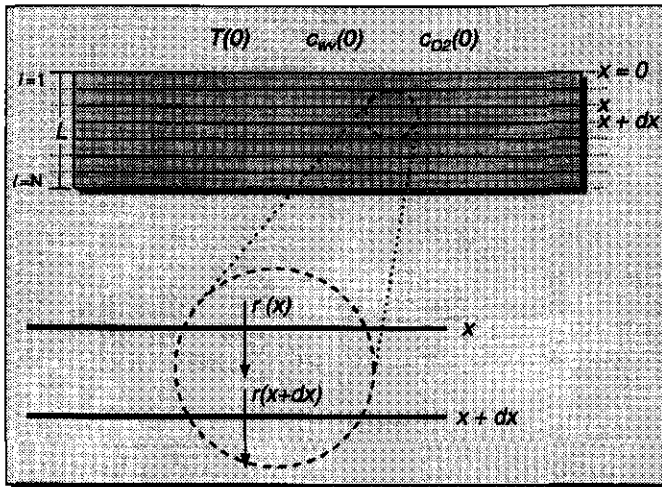


**Figure 1:** Schematic presentation of the tray fermentor used in model development.  $r$  is an undefined mass transport rate. The arrows show the direction of mass transfer at which  $r > 0$ . The other indices are explained in the text and in Table 1.

transfer resistance in the top of the bed are assumed to be absent. The models predict biomass glucosamine concentration, temperature, and oxygen, water and dry matter concentration in the tray.

The models described in this chapter start with calculating biomass glucosamine levels based on the logistic equation (see Appendix). The respiration activity is taken proportional to the amount of biomass glucosamine. The production rates of heat and water, and the consumption rate of dry matter are calculated from the respiration rates. Temperature is calculated from the water and enthalpy balances.

**Respiration activity.** Respiration activity is correlated to the amount of biomass glucosamine present, using the linear-growth model (see Appendix). An important issue in calculating respiration activity is the description of the decline in activity after the increase of glucosamine has stopped. This decline is described as a decline in specific activity by the zero-order equation (a7) given in the Appendix. The coefficients in this equation are obtained by respiration activity measurements of biomass at the end of the growth phase, i.e. for biomass with  $\mu(t) \leq \mu_{\max}/100$ . The argument  $\mu(t) \leq \mu_{\max}/100$  was an arbitrary choice (9, 12). Combination of equations (a1) and (a5) reveals that  $\mu(t) \leq \mu_{\max}/100$  when  $G(t) \geq 0.99 \cdot G_{\max}$ . This condition can occur at the end of the growth phase, but also when  $G_{\max}$  decreases as a result of increased temperature (12).

Equation (a7) was obtained from experiments under isothermal conditions. During large-scale SSF the temperature increases and decreases. For description of non-isothermal, dynamic systems three different interpretations can be given of equation (a7), resulting in three models:

- (i) the decline only occurs when  $\mu(t) \leq \mu_{\max}/100$  (temporary-decline model,  $M_{\text{temp}}$ ),
- (ii) the decline occurs once  $\mu(t) \leq \mu_{\max}/100$  (partial-decline model,  $M_{\text{part}}$ ), and
- (iii) the decline is always present (continuous-decline model,  $M_{\text{cont}}$ ).

Simulations obtained with these three models are compared with simulations in which the decline in specific activity is absent (model without decline,  $M_{\text{none}}$ ) to demonstrate the effect of including inactivation kinetics in the models.

The four kinetic models are incorporated in the fermenter model as follows.

**Temporary-activity model,  $M_{\text{temp}}$ :** For  $M_{\text{temp}}$  two moments in time have to be defined:  $t_d$ , the moment the decline starts, and  $t_r$ , the moment the decline stops. In  $M_{\text{temp}}$ , a decline in specific activity only occurs when  $\mu(t) \leq \mu_{\max}/100$ . This means that the decline starts at  $t_d$ , when  $\mu(t_d) = \mu_{\max}/100$ , and stops at  $t_r$  when  $\mu(t_r)$  becomes larger than  $\mu_{\max}/100$  again. The specific activity in  $M_{\text{temp}}$  is described by equations (1) as the replacement of equations (a4) and (a7).

$$\begin{aligned}
 \text{for } 0 \leq t < t_d : \quad q(t) &= \frac{1}{Y} \cdot \mu(t) + m_0 \\
 \text{for } t_d \leq t < t_r : \quad q(t) &= \frac{1}{Y} \cdot \mu(t) + m_0 - m_d \cdot (t - t_d) \\
 \text{for } t_r \leq t : \quad q(t) &= \frac{1}{Y} \cdot \mu(t) + m_0 - m_d \cdot (t_r - t_d)
 \end{aligned} \tag{1}$$

If growth has ceased (i.e.  $\mu = 0$ ),  $m_0 = 2.18 \times 10^{-3} \text{ mol} \cdot \text{s}^{-1} \cdot \text{kg}^{-1}$ , and  $m_d = 1.7 \times 10^{-6} \text{ mol} \cdot \text{s}^{-2} \cdot \text{kg}^{-1}$  (12),

complete inactivation, i.e.  $m_0 = m_d \cdot (t - t_d)$ , is reached when  $(t - t_d)$  is about 36 h.

**Partial-decline model,  $M_{\text{part}}$ :** In  $M_{\text{part}}$  the decline starts at  $t_d$  when  $\mu(t)$  becomes equal or smaller than  $\mu_{\text{max}}/100$ . After  $t_d$ , the decline remains present even if  $\mu(t)$  might become larger than  $\mu_{\text{max}}/100$  again. In this approach, equation (2) is used instead of equations (a4) and (a7):

$$\begin{aligned} \text{for } 0 \leq t < t_d: \quad q(t) &= \frac{1}{Y} \cdot \mu(t) + m_0 \\ \text{for } t_d \leq t: \quad q(t) &= \frac{1}{Y} \cdot \mu(t) + m_0 - m_d \cdot (t - t_d) \end{aligned} \quad (2)$$

If  $m_0 = 2.18 \times 10^{-3} \text{ mol} \cdot \text{s}^{-1} \cdot \text{kg}^{-1}$ , and  $m_d = 1.7 \times 10^{-8} \text{ mol} \cdot \text{s}^{-2} \cdot \text{kg}^{-1}$  (12), complete inactivation, i.e.  $m_0 = m_d \cdot (t - t_d)$ , is reached when  $(t - t_d)$  is about 36 h.

**Continuous-decline model,  $M_{\text{cont}}$ :** Decline of the specific activity in  $M_{\text{cont}}$  is always present and independent of  $\mu$ . The course of specific activity over time is described by equation (3), as the replacement of equations (a4) and (a7).

$$q(t) = \frac{1}{Y} \cdot \mu(t) + m_0 - m_d \cdot t \quad (3)$$

In this model, the decline starts from the beginning of the fermentation. This means that the value of  $m_0$  in  $M_{\text{cont}}$  has to be increased in relation to the value in  $M_{\text{temp}}$  and  $M_{\text{part}}$ , and the value of  $Y$  lowered. The value of  $m_0$  in  $M_{\text{cont}}$  is obtained by extrapolation, as is visualized in Figure 2 for 299 K. The value of  $Y$  is obtained by fitting equation (3) through the measured specific

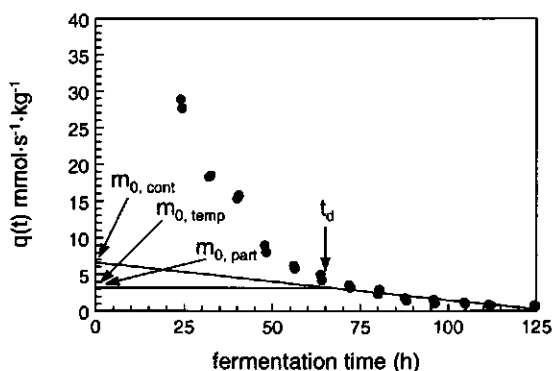


**Figure 2:** Specific activity over time at 299 K (●), showing the moment  $t_d$  at which  $\mu = \mu_{\text{max}}/100$ .  $m_0$  of the  $M_{\text{temp}}$  and the  $M_{\text{part}}$  model ( $m_{0,\text{temp}}$  and  $m_{0,\text{part}}$ , respectively) and  $m_0$  of the  $M_{\text{cont}}$  model ( $m_{0,\text{cont}}$ ) are shown. The declining solid line represents  $m_{0,\text{cont}} - m_d \cdot t$ .  $q(t)$  is given in mmol  $\text{O}_2$  per second per kg glucosamine.

activity data and is ca. 70% of that in  $M_{\text{temp}}$  and  $M_{\text{par}}$  (results not shown). With the value of  $m_0 = 7.19 \times 10^{-3} \text{ mol} \cdot \text{s}^{-1} \cdot \text{kg}^{-1}$  and an  $m_d$  at 299 K of about  $1.7 \times 10^{-8} \text{ mol} \cdot \text{s}^{-2} \cdot \text{kg}^{-1}$  (12), maintenance activity, i.e.  $m_0 - m_d \cdot t$ , is zero within ca. 118 h after  $t=0$ . At that time, complete inactivation is reached, regardless of the value of  $\mu$ .

**Model without decline,  $M_{\text{none}}$ :** The fourth model does not include a decline in specific activity. In this case equation (a7) is omitted, making equation (a4) valid for the whole fermentation period. In fact,  $M_{\text{none}}$  is the linear-growth model as described in the Appendix.

**Consumption and production rates:** The respiration rates, i.e. oxygen consumption rate ( $r_{\text{O}_2}$ ) and carbon dioxide production rate ( $r_{\text{CO}_2}$ ), are calculated by multiplying the specific activity  $q$  in mol  $\text{O}_2$  or  $\text{CO}_2$  per kg glucosamine per second, with  $G$ , being the amount of glucosamine present, expressed as kg glucosamine per kg initial dry matter, and  $c_{\text{dm}}(0)$  the initial amount of dry matter in kg per  $\text{m}^3$  fermenter :

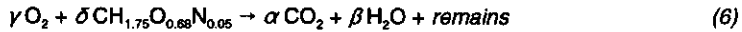
$$r = q \cdot G \cdot c_{\text{dm}}(0) \quad (4)$$

$r$  is either  $r_{\text{O}_2}$  or  $r_{\text{CO}_2}$  in mol per second per  $\text{m}^3$  fermenter. Dry matter consumption rate,  $r_{\text{dm}}$  in kg dry matter per second per  $\text{m}^3$  fermenter, results from the relationship between  $\text{CO}_2$  production and dry matter weight loss (9):

$$r_{\text{dm}} = -r_{\text{CO}_2} \cdot M_{\text{C-mol}} \quad (5)$$

$M_{\text{C-mol}}$  is the molecular weight of the substrate on a C-mol base (kg per C-mol substrate).

The amount of water produced from wheat bran is calculated as follows. The water production rate,  $r_w$  in kg water per second per  $\text{m}^3$  fermenter, is supposed to be related to  $\text{CO}_2$  production rate. Oxidation of wheat bran, which composition on a C-mol basis is  $\text{CH}_{1.75}\text{O}_{0.68}\text{N}_{0.05}$  (10), is supposed to occur according to equation (6).



In this equation, the term *remains* stands for products, not *per se* being biomass. The number of moles of water produced per mole  $\text{CO}_2$  varies during the course of fermentation. The ratio  $\beta/\alpha$  is therefore used as a variable, which value will be evaluated later. The water production rate,  $r_w$  in kg water per second per  $\text{m}^3$  fermenter, is accordingly described by equation (7).

$$r_w = r_{\text{CO}_2} \cdot M_{\text{H}_2\text{O}} \cdot \frac{\beta}{\alpha} \quad (7)$$

$M_{\text{H}_2\text{O}}$  is the molecular weight of water, which is 0.018 kg per mol water.

The production rate of heat,  $r_h$  in J per second per  $\text{m}^3$  fermenter, is assumed to be proportional to the oxygen consumption rate (13):

$$r_H = -460 \times 10^3 \cdot r_{O_2} \quad (8)$$

**Mass and enthalpy balances:** The water balance describes liquid water in the solid phase and water vapour in the gas phase. Each phase occupies about half of the fermenter volume. In the solid phase, which consists of moistened substrate, transport of water is assumed to be negligible compared to the diffusion of water vapour in the gas phase. In the models it is assumed that there is no difference in temperature and water activity between the gas and the solid phase.

**Water balance:** Under the circumstances outlined above, there are three processes of importance for the water balance. The first is the production of water by the microorganism. The second is evaporation of water, which is generally seen as most effective for cooling SSF (14). The third process is the diffusion of water vapour from high to low concentrations in the fermentation bed. The combination of these three processes leads to equation (9).

$$\frac{\partial c_w}{\partial t} = r_w - \left[ \frac{\partial c_{wv}}{\partial t} - D_{wv} \cdot \frac{\partial^2 c_{wv}}{\partial x^2} \right] \quad (9)$$

$\partial c_w / \partial t$  is the change in water concentration in kg water per m<sup>3</sup> fermenter per second. Rate  $r_w$  is already given in equation (7). The term  $\partial c_{wv} / \partial t$  represents the change in water vapour concentration due to changes in temperature and water and dry matter concentrations. The term  $\partial c_{wv} / \partial t$  is obtained by differentiation of equation (10).

$$c_{wv} = \epsilon \cdot a_w \cdot c_{sat} \quad (10)$$

In equation (10),  $c_{wv}$  is the concentration of water vapour (in kg water vapour per m<sup>3</sup> fermenter), which depends on the temperature-dependent concentration of water vapour in water-saturated air ( $c_{sat}$ ), water activity ( $a_w$ ), and  $\epsilon$ , the fraction of air in the fermenter bed. The concentration of water vapour in saturated air depends on temperature  $T$  and can be described by an Arrhenius-type equation (equation (11)).

$$c_{sat} = \exp \left[ 10.653 - \frac{4111}{T} \right] \quad (11)$$

Equation (11) was obtained by fitting the relationship between temperature and water concentration of saturated air, as obtained from a standard physics text book (15). As temperature is a function of time, equation (11) can be rewritten into:

$$\frac{\partial c_{sat}}{\partial t} = \frac{4111}{T^2} \cdot \exp \left[ 10.653 - \frac{4111}{T} \right] \cdot \frac{\partial T}{\partial t} \quad (12)$$

The  $a_w$  was determined at 298 K by measuring the relative humidity of the gas phase in equilibrium with wet wheat bran at different moisture contents, using the Novasina EEJA-6



(Novasina, Pfäffikon, Switzerland). Its correlation with the moisture content, expressed as  $c_w/c_{dm}$  in kg water per kg dry matter, is described by equation (13) and shown in Figure 3. It is assumed to be valid within the temperature range of the fermentation and not to be influenced by changes in dry matter composition during the fermentation.

$$a_w = 0.7254 + \frac{0.2670}{1 + \left[ \frac{1}{0.2395} \cdot \frac{c_w}{c_{dm}} \right]^{-2.2}} \quad (13)$$

If it is assumed that the fermenter bed does not shrink, the fraction of air in the fermenter,  $\epsilon$ , can be defined as:

$$\epsilon = 1 - \left[ \frac{c_{dm}}{\rho_{dm}} + \frac{c_w}{\rho_w} \right] \quad (14)$$

with  $\rho_{dm}$  and  $\rho_w$  being the densities of dry matter and water in kg dry matter per m<sup>3</sup> dry matter and kg water per m<sup>3</sup> water, respectively.

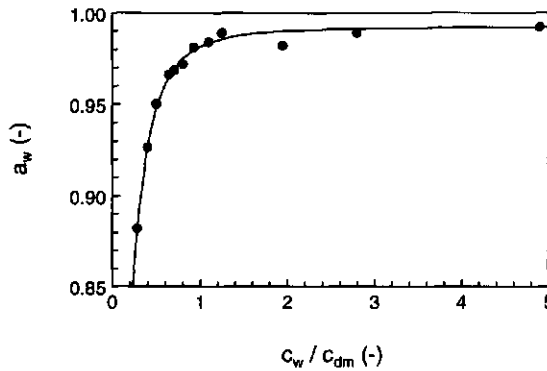


**Figure 3:** Relationship between water content of the solid phase ( $c_w/c_{dm}$ , kg water per kg dry matter) and water activity ( $a_w$ ). The experimental results (●) and the fit of equation (13) (solid line) are shown.

Now that all terms in equation (10) are known,  $\partial c_w / \partial t$  can be calculated.

The last term in equation (9), the second derivative of water-vapour concentration ( $\partial^2 c_w / \partial x^2$ ), is obtained numerically as will be explained later. To simplify the calculations, the fermenter bed is approached as a homogeneous (non-porous) system.  $c_{ww}$  is given in kg water vapour per m<sup>3</sup> fermenter bed, i.e. it is the product of the concentration in the gas phase of the fermenter bed and  $\epsilon$  (see equation (10)). The effective water vapour diffusion coefficient,  $D_{ww}^*$ , is given in m<sup>2</sup>

fermenter bed per second. For the present the effective diffusion coefficient is assumed not to change when changes in dry matter and water content in the fermenter bed occur.

**Enthalpy balance:** With the models described here we intend to evaluate the effects of different descriptions of inactivation of microbial activity on biomass and temperature patterns in a tray SSF. Temperature plays a key role in this evaluation and thus the transport of heat in the fermenter bed is crucial. Three processes of heat transport are important in a tray fermenter: conduction of heat, convection and diffusion of water vapour. In this theoretical evaluation heat transport is simulated as conduction of heat and diffusion of water vapour.

Variation in heat transport is accomplished by varying the heat-transfer coefficient,  $\lambda$ , and the water vapour diffusion coefficient,  $D_{wv}^*$ . The effects of variation in  $\lambda$  and  $D_{wv}^*$  on temperature and biomass patterns are thus assumed to cover the effects of free convection.

The system described in the enthalpy balance consists of the components dry matter, water present in the solid phase and water vapour. The dry air in the gas phase is assumed not to contribute significantly to the enthalpy in this system, and is neglected.

The enthalpy of the system,  $H$ , is the sum of the enthalpies of all components  $j$ :

$$H = \sum (c_j \cdot h_j) \quad (15)$$

In equation (15),  $c$  is the concentration and  $h$  is the molar enthalpy of component  $j$ . The latter is defined as

$$h_j = c_{p,j} \cdot (T - T_{ref,j}) + \Delta H_j \quad (16)$$

In equation (16),  $c_p$  is the specific heat of component  $j$  at constant pressure in J per kg per K, and  $T_{ref}$  is the temperature for which  $c_p$  and  $\Delta H$ , the enthalpy of phase transition (J per kg), are given.

Considering the components dry matter, water in the solid phase and water vapour, the change of enthalpy,  $\partial H / \partial t$  in J per second per  $m^3$  fermenter, can be described by equation (17).

$$\begin{aligned} \frac{\partial H}{\partial t} = & c_{p,dm} \cdot c_{dm} \cdot \frac{\partial T}{\partial t} + c_{p,dm} \cdot (T - T_{ref,dm}) \cdot \frac{\partial c_{dm}}{\partial t} \\ & + c_{p,w} \cdot c_w \cdot \frac{\partial T}{\partial t} + c_{p,w} \cdot (T - T_{ref,w}) \cdot \frac{\partial c_w}{\partial t} \\ & + c_{p,wv} \cdot c_{wv} \cdot \frac{\partial T}{\partial t} + c_{p,wv} \cdot (T - T_{ref,wv}) \cdot \frac{\partial c_{wv}}{\partial t} + \Delta H_w \cdot \frac{\partial c_{wv}}{\partial t} \end{aligned} \quad (17)$$

In equation (17),  $c_{p,dm}$ ,  $c_{p,w}$  and  $c_{p,wv}$  are the specific heat of dry matter, water and water vapour, respectively, in J per kg per K. Values of  $c_{dm}$ ,  $c_w$  and  $c_{wv}$  are expressed in kg per  $m^3$  fermenter.

accumulation rate values multiplied with the time step,  $dt$ , to the original value.

Simulations started with wetted wheat bran of 53% w/w moisture content at 298 K. In the fermenter bed initially 48% of the volume is occupied by the wet substrate.

The tray is supposed to be placed in an environment with a constant relative humidity corresponding to an initial  $a_w$  of 0.98 of the substrate. The initial water-vapour concentration resulted from equation (10) and amounts to 42.3 g per  $m^3$  air. The bed height was  $2L = 0.20$  m, of which  $L$  was divided into 20 steps.

To evaluate biomass growth patterns under different situations regarding heat dissipation,  $\lambda$  was varied between the values that represent the situation in which water is absent and the situation in which dry matter is absent. Thus, glucosamine contents at different depths in the fermentation bed were calculated using arbitrary values of  $\lambda$  between the approximated heat conduction coefficients of wood, as a comparable substance, and that of water (0.15 and 0.60  $J \cdot m^{-1} \cdot s^{-1} \cdot K^{-1}$ , respectively). The values of  $\lambda$  were assumed to remain constant during the fermentations. Heat transfer by convection, as explained before, was not included in the models, but its effect on the fermentation is assumed to be evaluated by variation of  $\lambda$ .

## Results and discussion

The simulation results obtained with the models are presented in three steps. First, the sensitivity of the models to variation in estimated values of parameters is evaluated. Then the results of the models without and with activity decline are described and discussed. Finally, the roles of oxygen, carbon dioxide and water concentration are discussed.

**Sensitivity analysis:** In the evaluation of the effect of temperature on SSF, four parameter values are estimated. These are  $c_{p, dm}$ ,  $D_{wv}^*$ ,  $B/\alpha$  and  $\lambda$ . The influence of variation in values of the first three parameters is evaluated on the basis of the temperature predicted. For this evaluation model  $M_{none}$  is used as a worst-case situation.

The importance of  $\lambda$  turned out to be larger than the first three parameters. The value of  $\lambda$  is measurable but may change significantly during fermentation as a result of changes in substrate composition and an increase in biomass. The influence of variation in  $\lambda$  on the simulations is evaluated for each of the four models with the help of temperature and of biomass glucosamine evolution. Results are discussed in detail below. Values of all other parameters are given in Table 1.

The value of the specific heat of wheat bran dry matter ( $c_{p, dm}$ ) is varied between 1500 and 3500  $J \cdot kg^{-1} \cdot K^{-1}$ , based on values for wood found in literature (15). The temperatures predicted with either of these values differed 2.2 K at most. This deviation was predicted at 32 h fermentation time in the 0.10 m layer of the fermentation bed. The results of simulations of the layers at 0.025, 0.05 and 0.10 m depth with  $c_{p, dm}=1500$  and  $c_{p, dm}=3500$  J per kg per K are shown in Figure 5. It can be concluded that variation in the value of  $c_{p, dm}$  between 1500 and 3500  $J \cdot kg^{-1} \cdot K^{-1}$  is of negligible importance for the simulation results.

The concentration of water vapour in the fermentation bed is adjusted to a value corresponding to the initial value of  $a_w$  of the substrate. Water vapour diffusion is therefore only expected to happen as a result of temperature changes. Water vapour diffusion affects temperature in two ways, by the contribution of water vapour in the overall enthalpy flux, and by the transition

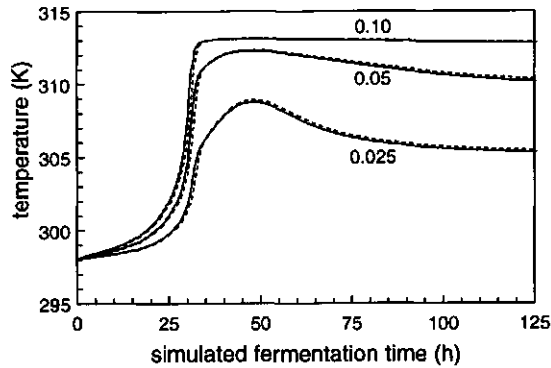


**Figure 5:** Effect of  $c_{p, dm}$  on temperature course predicted by the  $M_{none}$  model. Values of  $c_{p, dm}$  used for evaluation were 3500 (---) and 1500 (—)  $J \cdot kg^{-1} \cdot K^{-1}$ . The temperature courses in the layers at 0.025, 0.05 and 0.10 m are shown.

enthalpy of water that evaporates. Both effects are expected to be small because the water vapour pressure remains low in the temperature range relevant for *Trichoderma reesei* QM9414. Simulations with model  $M_{none}$  confirm these expectations. Largest temperature differences between simulations with  $D_{ww}^* = 5.2 \times 10^{-6}$  and  $D_{ww}^* = 5.2 \times 10^{-8} m^2$  per second were found after 32 h fermentation time at 0.10 m depth in the fermentation bed, and amounted to only 0.3 K (results not shown). The influence of  $D_{ww}^*$  on temperature can be neglected. Therefore, our assumption that the fermenter bed is homogeneous and non-porous is of minor importance.

As described by equation (7), the amount of water produced by the microorganism is related to the amount of carbon dioxide produced. The ratio between both, defined by  $\beta/\alpha$ , is expected to vary during a fermentation. Therefore, values of  $\beta/\alpha$  of 0.5 and 1.0 were evaluated. The effect of this variation is low. A maximum temperature difference was predicted at 0.10 m depth after 32 h of fermentation, and amounted to only 0.9 K (results not shown). In these simulations, the water content was predicted to increase from 0.53 to 0.67 and 0.68 kg water per kg wet substrate for  $\beta/\alpha$  being 0.5 and 1.0, respectively. From this minor influence it can be concluded that the change in water content in the simulations is the result of a decrease in dry matter content rather than water production or evaporation.

**Decline in specific activity:** The four models,  $M_{none}$ ,  $M_{temp}$ ,  $M_{perf}$  and  $M_{cont}$ , are used to predict biomass glucosamine evolution and temperature during a fermentation lasting 400 h. The results of these predictions will be discussed below for each model separately. Figure 6 shows the glucosamine and temperature evolution. Figure 7 shows the influence of  $\lambda$  on glucosamine

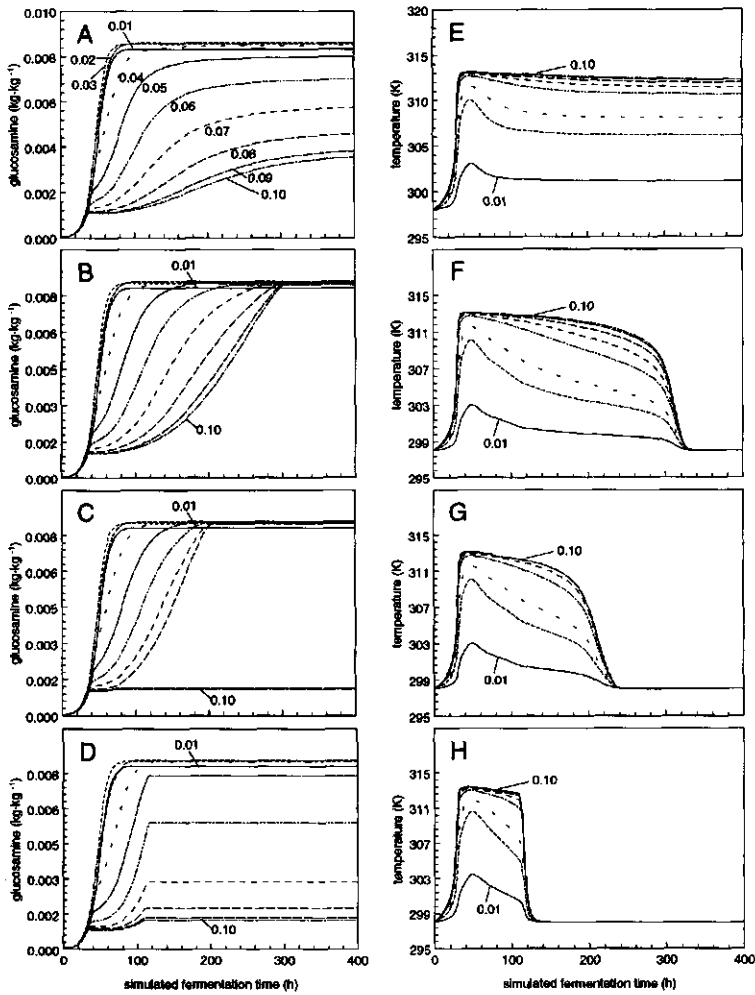


**Figure 6:** Evolution of biomass glucosamine (A-D) and corresponding temperature (E-H) in different layers of the fermentation bed as simulated with the values of  $\lambda$ ,  $c_{p, dm}$  and  $D_{ww}^*$  being  $0.45 \text{ J} \cdot \text{mol}^{-1} \cdot \text{s}^{-1} \cdot \text{K}^{-1}$ ,  $2720 \text{ J} \cdot \text{kg}^{-1} \cdot \text{K}^{-1}$  and  $1.5 \cdot 10^{-6} \text{ m}^2 \cdot \text{s}^{-1}$ , respectively. Results of the models  $M_{\text{none}}$  (A and E),  $M_{\text{temp}}$  (B and F),  $M_{\text{part}}$  (C and G) and  $M_{\text{cont}}$  (D and H) are shown. The type of lines in graph A for the layers of 0.01 to 0.10 m are accordingly used in the graphs B to H. Glucosamine concentration is given in kg glucosamine per kg initial dry matter.

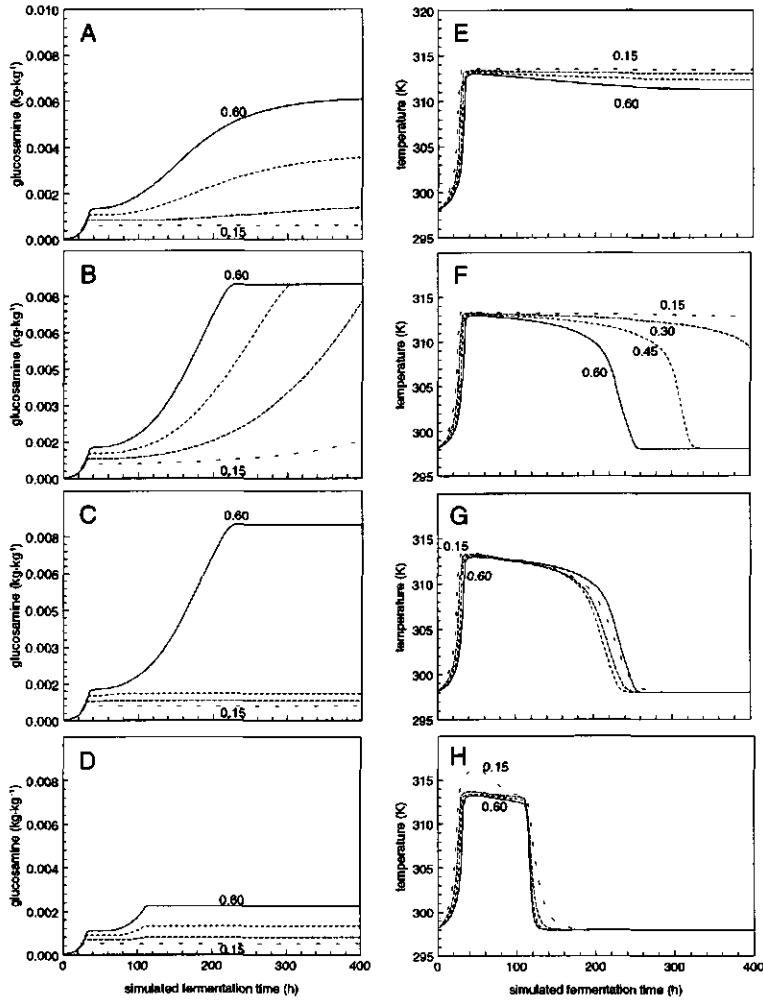


**Figure 7:** Biomass glucosamine (A-D) and corresponding temperature (E-H) patterns during 400 h of simulated fermentation at 10 cm bed depth predicted by the models  $M_{\text{none}}$  (A and E),  $M_{\text{temp}}$  (B and F),  $M_{\text{part}}$  (C and G) and  $M_{\text{corr}}$  (D and H). Values of the effective heat transfer coefficient,  $\lambda$ , used are 0.60 (—), 0.45 (---), 0.30 (— · —) and 0.15 J·m<sup>-1</sup>·s<sup>-1</sup>·K<sup>-1</sup> (····). Glucosamine concentration is given in kg glucosamine per kg initial dry matter.

and temperature in the centre of the fermentation bed (at 0.10 m depth).

**Model without decline,  $M_{none}$ :** The first results presented are those of the model without decline in maintenance activity,  $M_{none}$ . This model has been used by several groups (3, 5, 8) in modelling SSF. It predicts biomass glucosamine and temperature patterns as given in Figure 6A and 6E, respectively.

The temperature is predicted to increase during the first 50 h of the fermentation (Figure 6E), and remains elevated during the rest of the fermentation period. The typical temperature course of an SSF, i.e. an increase followed by a slow decrease, cannot be predicted by the  $M_{none}$  model.

Biomass glucosamine, predicted by  $M_{none}$ , reaches the maximum attainable glucosamine level of ca. 8.6 g per kg initial dry matter (Figure 6A) only in the outer 4 cm of the bed. The increase in glucosamine in the inner 6 cm is suppressed by the elevated temperatures. The glucosamine patterns predicted by  $M_{none}$  resemble experimental observations since fungal growth is hindered in the inner layers of an SSF tray (17, 18, 19). This is probably the reason why such models were assumed to be valid.

The effect of increased heat transfer is visible in the Figures 7A and 7E. The maximum temperature during a fermentation is predicted to remain below the maximum temperature for growth of the fungus,  $T_{max}$ , unless  $\lambda$  is chosen to be lower than  $0.05 \text{ J}\cdot\text{s}^{-1}\cdot\text{m}^{-1}\cdot\text{K}^{-1}$  (results not shown). In that case a temperature of 320 K is reached.

Increase of heat transfer resulted in locally lower temperatures only if the maximum attainable glucosamine level was reached (results not shown). If not, temperature remained close to maximal (see Figure 7E).

Due to the increased heat transport, the number of layers in which the maximum attainable glucosamine level is reached increases. At sufficiently high heat transport, the maximum attainable glucosamine level is predicted to be found in all layers of the bed within a fermentation period less than 400 h (results not shown). This, however, could not be simulated with the values of  $\lambda$  up to  $0.60 \text{ J}\cdot\text{m}^{-1}\cdot\text{s}^{-1}\cdot\text{K}^{-1}$ .

**Model with temporary decline,  $M_{temp}$ :** A temporary decline in specific activity, constant in time, might be expected when circumstances are temporarily unfavourable. For instance, a temporarily high temperature or low oxygen concentration might result in irreversible inactivation as long as these circumstances occur. Once favourable circumstances are re-established, the inactivation process stops in this model.

The  $M_{temp}$  model predicts a slow decline in temperature in the period after the maximum temperature is reached (Figure 6F). This decline accelerates when the number of layers that reach the maximum attainable glucosamine level increases and proceeds until activity is zero (Figure 6B). The temperature decline rates are initially much smaller than rates reported in the literature (1, 2), but finally are of the same order of magnitude.

All layers in the fermenter bed are predicted to finally reach the maximum attainable glucosamine level. The deepest layer reaches this level some 300 h after the start of fermentation (Figure 6B).

The effect of increased heat removal on biomass glucosamine and temperature (See Figure 7B and 7F) is similar to that in the  $M_{none}$  model. As long as the glucosamine level is below the maximum attainable level, the temperature remains close to maximal. The maximum attainable

glucosamine level is reached earlier (and in more layers) when heat transfer is increased.

**Model with partial decline,  $M_{\text{part}}$ :** If a substrate component becomes exhausted or when a product concentration becomes toxic, inactivation of the non-growing biomass is expected to occur according to the  $M_{\text{part}}$  model. Once the inactivation starts it continues constant in time, until biomass is completely inactivated.

The difference between the predictions in the  $M_{\text{temp}}$  model and those in the  $M_{\text{part}}$  model are shown in the temperature patterns (Figure 6F and 6G). In the  $M_{\text{part}}$  model, biomass is inactivated in the deepest layers within 80 h of simulated fermentation time (see Figure 6C) and does not contribute any more to heat production. Therefore, the temperature decrease occurs earlier than in the  $M_{\text{temp}}$  model.

The biomass glucosamine can reach its maximum attainable level only in the outer layers. The difference between these outer layers and the layers in which biomass is completely inactivated is a sharp border (results not shown).

Increase of heat transfer is predicted to have a small effect on the temperature course (Figure 7G), but a large effect on the biomass (Figure 7C). The border of overgrown substrate moves towards the core of the fermentation bed. At a  $\lambda$  of  $0.6 \text{ J}\cdot\text{m}^{-1}\cdot\text{s}^{-1}\cdot\text{K}^{-1}$  the most inner layer of the fermentation bed is predicted to be overgrown in 225 h.

**Model with continuous decline,  $M_{\text{cont}}$ :** The results obtained during experiments under isothermal conditions do not really allow us to define when inactivation starts. Therefore, the moment inactivation starts, i.e. at  $\mu=0.01\cdot\mu_{\text{max}}$  was arbitrarily chosen. If, for instance, ageing of the biomass plays a role in inactivation, a decline of specific activity might occur during the whole fermentation independent of  $\mu$ . This is simulated by the  $M_{\text{cont}}$  model. The decline starts as soon as the fungus starts to grow.

The total amount of measurable activity depends on the combined result of biomass growth, maintenance and inactivation. Within the temperature range predicted, the decline coefficient ( $m_d$ ) is less temperature-sensitive than  $\mu_{\text{max}}$  (12). Therefore, a situation might occur in which  $m_d\cdot m_b\cdot t$  becomes zero, and thus complete inactivation occurs, while temperature allows  $\mu_{\text{max}}$  to be relatively high. This phenomenon results in an abrupt stop of biomass growth as is visible after a little more than 100 h in the layers halfway the middle of the fermentation bed (see Figure 6D).

Temperature increases only during a restricted period (Figure 6H). The length of this period is almost independent of heat transfer (Figure 7H). An increase in heat transfer only affects the level of glucosamine reached within this period (Figure 7D).

Figure 7H also shows that temperatures rise above  $T_{\text{max}}$  when  $\lambda$  is  $0.15 \text{ J}\cdot\text{m}^{-1}\cdot\text{s}^{-1}\cdot\text{K}^{-1}$  or lower.  $T_{\text{max}}$  is predicted to be exceeded by the other models, which have a lower value of  $m_d$ , when  $\lambda$  was smaller than  $0.05 \text{ J}\cdot\text{m}^{-1}\cdot\text{s}^{-1}\cdot\text{K}^{-1}$ . An increase of temperature above  $T_{\text{max}}$  must be assigned to maintenance activity, since growth stops above  $T_{\text{max}}$ .

Inhibition of growth and activity of biomass in the inner layers of the substrate bed is a feature of a tray SSF generally recognized (17, 18, 19, 20, 21). However, most practical observations are done between 50 and 100 h, i.e. 4 - 8 times shorter than used for predictions in this study. Restricted overgrowth of the substrate is predicted in this study by all four models during the first 100 h of fermentation. In this period, inclusion of inactivation kinetics does not contradict



the results of measurements and simulations done by the other groups. The importance of inactivation kinetics lies in longer-lasting fermentation periods.

The models  $M_{\text{none}}$  and  $M_{\text{cont}}$  still predict incomplete overgrowth after 400 h. These two models have other features which are less realistic. The first model misses the description of decline in activity which is obviously present (12) and predicts everlasting heat production. The  $M_{\text{cont}}$  model represents inactivation of the biomass dependent only on time. This would suggest that, under normal circumstances, biomass has only a restricted period of activity and growth after spore germination, independent of the availability of substrate.

Both the  $M_{\text{part}}$  and the  $M_{\text{temp}}$  model predict complete overgrowth of the substrate during a 400 h fermentation, but this holds for the  $M_{\text{part}}$  model only when heat transfer is sufficient. Incomplete overgrowth is predicted by the  $M_{\text{part}}$  model in combination with a decline of temperature at the end of fermentation. In this respect it differs from the  $M_{\text{none}}$  model which does not predict the temperature decline.

It cannot be concluded whether  $M_{\text{part}}$  or  $M_{\text{temp}}$  approaches *in vivo* inactivation in SSF best. In practice, other phenomena, such as sporulation and activity of hydrolysing enzymes, may start to play an important role in long fermentation periods, making it hard to correlate fermentation results to one of these two models.

The description of decline of specific activity is the result of measurements under isothermal conditions without limitation (9). In practice, under the non-isothermal conditions that occur in up-scaled SSF processes, other biological and physical effects may play an important role in inactivation. For instance, delayed response of growth of biomass to a temperature increase would result in higher temperatures than predicted here. This might lead to temperatures above  $T_{\text{max}}$  and thus result in cessation of growth and enhanced inactivation.

**Oxygen, carbon dioxide and water:** One of the physical phenomena in SSF denoted earlier as responsible for growth of biomass to limited depths is the limitation of oxygen (17, 22). Since the model takes oxygen consumption into account, a decrease of oxygen concentration can be calculated with equation (21). It hardly needs noting that the effect of oxygen on biomass growth and activity is not included in the models.

Figure 8 shows the results of calculations of the course of  $pO_2$  in time in the layer at 0.10 m depth at different values of  $\lambda$  and effective-diffusion coefficient of oxygen ( $D^*_{O_2}$ ). Model  $M_{\text{none}}$  is used to calculate the oxygen concentration  $c_{O_2}$  in mol per  $m^3$  fermenter as a worst-case situation. The simulations reveal that oxygen limitation is dependent on two processes: oxygen transport and heat transfer, represented in the models by two parameters:  $D^*_{O_2}$  and  $\lambda$ . At high values of  $\lambda$ , oxygen is more rapidly limiting (Figure 8A) than at low values of  $\lambda$  (Figure 8C). This is explained by the fact that at high heat transfer rates, biomass grows at higher growth rates and thus consumes oxygen more rapidly. Figure 8A-C show that oxygen is limiting, at values of  $\lambda$  between 0.15 and 0.60  $J \cdot m^{-1} \cdot s^{-1} \cdot K^{-1}$ , if the value of  $D^*_{O_2}$  is 1/20 or less of the effective diffusion coefficient of oxygen in air.

These simulations are supported by the findings of Rathbun and Shuler (17) for fast-growing *Rhizopus oligosporus* on soya beans. They measured oxygen and temperature in layers of a small fermentation chamber placed in an isothermal environment. Oxygen first became limiting in those layers where temperature did not reach the maximum temperature for growth. These layers were on the bottom of the chamber where heat transfer to the surroundings was highest.

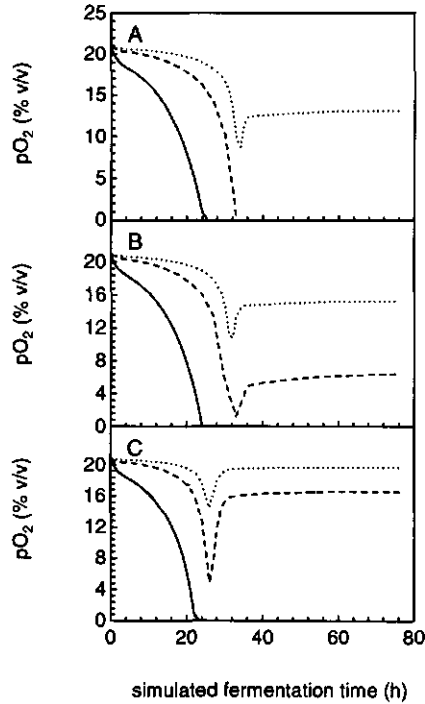


**Figure 8:** Influence of the value of the effective diffusion coefficient ( $D_{O_2}^*$ ) on the course of partial oxygen pressure predicted by the  $M_{\text{none}}$ -model with  $\lambda$  being 0.60 (A), 0.45 (B) and 0.15 (C)  $\text{J} \cdot \text{m}^{-1} \cdot \text{s}^{-1} \cdot \text{K}^{-1}$ . Values of  $D_{O_2}^*$  used for calculation are  $9.3 \cdot 10^{-7}$  (—),  $4.2 \cdot 10^{-6}$  (---) and  $1.0 \cdot 10^{-5} \text{ m}^2 \cdot \text{s}^{-1}$  (· · ·).  $pO_2$  is given in volume percentage oxygen per volume air fraction.

Ghildyal *et al.* (23) measured oxygen concentration at different depths in a tray SSF of *Aspergillus niger* on wheat bran. Although *A. niger* grows faster than *Trichoderma reesei* and maximum respiration activities were measured at 12 h fermentation, complete depletion of oxygen did not occur. The oxygen-concentration and enzyme-activity profiles Ghildyal *et al.* measured at different depths of up to 0.24 m demonstrated that oxygen is not the growth-limiting parameter in a wheat bran bed. In a separate report these authors concluded that temperature is the key parameter (20).

Whether oxygen concentration plays a role in the formation of biomass in SSF in general does not only depend on oxygen concentration, oxygen diffusion rate, rate of heat transfer and oxygen consumption rate, but also on the sensitivity of the biomass to lower oxygen

concentrations which is expected to be significant (24). The sensitivity of biomass to low oxygen concentrations has to be determined in independent experiments using glucosamine as the biomass parameter to include the influence of oxygen on biomass growth and activity in our models. This is an important topic for future research on SSF.

What holds for oxygen also holds for carbon dioxide since the amount of carbon dioxide produced in the SSF bed may be expected to be of the same order of magnitude as the amount of oxygen consumed (17, 23). Carbon dioxide at low concentrations might have a positive effect on microbial growth, but is inhibiting at high concentrations (24, 25).

Water activity is another important parameter. However, the water content inside the fermentation bed is predicted to remain above the initial water content of 53% w/w in the wetted substrate. This is expected since the water vapour diffusion rate, which reflects dissipation of water vapour and hence of water, is low as a result of small differences in water vapour concentrations between the fermentation bed and the environment. Maximum water content was predicted to be close to 70% w/w at those locations where most biomass glucosamine is predicted.

Based on these simulation results, it can be concluded that water evaporation is of minor importance in cooling SSF in a tray under these conditions. The situation is presumed to be different when the tray is placed in an environment with a lower relative humidity than simulated here. In that case, diffusion of water vapour towards the environment increases, allowing more water to evaporate inside the bed, with a consequent increase in the contribution of evaporation to cooling and, probably more important, an increased effect of water activity on biomass growth and activity.

Increased water vapour transport is also obtained by convection, which can result from differences in temperature in a tray and from forced aeration as in a packed bed. Inclusion of free convection in the models is also one of our future research topics. For the time being, the effect of free convection on biomass glucosamine evolution and temperature in the models described here is simulated by the relatively high values of  $\lambda$ .

Besides an effect on water vapour transport, free convection also has a significant effect on oxygen and carbon dioxide transport. Increased free convection will lead to increased heat dissipation, delayed oxygen exhaustion and less carbon dioxide accumulation with a concomitant effect on biomass and temperature patterns.

## Conclusions

The four models differ in their description of inactivation of biomass. Omission of inactivation results in unrealistic temperature courses, but can predict biomass patterns which may be observed in practice. Inclusion of inactivation kinetics can predict more realistic temperature patterns. Inclusion is done in three ways, the  $M_{\text{core}}$  model resulting in the least likely predictions. The most probable results are predicted by the  $M_{\text{part}}$  and  $M_{\text{temp}}$  models. The  $M_{\text{temp}}$  model predicts complete overgrowth of the substrate, although it takes quite some time to accomplish this. The  $M_{\text{part}}$  model predicts restricted growth of biomass in the inner layers of the tray. An explanation for this can be looked for in irreversibly unfavourable circumstances, like substrate limitation and product toxicity.

The  $M_{\text{part}}$  and  $M_{\text{unp}}$  models predict overall increased biomass yields with longer-lasting fermentation periods. These longer periods, however, do not necessarily result in increased efficiencies of the fermentations since other phenomena (such as sporulation and hydrolysing enzymes) may start to play a spoiling part.

Heat transfer in the fermentation bed is an important parameter and determines to a large extent the biomass and temperature patterns of the fermentation. Oxygen concentration in deeper layers of the fermentation bed only approaches zero at high heat-transfer rates. Desiccation of the substrate was predicted not to occur. Temperature is therefore assigned to be the key parameter in the fermentation process and oxygen concentration only to a lesser extent.

**Table 1:** List of symbols and values of constants used in the models.

**Variables in time, temperature and place**

$a_w$	water activity of substrate	-
$c_{\text{dm}}$	dry matter concentration	kg per m <sup>3</sup> fermenter
$c_{\text{O}_2}$	oxygen concentration	mol per m <sup>3</sup> fermenter
$c_{\text{sat}}$	water concentration in water-saturated air	kg per m <sup>3</sup> fermenter
$c_w$	water concentration	kg per m <sup>3</sup> fermenter
$c_{\text{wv}}$	water vapour concentration	kg water per m <sup>3</sup> fermenter
$c_{p, \text{dm}}$	specific heat of dry matter	J per kg dry matter per K
$dt$	time step	s
$D_{\text{wv}}^*$	effective diffusion coefficient of water vapour in fermenter	m <sup>2</sup> per s
$D_{\text{O}_2}^*$	effective diffusion coefficient of O <sub>2</sub> in fermenter	m <sup>2</sup> per s
$G$	glucosamine concentration	kg per kg initial dry matter
$G_{\text{max}}$	maximum attainable glucosamine level	kg per kg initial dry matter
$H$	enthalpy of fermenter system	J per s per m <sup>3</sup> fermenter
$h_j$	enthalpy of a component $j$	J per s per kg
$i$	layer in fermentation bed	-
$j$	component of substrate	-
$m_d$	specific activity decline rate	mol per s per kg glucosamine
$N$	number of layers	-
$q$	specific-respiration activity	mol per s per kg glucosamine
$r_{\text{evap}}$	water evaporation rate	kg water per s per m <sup>3</sup> fermenter
$r_{\text{O}_2}$	oxygen consumption rate	mol O <sub>2</sub> per s per m <sup>3</sup> fermenter
$r_{\text{CO}_2}$	carbon dioxide production rate	mol CO <sub>2</sub> per s per m <sup>3</sup> fermenter
$r_H$	heat production rate	J per s per m <sup>3</sup> fermenter
$r_{\text{dm}}$	dry matter consumption rate	kg dry matter per s <sup>1</sup> per m <sup>3</sup> fermenter
$r_w$	water production rate	kg H <sub>2</sub> O per s per m <sup>3</sup> fermenter
$T$	temperature	K
$t$	time	s
$t_d$	time at which a decline of specific activity starts	s
$t_s$	time at which a decline of specific activity stops	s
$Y$	yield of glucosamine on O <sub>2</sub> or CO <sub>2</sub>	kg glucosamine per mol
$x$	vertical position coordinate	m
$\beta/\alpha$	H <sub>2</sub> O/CO <sub>2</sub> ratio	mol H <sub>2</sub> O per mol CO <sub>2</sub>
$\epsilon$	fraction of air	m <sup>3</sup> air per m <sup>3</sup> fermenter
$\lambda$	effective heat transfer coefficient in fermenter	J per m per s per K
$\mu$	specific-growth rate	per s
$\mu_{\text{max}}$	maximum specific-growth rate	per s

Table 1 (cont.)

## Constants

$c_{dm}(0)$	initial dry matter content	206	kg per m <sup>3</sup> fermenter	(a)
$c_w(0)$	initial water concentration	232	kg water per m <sup>3</sup> fermenter	(c)
$c_{p,w}$	specific heat of water ( $T_{ref} = 373$ K)	4216	J per kg per K	(e)
$c_{p,ww}$	specific heat of water vapour ( $T_{ref} = 273$ K)	2000	J per kg per K	(e)
$E_a$	activation energy	$327 \times 10^3$	J per mol	(b)
$G(0)$	initial glucosamine concentration	$0.029 \times 10^{-3}$	kg per kg initial dry matter	(c)
$\Delta H_w$	evaporation enthalpy of water ( $T_{ref} = 373$ K)	$22.7 \times 10^5$	J per kg	(e)
$k_{md}$	specific death rate	$1.312 \times 10^{-9}$	mol per s <sup>2</sup> per kg glucosamine	(b)
$L$	bed height	0.10	m	(a)
$M_{C-mol}$	molecular weight of substrate	32.6	g per C-mol	(b)
$M_{H_2O}$	molecular weight of water	18	g per mol	(e)
$m_{d,0}$	basic specific activity decline rate	$17.28 \times 10^{-9}$	mol per s <sup>2</sup> per kg glucosamine	(b)
$m_b$	maintenance coefficient	$2.18 \times 10^{-3}$	mol per s per kg glucosamine	(b)
$p$	air pressure	$10.13 \cdot 10^6$	N per m	(a)
$pO_2(0)$	partial oxygen pressure	20.9	% v/v	(a)
$R$	gas constant	0.314	J per mol per K	(e)
$T(0)$	ambient temperature	298	K	(a)
$T_{min}$	virtual minimum temperature for growth	263	K	(b)
$T_{max}$	maximum temperature for growth	313.7	K	(b)
$T_{ref}$	reference temperature		K	(e)
$\rho_{dm}$	density of dry matter	840	kg per m <sup>3</sup> dry matter	(d)
$\rho_w$	density of water	994	kg per m <sup>3</sup> water	(e)

## Coefficients

$a_1$	for description of $G_{max}(T)$	$4.056 \times 10^{-4}$	kg <sup>0.5</sup> per K per kg <sup>0.5</sup> initial dm	(b)
$a_2$	for description of $G_{max}(T)$	75	K	(b)
$a_3$	for description of $G_{max}(T)$	0.694	per K	(b)
$b_1$	for description of $\mu_{max}(T)$	$1.524 \times 10^{-4}$	s <sup>-0.5</sup> per K	(b)
$b_2$	for description of $\mu_{max}(T)$	0.544	per K	(b)
$d_1$	for description of $Y(T)$	$1.187 \times 10^{-3}$	kg glucosamine per mol	(b)
$d_2$	for description of $Y(T)$	$1.968 \times 10^{-3}$	kg glucosamine per mol	(b)
$d_3$	for description of $Y(T)$	301	K	(b)
$d_4$	for description of $Y(T)$	3.67	K	(b)

(a): this chapter, (b): reference (12), (c): reference (9), (d): reference (10), (e): reference (15)

## References

- Lai, M.N., Chang, F.W., Wang, H.H. (1991) Application of pseudo-steady heat conduction model for solid-state fermentation of sorghum mash. *Nippon Shokuhin Kogyo Gakkaishi* **38** 226-234
- Soccol, C.R., Stertz, S.C., Raimbault, M., Pinheiro, L.I. (1995) Biotransformation of solid waste from cassava starch production by *Rhizopus* in solid state fermentation. Part 3: Scale-up studies in different bioreactors. *Arq. Biol. Technol.* **38** 1319-1326
- Saucedo-Castañedo, G., Gutiérrez-Rojas, M., Bacquet, G., Raimbault, M., Viniegra-González, G. (1990) Heat transfer simulation in solid substrate fermentation. *Biotechnol Bioeng.* **35** 802-808
- Wang, H.H., Wu, T.Z., Hsu, J.P., Tsai, Y.S. (1991) A kinetic analysis of sorghum brewing - a typical solid-state fermentation. *Nippon Shokuhin Kogyo Gakkaishi* **38** 716-721
- Szewczyk, K.W., Myszka, L. (1994) The effect of temperature on the growth of *A. niger* in solid-state fermentation. *Bioprocess Engin.* **10** 123-126

- 6 Sangsurasak, P., Mitchell, D.A. (1995) Incorporation of death kinetics into a 2-dimensional dynamic heat transfer model for solid-state fermentation. *Chem. Engin. J.* **64** 253-260
- 7 Rajagopalan, S., Modak, J.M. (1995) Modeling of heat and mass transfer for solid state fermentation process in tray bioreactor. *Bioprocess Engin.* **13** 161-169
- 8 Gutiérrez-Rojas, M., Auria, R., Benet, J.C., Revah, S. (1995) A mathematical model for solid-state fermentation of mycelial fungi on inert support. *Chem. Engin. J.* **60** 189-198
- 9 Smits, J.P., Rinzeema, A., Tramper, J., Sonsbeek, H.M. van, Knol, W. (1996a) Solid-state fermentation of wheat bran by *Trichoderma reesei* QM9414: substrate composition changes, C-balance, enzyme production, growth and kinetics. *Appl. Microbiol. Biotechnol.* **46** 489-496
- 10 Smits, J.P., Rinzeema, A., Tramper, J., Schlösser, E.E., Knol, W. (1996b) Accurate determination of process variables in solid state fermentation system. *Process Biochem.* **31** 669-678.
- 11 Pirt, S.J. (1965) The maintenance energy of bacteria in growing cultures. *Proc. Royal. Soc. of London* **163** 224-231
- 12 Smits, J.P., Rinzeema, A., Tramper, J., Sonsbeek, H.M. van, Hage, J.C., Kaynak, A., Knol, W. (1997) The influence of temperature on kinetics in solid-state fermentation. In press *Enzyme Microb. Technol.*
- 13 Riet, van 't, K., Tramper, J. (1991) in: *Basic bioreactor design*. Marcel Dekker, inc. New York
- 14 Laukevics, J.J., Aspite, A.F., Viesturs, U.S., Tengerdy, R.P. (1984) Solid substrate fermentation of wheat straw to fungal protein. *Biotechnol. Bioeng.* **26** 1465-1474
- 15 Weast, R.C., Astle, M.J. (ed.) In: *CRC Handbook of Chemistry and Physics* vol 61 (1980) CRC Press, Inc. Boca Raton
- 16 Press, W.H., Tenkolsky, S.A., Vetterling, W.T., Flannery, B.P. (1992) In: *Numerical recipes*, Cambridge University Press, Cambridge
- 17 Rathbun, B.L., Shuler, M.L. (1983) Heat and mass transfer effects in static solid-substrate fermentations: design of fermentation chambers. *Biotechnol. Bioeng.* **25** 929-938
- 18 Doelle, H.W., Mitchell, D.A., Rolz, C.E. (1992) In: *Solid substrate cultivation*. Elsevier Appl. Sci., Essex.
- 19 Raghava Rao, K.S.M.S., Gowthaman, M.K., Ghildyal, N.P., Karanth, N.G. (1993) A mathematical model for solid-state fermentation in tray bioreactors. *Bioprocess Engin.* **8** 255-262
- 20 Ghildyal, N.P., Ramakrishna, M., Lonsane, B.K., Karanth, N.G., Krishnaiah, M.M. (1993) Temperature variations and amylglucosidase levels at different bed depths in a solid state fermentation system. *Chem. Engin. J.* **51** B17-B23
- 21 Rajagopalan, S., Modak, J.M. (1994) Heat and mass transfer simulation studies for solid-state fermentation processes. *Chem. Engin. Sci.* **49** 2187-2193
- 22 Mudget, R.E. (1980) Controlled gas environments in industrial fermentations. *Enzyme Microb. Technol.* **2** 273-280
- 23 Ghildyal, N.P., Ramakrishna, M., Lonsane, B.K., Karanth, N.G. (1992) Gaseous concentration gradients in tray type solid state fermentors - Effect on yields and productivities. *Bioprocess Engin.* **8** 67-72
- 24 Bajracharya, R., Mudgett, R.E. (1980) Effects of controlled gas environments in solid-substrate fermentations of rice. *Biotechnol. Bioeng.* **22** 2219-2235
- 25 Reu, J. de. (1995) Solid-substrate fermentation of soya beans to tempe. Thesis Agricultural University Wageningen

### - Appendix -

Glucosamine is the building block of chitin in the fungal-cell wall. Its content in an SSF system is a measure for the amount of biomass present and replaces the biomass parameter in the models used here.

Glucosamine content and respiration activity during the fermentation of wheat bran by *Trichoderma reesei* QM 9414 at different temperatures were described by Smits *et al.* (9, 12). The mathematical descriptions of the influence of time and temperature on glucosamine and respiration activity resulting from these studies are summarized here.

The increase in rate of glucosamine at constant temperature is described with the logistic equation:

$$\frac{dG(t)}{dt} = \mu_{\max} \cdot G(t) \cdot \left[1 - \frac{G(t)}{G_{\max}}\right] \quad (a1)$$

in which  $dG/dt$  is given in kg glucosamine per kg initial dry matter per second.

Maximum glucosamine content,  $G_{\max}$  in kg glucosamine per kg initial dry matter, is described as a function of temperature by:

$$G_{\max}(T) = [a_1 \cdot (T - a_2) \cdot (1 - \exp(a_3 \cdot (T - T_{\max})))^2] \quad (a2)$$

Maximum specific-growth rate,  $\mu_{\max}$  in  $s^{-1}$ , is described as a function of temperature by:

$$\mu_{\max}(T) = [b_1 \cdot (T - T_{\min}) \cdot (1 - \exp(b_2 \cdot (T - T_{\max})))^2] \quad (a3)$$

$T_{\min}$  and  $T_{\max}$  are the minimum and maximum temperature for growth in K, respectively.  $a_1$  to  $a_3$  and  $b_1$  and  $b_2$  are constants.

The highest maximum attainable glucosamine concentration is ca. 8.5 g glucosamine per kg initial dry matter, which is reached after isothermal growth at ca. 305 K. The highest  $\mu_{\max}$  is reached at approximately the same temperature and amounts to  $0.4 \times 10^{-6} s^{-1}$ .

The specific respiration activity  $q$ , i.e. oxygen consumption or carbon dioxide production rate in mol per second per kg glucosamine, is described by the linear-growth model:

$$q(t) = \frac{1}{Y} \cdot \mu(t) + m_0 \quad (a4)$$

Here,  $\mu(t)$  is the specific-growth rate in  $s^{-1}$ , as described by equation (a5).

$$\mu(t) = \frac{1}{G(t)} \cdot \frac{dG(t)}{dt} \quad (a5)$$

$m_0$  is the maintenance coefficient in mol  $O_2$  or  $CO_2$  per second per kg glucosamine, and  $Y$  is the yield factor in kg glucosamine per mol  $O_2$  or  $CO_2$ , whose dependence on temperature can be described by:

$$Y(T) = d_1 + d_2 \cdot \exp(-0.5 \cdot [\frac{T - d_3}{d_4}]^2) \quad (a6)$$

In equation (a6),  $d_1$  to  $d_4$  are constants.

The specific activity declines after growth has ceased, i.e. after  $t_d$  when  $\mu(t_d) = \mu_{\max} / 100$ . This decline is described over time by equation (a7), in which the contribution of growth is neglected.

$$q(t) = m_0 - m_d \cdot (t - t_d) \quad (a7)$$

for  $t \geq t_d$

The course of the specific activity decline rate,  $m_d$  in mol per second per kg glucosamine, for biomass growing at a specific-growth rate of  $\mu(t) \leq \mu_{\max} / 100$ , is described by the Arrhenius-type equation as a function of temperature:

$$m_d(T) = m_{d,0} + k_{md} \cdot \exp\left[-\frac{E_a}{R} \cdot \left(\frac{1}{T} - \frac{1}{T_{\max}}\right)\right] \quad (a8)$$

In equation (a8),  $m_{d,0}$  is the basic specific-activity decline rate (mol·s<sup>-2</sup> per kg glucosamine),  $k_{md}$  is the specific death rate (mol·s<sup>-2</sup> per kg glucosamine),  $E_a$  is the activation energy of inactivation (J·mol<sup>-1</sup>), and  $R$  is the gas constant (J·mol<sup>-1</sup>·K<sup>-1</sup>).

$m_d$  describes the linear decline of specific activity of non-growing biomass in time. The maintenance coefficient  $m_0$  is assumed to be constant in time and thus  $m_d$ , in fact, describes the change in the amount of active biomass contributing to the specific activity. This means that, finally,  $q(t)$  becomes zero because of the increase in the amount of inactivated biomass.



## Summary

The logistic equation and the linear-growth model are often used in models for solid-state fermentation (SSF). The logistic equation is used to describe the evolution of total biomass and does not discriminate between growing active, non-growing active and inactive biomass. The linear-growth model, on the other hand, describes the activity necessary for growth and maintenance and does not deal with inactive biomass. Using the combination of both in a mathematical model for predicting temperature, oxygen and biomass patterns in SSF appears not to be sufficiently detailed. The inclusion of inactivation of biomass in the model is mandatory to predict simultaneously restricted biomass growth and temperature decline during fermentation. Inclusion of the dependence of biomass growth and activity on reversible variables, such as temperature and oxygen concentration, does result in inhibition but cannot terminate biomass growth and activity.

This chapter evaluates the implementation of logistic equation and the linear-growth model in modelling fungal SSF and discusses the need for research efforts focused on the post-growth stage. It is concluded that the combination of logistic equation and linear-growth model is only suitable to describe fungal SSF if, for instance, time- or substrate-dependent inactivation kinetics are incorporated as well.

## Introduction

Fermentation of substrates under conditions of limited water availability, so-called solid-state fermentation (SSF), has been applied for centuries for the production of food and feed. Examples are the production of tempeh and koji, which are important protein and enzyme products, respectively, in the food industry of the Far East. Many other applications of SSF are described in scientific literature, such as production of hydrolytic enzymes, pigments, antibiotics, ethanol and protein (1).

Advantages of SSF over submerged fermentations lie in the absence of excess water: high productivity, simple technique, reduced energy requirement, low waste water output, and elimination of foam problems. A typical SSF contains between 40 and 80% w/w water (2). Generally, volumetric yields are high and substrates are usually cheap insoluble agricultural products. An SSF forms a typical environment close to the natural habitat of fungi (3). Fungi are therefore most successfully applied in SSF.

The main feature of an SSF is the inhomogeneous distribution of biomass or related products in, especially, a tray fermenter bed (1, 4, 5, 6). Several studies have attempted to describe the development of this inhomogeneity. High temperature and low oxygen concentration are believed to be the most important factors (7).

Nowadays, fast-calculating computers ease mathematical modelling of SSF for simulation, design and optimization studies. These models describe the biological and physical processes involved in SSF and predict the course of fermentation even when alterations of physical variables are involved. Several of such mathematical models described in the literature contribute to a better understanding of the intrinsic difficulties of SSF.

## Steps in modelling SSF

In modelling SSF, several steps can be distinguished. The first is the description of biomass

evolution and the second is correlation of biomass amount with its activity. Then the description of the influence of environmental parameters, such as temperature and oxygen, carbon-dioxide and water content, on the first two steps follows. In addition to the description of these biological processes of growth and activity, physical processes such as mass and heat transfer, evaporation, condensation, convection and conduction, and the effect of biological processes on these physical processes, have to be included in the mathematical model. This chapter provides a closer look at modelling SSF by evaluating the first three steps mentioned above. How these steps are taken and what the consequences are for the model predictions of biomass, temperature and oxygen concentration is evaluated.

### Description of fungal biomass

The most widely used equation for describing the evolution of biomass or biomass-related parameters in an SSF system is the logistic equation, equation (1) (see Table 1 and refs. 8, 9, 10, 11).

$$\frac{dX}{dt} = \mu_{\max} \cdot X \cdot \left[1 - \frac{X}{X_{\max}}\right] \quad (1)$$

Here,  $X$  is the actual amount of biomass,  $\mu_{\max}$  is the maximum specific-growth rate and  $X_{\max}$  is the maximum attainable amount of biomass. If dormant spores are used as inoculum in a fermentation, a lag phase should be considered before biomass increases. During this lag phase,  $dX/dt$  is zero and  $X$  is equal to  $X_0$ , the initial amount of viable biomass.

Since a large problem in SSF is the quantitative separation of biomass from its substrate, usually concentrations of biomass-related constituents are measured and used, such as the amounts of glucosamine (8, 11, 12), protein (13, 14, 15), ATP (16, 17),  $\text{CO}_2$  (9) and  $\text{O}_2$  (5, 18). Alternatively, the pressure drop over a packed bed has been correlated to biomass growing on an inert carrier (19) and used in modelling as well (20).

The applicability of the logistic equation for some biomass-replacing parameters is shown in several studies (9, 11, 15). Sometimes only a few data are used, mainly on the exponential-growth phase of biomass (5, 21), or the applicability is not experimentally proven at all (14). In most studies mentioned, a constant relationship is assumed between the biomass-related parameter and biomass dry matter. However, this may not be the case. For instance, glucosamine content may vary with age of fungal biomass (22, 23). The quotient glucosamine per biomass dry matter can easily be measured in a culture grown in liquid, but may not be valid for a culture growing under SSF conditions (11). The same holds for protein and ATP: the amount per biomass may not be constant. The dilemma of correlating  $\text{CO}_2$  produced or  $\text{O}_2$  consumed with the amount of fungal biomass is related with the applicability of the linear-growth model of Pirt (24) to fungal biomass. This subject is discussed in more detail below under "Correlating fungal biomass to respiration activity".

### The effect of temperature on fungal-biomass growth

The effect of temperature on growth of fungal biomass (or the related variable, which will also be called biomass hereinafter) received only moderate attention so far in scientific literature on

Because of these transitions it can be concluded that the correlations with metabolic activity, described by equation (5), (6) or (7), are at best approximations. If differentiation of fungal biomass into growing active and non-growing active hyphal parts explains the deviation from the linear-growth model, as described above, it would mean that not only the effect of temperature on the amount of biomass and the coefficient  $Y$  and  $m_o$  need to be described, but also the effect on this differentiation process. The effect of temperature on the inactivation process is already described in a preliminary, non-mechanistic way by the effect of temperature on  $m_o$  in equation (5) (39). An Arrhenius-type equation was used, showing the exponential increase of the inactivating effect on fungal biomass at increasing temperatures. Regarding the importance of the including inactivation kinetics, the models of Sargentanis *et al.* (15) and Smits *et al.* (39) give insight into the consequences of the use of equation (6). The models predict that temperature remains elevated during the fermentation period unless inactivation of biomass occurs, allowing the temperature to decrease.

### Implementation of the effect of temperature and oxygen

Due to microbial activity, heat is produced. A constant ratio between oxygen consumption rate (40) or substrate consumption rate (41) and heat production rate has been described. The heat production might result in a temperature increase, depending on several physical processes, such as heat transfer (by conduction or convection) and evaporation of water, and the heat capacity of the substrate and other components.

Descriptions of temperature dependence of fungal growth and respiration activity mentioned above are results of experiments done under isothermal conditions. In a fermentation bed, however, temperature is not constant. It increases during the initial stage of fermentation, and decreases when heat production ceases, as shown for a large-scale fermentation by Lai *et al.* (42). Usually, heat transfer at a side of a fermenter bed adjacent to the environment differs from heat transport in the centre. Therefore, temperature increase is dependent on the location in the bed. Whether mathematical descriptions of the effect of temperature obtained from isothermal experiments can be used as such for describing non-isothermal fermentations remains a subject for further research. For the time being, we assume the impact to be small as compared to the impact of choosing the linear-growth model.

The effect of increased temperature on biomass will, at a certain moment, result in a decline of growth rate and activity and a corresponding change in heat production. Because of heat removal to the environment, temperature decreases again and biomass growth rate may tend to increase, with consequences for heat production. The overall process is a feedback interaction between temperature and biomass growth and activity. Therefore, it is not likely that high temperatures determine the final biomass concentration. This is most probably determined by another irreversible limitation.

What is predicted to be the effect of temperature on maintenance activity depends on which version of linear-growth model is chosen: equation (5), (6) or (7). In the first linear-growth model, equation (5), maintenance activity is omitted, so heat production is zero after  $\mu$  is zero (17, 27, 28, 32). At the end of the process, temperature is predicted to be equal to the temperature of the environment.

In the second linear-growth model, equation (6), temperature will remain above ambient

temperature unless heat transfer rates are sufficiently high to remove the heat produced by maintenance activity. The third model, equation (7), predicts a decrease in temperature until ambient temperature is reached, but only after  $\mu$  has become close to zero due to a growth-inhibiting effect.

A similar effect as with temperature is seen with oxygen concentration. Oxygen is consumed and thus its concentration decreases. Using the first linear-growth model, equation (5), to describe oxygen consumption will result in a concentration increase at the moment biomass growth ceases with the rate of diffusion (5). The second linear-growth model, equation (6), will predict the oxygen concentration to remain low unless oxygen diffusion is extremely high. The third linear-growth model, equation (7) predicts a slow increase in oxygen concentration after growth has stopped.

High temperature and oxygen limitation are both said to be the primary cause of inhibited growth of the fungus on the substrate (1, 4, 5). However, mathematical models predict that temporarily unfavourable circumstances, like high temperature and low oxygen concentration, do not prevent maximum attainable biomass levels throughout the fermentation bed to be reached. These circumstances theoretically only delay complete overgrowth of the substrate (39). This means that with longer fermentation periods, complete overgrowth can be accomplished. A technical problem with long-lasting large-scale fermentations is in maintenance of sterility over this period. Growth of unwanted microorganisms does not only mean unwanted consumption of substrate and product formation, but also might raise the temperature of the fermentation bed above the value of  $T_{max}$  with subsequently disastrous effects on the fungus. Despite the importance of aseptic operating in SSF, aseptic (pilot-scale) fermenters are rarely described (43).

Another problem of long-lasting fermentation periods can be the stability of the fermentation product, especially when biologically active compounds such as enzymes are produced. For instance, one part of the fermentation bed might not have reached the maximum attainable biomass level yet, while other parts did and biomass started to sporulate. In the meantime, the fermentation product may deteriorate and certain enzymes may be inactivated due to hydrolytic activity. In these situations, long fermentations neither contribute to efficiency nor increase the quality of the fermentation product.

### Future perspectives of SSF

In SSF research described in the literature, most attention seems to be focused on the growth phase of fungal biomass. Based on the discussion above, it can be concluded that more attention should be paid to the post-growth phase of fermentation. This phase is important especially for processes in which secondary metabolites are produced. The post-growth phase is also important for processes on a large scale where inhomogeneity determines efficiency of the fermentation.

In large-scale tray fermentations high growth rates of the fungus are found only in the outside layers of the substrate bed. Inside the bed, growth occurs under sub-optimal conditions of inhibiting high temperatures, oxygen depletion or elevated carbon dioxide concentrations. The physiology of the fungus growing under these circumstances is unknown. Therefore, more

attention should be paid to the behaviour of fungal biomass growing under sub-optimal conditions. Not only growth and activity, but also product formation might be different. This might explain why yields obtained in SSF may be significantly higher than those in liquid fermentation (44).

The application of results of glucosamine analysis in modelling SSF showed to be a good alternative to total biomass in modelling SSF. Growth, respiration activity and inactivation of fungi can be described with glucosamine as the biomass parameter. To use glucosamine in describing activities other than respiration seems also quite promising. For instance, production of xylanase and protease during growth of *Trichoderma reesei* QM9414 on wheat bran was shown to be constant in relation to glucosamine production (11). Modelling of enzyme production in SSF might thus be eased by knowing the glucosamine content. The potential of glucosamine in describing fungal growth may be extended if the results are combined with those of other measurements, such as ATP, RNA and DNA. If each measurement covers a different type of fungal biomass (active growing, active non-growing and inactive), the combination will open a new world of possibilities regarding fungal kinetics and modelling.

Unexplored are the application possibilities of SSF in fundamental physiological research. Fungal growth, differentiation and sporulation depend on the processes on a micro scale, and thus sensitive image analysis techniques, combined with powerful computer technology, are needed to open new areas of research. Since the location of the biomass in the fermentation layer does not change in static SSF, the combination of SSF with activity measurement and image analysis techniques might be very fruitful.

## Conclusions

The combination of the logistic equation, for describing fungal biomass evolution, and the linear-growth model, for correlating fungal biomass to activity, does not offer sufficiently detailed possibilities to describe an SSF. Inactivation of biomass, which obviously occurs, must also be described mathematically dependent on a irreversible physical parameter such as substrate concentration or time. Several researchers attribute the observed restricted biomass growth in a fermentation bed to the effect of mass and heat transfer limitations on biomass, but these will predict either everlasting heat production or complete overgrowth of the substrate with increased fermentation time.

The lack of details results from the fact that both the logistic equation and the linear-growth model do not allow discrimination of biomass in the classes of active growing, active non-growing and inactivated biomass. Much research has already been devoted to the description of the mechanism underlying fungal growth and differentiation. Especially germination of spores and the following growth phases are well described (45). For correlating fungal biomass to activity, image analysis techniques in combination with computer technology are promising.

## List of symbols and abbreviations

CPR	carbon dioxide production rate	mol CO <sub>2</sub> -s <sup>-1</sup> per kg substrate
<i>l</i>	respiration activity	mol-s <sup>-1</sup> per kg substrate
<i>m</i> <sub>0</sub>	maintenance coefficient	mol-s <sup>-1</sup> per kg biomass
<i>m</i> <sub>d</sub>	decline coefficient	mol-s <sup>-1</sup> per kg biomass
<i>q</i>	specific respiration activity	mol-s <sup>-1</sup> per kg biomass
<i>t</i>	time	s
<i>t</i> <sub>d</sub>	period of decline in activity	s
<i>Y</i>	yield factor of biomass on activity	kg biomass per mol
<i>X</i>	amount of biomass	kg biomass
<i>X</i> <sub>0</sub>	initial amount of viable biomass	kg biomass
<i>X</i> <sub>max</sub>	maximum attainable amount of biomass	kg biomass
<i>μ</i>	specific-growth rate	s <sup>-1</sup>
<i>μ</i> <sub>max</sub>	maximum specific-growth rate	s <sup>-1</sup>

## References

- Doelle, H.W., Mitchell, D.A., Rolz, C.E. (1992) in: Solid substrate cultivation. Elsevier Appl. Sci., Essex.
- Cannel, E., Moo-Young, M. (1980) Solid-state fermentation systems. *Process Biochem.* **15** 2-7
- Raimbault, M., Alazard, D. (1980) Culture method to study fungal growth in solid-state fermentation. *Eur. J. Appl. Microbiol.* **9** 199-209
- Rathbun, B.L., Shuler, M.L. (1983) Heat and mass transfer effects in static solid-substrate fermentation: design of fermentation chambers. *Biotechnol. Bioeng.* **25** 929-938
- Raghava Rao, K.S.M.S., Gowthaman, M.K., Ghildyal, N.P., Karanth, N.G. (1993) A mathematical model for solid state fermentation in tray bioreactors. *Bioprocess Engin.* **8** 255-262
- Ghildyal, N.P., Ramakrishna, M., Lonsane, B.K., Karanth, N.G., Krisnaiah, M.M. (1993) Temperature variations and amyloglucosidase levels at different bed depths in a solid state fermentation system. *The Chem. Engin. J.* **51** B17-B23
- Lonsane, B.K., Ghildyal, N.P., Budiatman, S., Ramakrishna, S.V. (1985) Engineering aspects of solid-state fermentation. *Enzyme Microb. Technol.* **7** 258-265
- Okazaki, N., Sugama, S., Tanaka, T. (1980) Mathematical model for surface culture of koji mold. *J. Ferment. Technol.* **58** 471-476
- Sato, K., Yoshizawa, K. (1988) Growth and growth estimation of *Saccharomyces cerevisiae* in solid-state ethanol fermentation. *J. Ferment. Technol.* **66** 667-673
- De Reu, J.C. (1995) Solid-substrate fermentation of soya beans to tempeh. Thesis Agricultural University Wageningen.
- Smits, J.P., Rinzema, A., Tramper, J., Sonsbeek, H.M. van, Knol, W. (1996) Solid-state fermentation of wheat bran by *Trichoderma reesei* QM9414: substrate composition changes, C-balance, enzyme production, growth and kinetics. *Appl. Microbiol. Biotechnol.* **46** 489-496
- Kim, J.H., Hosobuchi, M., Kishimoto, M., Seki, T., Yoshida, T., Taguchi, H., Ryu, D.D.Y. (1985) Cellulase production by a solid state culture system. *Biotechnol. Bioeng.* **27** 1445-1450
- Rodriguez-Leon, J.A., Sastre, L., Echevarria, J., Delgado, G., Bechstedt, W. (1988) A mathematical approach for the estimation of biomass production rate in solid-state fermentation. *Acta Biotechnol.* **8** 307-310

The influence of temperature on specific growth rate, maximum attainable biomass, glucosamine level and yield of glucosamine on oxygen consumption or carbon-dioxide production could be described with a (modified) Ratkowsky equation or a Gaussian curve. The influence of temperature on the maintenance coefficient was negligible.

These mathematical equations were combined with conservation laws describing mass and heat transfer in a simulation model. Inactivation, as described under isothermal conditions, was implemented in three different ways, which resulted in the models  $M_{\text{part}}$ ,  $M_{\text{temp}}$  and  $M_{\text{cont}}$ . In the  $M_{\text{part}}$  model, inactivation starts when the specific growth rate becomes equal to or less than 1% of its maximum value. The inactivation continues until no activity is left. In the  $M_{\text{temp}}$  model, inactivation starts for the same reason, but stops when the specific growth rate is more than 1% of its maximum value again. In the  $M_{\text{cont}}$  model, inactivation is continuously effective, immediately from the start of fermentation.

The temperature and biomass evolution in a tray SSF predicted by these three models are compared with a model in which inactivation is omitted. The results show the importance of describing the inactivation in modelling SSF. Without this, unrealistic temperature and biomass glucosamine patterns are predicted.

The  $M_{\text{part}}$  model, representing inactivation due to substrate limitation or product toxicity, predicts temperature and biomass patterns described in the literature: restricted biomass growth and decrease in temperature at the end of fermentation. The mathematical models reported thus far in the literature predict restricted growth or a decrease in temperature. Although the combination of the logistic equation, for describing fungal biomass in time, and the linear-growth model, for correlating the respiration activity to biomass, is most often used in scientific literature on modelling SSF, it is insufficiently detailed. The logistic equation is shown to be applicable to the glucosamine measurement results, but the glucosamine determination cannot distinguish between active growing, active non-growing and inactive biomass. The total amount of these three types of biomass is described by the logistic equation, while the linear-growth model only describes the first two types. It is therefore suggested to focus research efforts on the description of the evolution of these three different forms of fungal biomass in time. Sensitive image analysis techniques, combined with computer technology, applied to fungal biomass growing under SSF conditions have the potential of being powerful tools to accomplish this target.

Het is in vaste-stoff fermentatie (SSF) onderzoek niet mogelijk schimmelbiomassa kwantitatief te scheiden van het substraat. Daarom is het moeilijk de biomassaontwikkeling in de tijd te meten. Alternatieven zijn voorhanden, waarvan het glucosaminegehalte veelbelovend is. Glucosamine is het monomeer van de celwandcomponent chitine en is daarom gerelateerd aan de hoeveelheid biomassa. De concentratie glucosamine in biomassa kan echter variëren in de tijd en is afhankelijk van de groeiomstandigheden.

In plaats van het glucosaminegehalte te gebruiken om de hoeveelheid biomassa te berekenen, zijn groei en activiteit van biomassa in dit onderzoek steeds gerelateerd aan de hoeveelheid glucosamine. Met deze beschrijvingen zijn wiskundige simulatiemodellen opgesteld waarmee glucosamine- en temperatuurpatronen in een SSF-bed voorspeld kunnen worden.

Het onderzoek is verricht aan de fermentatie van tarwezemelen door de schimmel *Trichoderma reesei* QM9414. De fermentaties zijn uitgevoerd in Petrischalen, in porties van 5 g, welke in een klimaatkast met constante temperatuur en luchtvochtigheid geplaatst werden. Monsters voor analyse werden genomen door Petrischalen uit de klimaatkast te nemen. Op deze wijze bleek het mogelijk droge-stofafname, glucosamine en respiratie-activiteit te meten met een standaard deviatie van minder dan 7% van de gemiddelde gemeten waarde. ATP en cellulase-activiteit bleken niet zo nauwkeurig te meten. Dit wordt toegeschreven aan de nodige voorbehandeling van het monstermateriaal voor ATP-analyse, en aan interacties tussen substraat en cellulase.

Zuurstofconsumptiesnelheid en koolzuurproductiesnelheid werden tegelijkertijd gemeten. In een fermentatieperiode van 125 uur werd circa 9 mmol per gram initiële droge stof aan CO<sub>2</sub> en O<sub>2</sub> respectievelijk geproduceerd en geconsumeerd. De toename aan glucosamine kon worden beschreven met een logistische curve. Het glucosaminegehalte verliep van 0,02 naar het maximum van 8,1 mg per gram initiële droge stof gedurende een 125-uurs fermentatie. De maximale specifieke groeisnelheid bedroeg 0,123 per uur.

De specifieke respiratie-activiteiten werden uitgerekend per hoeveelheid glucosamine. De correlatie met de specifieke groeisnelheid bleek af te wijken van het lineaire groeimodel. Een verklaring werd gezocht in de verschillende gedifferentieerde vormen waarin schimmelbiomassa aanwezig kan zijn. De afwijking werd geconstateerd tijdens de initiële groeifase van de schimmel. Deze afwijking zal echter van weinig invloed zijn op de resultaten van de simulatiemodellen waarin het lineaire groeimodel wordt gebruikt omdat de hoeveelheid biomassa in deze fase gering is en dus de voorspelde activiteiten gering zijn.

De afname in respiratie-activiteit nadat de toename in biomassa is gestopt, bleek wel significant. Deze afname, inactivering genoemd, werd toegeschreven aan de afname in de hoeveelheid actieve, niet-groeiende biomassa. De snelheid waarmee deze inactivering plaatsvond onder isotherme omstandigheden bleek constant in de tijd, maar nam exponentieel toe met een toenemende temperatuur boven de maximale groeitemperatuur.



De invloed van temperatuur op de maximale specifieke groeisnelheid, het maximaal haalbare glucosaminegehalte en de yield factor konden met een (gemodificeerde) Ratkowsky-vergelijking en een Gauss-kromme worden beschreven. De invloed van de temperatuur op de onderhoudscoëfficiënt bleek nihil.

De wiskundige vergelijkingen uit het onderzoek werden gecombineerd met vergelijkingen voor massa en warmtetransport tot de uiteindelijke simulatiemodellen. De beschrijving van de inactivering leverde drie modellen op:  $M_{part}$ ,  $M_{temp}$  en  $M_{cont}$ . In het  $M_{part}$ -model start de inactivering op het moment dat de specifieke groeisnelheid onder de 1% van de maximale waarde komt. In tegenstelling tot het  $M_{temp}$ -model blijft de inactivering in het  $M_{part}$  model effectief wanneer de specifieke groeisnelheid weer boven de 1% van de maximale waarde komt. Het  $M_{cont}$ -model gaat ervan uit dat inactivering vanaf het begin van de fermentatie continu effectief is. De voorspellingen van de drie modellen zijn vergeleken met het model waarin de inactivering niet is opgenomen. De resultaten laten het belang van het beschrijven van de inactivering zien. Zonder dat worden onrealistische temperatuur- en biomassapatronen voorspeld.

In vergelijking met de modellen die in de literatuur zijn beschreven, geeft vooral het  $M_{part}$ -model, dat de situatie bij substraatlimitatie simuleert, patronen die in de literatuur beschreven zijn: beperkte biomassagroei en afname van temperatuur aan het eind van de fermentatie. De modellen uit de literatuur voorspellen òf beperkte biomassagroei òf een afname in temperatuur aan het eind van de fermentatie.

Hoewel de combinatie van logistische vergelijking voor beschrijving van de ontwikkeling van schimmelbiomassa en het lineaire-groeimodel voor beschrijving van respiratie-activiteit in de wetenschappelijke literatuur veel voor het modelleren van SSF wordt gebruikt, blijkt uit dit onderzoek dat deze combinatie onvoldoende gedetailleerd is. De logistische vergelijking is van toepassing op het beschrijven van de toename aan glucosamine in de tijd, maar het glucosamine vertegenwoordigt actieve groeiende, actieve niet-groeiende en inactieve biomassa. Het lineaire-groeimodel is echter alleen van toepassing op actieve groeiende en actieve niet-groeiende biomassa.

Meer onderzoek is nodig om een gedetailleerde beschrijving van de verschillende vormen van schimmelbiomassa onder SSF condities te verkrijgen. Beeldanalysetechnieken in combinatie met computertechnologie bieden potentiële mogelijkheden om dit doel te bereiken.

## Curriculum Vitae

---

Johannes Petrus Smits werd op 26 november 1958 geboren te Bergh. Na de HAVO aan het St. Ludgercollege te Doetinchem met succes te hebben doorlopen volgde hij de HBO-A opleiding tot klinisch chemisch analist aan de OLAN te Arnhem, welke hij in 1979 met het halen van het diploma afrondde. Aansluitend volgde hij de HBO-B opleiding tot biochemisch analist aan de HMLS te Oss waarvan hij in 1982 het diploma behaalde. Na een jaar brak hij de daarop volgende MO-A Natuur- en Scheikunde studie aan de Katholieke Universiteit Nijmegen af om te gaan werken als onderzoekmedewerker binnen de groep Industriële Microbiologie van prof. dr. ir. J.A.M. de Bont aan de Landbouwniversiteit Wageningen. Samen met de toenmalige promovendus W.J.J. van den Tweel onderzocht hij de mogelijkheden van hydroxylering van aromaten met behulp van micro-organismen.

Sinds 1987 is hij werkzaam als researchmedewerker binnen het biotechnologisch onderzoek bij TNO Voeding in Zeist. Na diverse microbieel fysiologische en procestechnologische onderzoeken raakte hij nauw betrokken bij nieuwe en reeds lopende vaste-stoff fermentatie onderzoeksprojecten. De resultaten uit één van de projecten, het tussen 1992 en 1995 uitgevoerde multi-client project *Kennisopbouw solid-state fermentatie*, vormen de basis voor dit proefschrift.

Bij het overdenken en schrijven van het nawoord realiseer ik pas wat de betekenis is van de vaak oh-zo clichématige dankbetuigingen in andere proefschriften. Nu realiseer ik me ook hoeveel mensen bij dit onderzoek direct en indirect betrokken zijn geweest die ik allemaal wil bedanken voor hun positieve inzet. Zonder iemand te willen vergeten en zonder een strikte volgorde aan te willen houden wil ik de volgende personen hier speciaal noemen.

Pim, zonder jouw overtuiging, inzicht, inzet en vastberadenheid zou het onderzoek nooit hebben geresulteerd in dit proefschrift. Je hebt je van begin af aan volledig ingezet voor dit onderzoek. Tijdens het onderzoek en de jaren erna probeerde je me te beschermen tegen zaken die een succesvolle afronding van de promotie in de weg zouden kunnen staan, ook al ging het wel eens ten koste van je eigen welbehagen. Jouw inzet en overtuiging gaven mij motivatie extra mijn best te doen op welslagen van deze promotie.

Arjen, de bijdrage van jouw kennis op het gebied van de proceskunde is onmisbaar gebleken in dit onderzoek. Je Mathcad files hebben me meerdere malen tot denken aangezet en, eerlijk gezegd, dat heeft me nogal wat avondjes gekost. Mede daardoor heb ik mijn inzicht in wiskundige vergelijkingen vergroot.

Hans, de wijze waarop je me motiveerde om mijn grenzen steeds verder te leggen dan ik oorspronkelijk van plan was heeft me geleerd ergens steeds het maximale eruit proberen te halen. Een enkele keer ging ik daarin te ver... , maar een hypothetisch model komt er nog wel. Henk, je benadering van "hou het maar eenvoudig, dat is al moeilijk genoeg" heeft ervoor gezorgd dat ik steeds door de bomen het bos in de gaten hield. Je was in staat steeds de zaken tot de juiste proporties terug te brengen.

Elvire, Ko, Aylin, Wiarda en Marika, jullie bijdragen zijn onmisbaar gebleken voor het onderzoek en het programmeren van Tomasito, ook al zijn ze niet altijd direct terug te vinden in dit proefschrift. Het was erg plezierig met jullie samen te werken.

De participanten binnen het multi-client project (Fons Peters, Hein Stam, Jan Hunik en Bart van Schie namens Unilever Research Laboratorium en Quest International BV; Tim Tersmette en Freddy Dekkers namens Bavaria BV; Ton Kerkenaar namens Denka International BV; Peter Dusseljee en Gert Groot namens Gist-brocades NV, en Rita Delrue en Wilma Taverne-Veldhuizen namens Cargill BV), jullie grote en kleine bijdragen in de loop van het project hebben ervoor gezorgd dat het project op het pad van de toegepaste wetenschap bleef, ofschoon jullie ons meerdere malen de gelegenheid gaven verder te kijken dan onze neus lang is. Het was bijzonder aangenaam met jullie samen te werken.

Cees, Mario, Pieter en Han, de kwaliteit en betrouwbaarheid van het werk dat jullie en jullie collega's hebben geleverd met het analyseren van de gefermenteerde monsters is van doorslaggevend belang geweest voor de goede afloop van het onderzoek. Jullie vakkundigheid geeft vertrouwen in de resultaten van het onderzoek.

Dirk, je taalcorrecties en je voorstellen voor aanpassing van de tekst hebben ervoor gezorgd dat taaie stukken beter leesbaar werden.

Wilhelm en je help-desk collega's, dit werk kon niet worden uitgevoerd zonder een computer met software, en die lijken vooralsnog niet zonder jullie service te kunnen.

Collega's in het lab en op het secretariaat, jullie bereidheid om mee te denken en zo af en toe, waar nodig, mee te helpen heb ik zeer gewaardeerd. Jullie collegialiteit en humor zijn onmisbaar voor mijn werkplezier.

Azkenik: Mònica, gure denbora librean lan egiten uzteagatik eduki duzun pazientziagatik. Zuk jarraitzen lagundu zenidan, nik lan hau sekula bukatuko ez nuelan pentsatzen nuenean. Asko eskertzen dizut eman didazun laguntza eta indar guztia, nahiz eta hemendik aurrera aspiradora etxean pasatzeko aitzakirik ez izan.

(Last but not least: Mònica, jij had het geduld om mij dit werk in *onze* vrije tijd te laten afmaken. Je haalde me over door te gaan op momenten dat ik dacht dat er nooit een eind aan kwam. Ik ben je erg dankbaar voor je steun. Helaas weet ik dat ik nu geen excuses meer heb om me niet voor het huishouden in te zetten.)

## Bibliography

---

- Van den Tweel, W.J.J., Smits, J.P., De Bont, J.A.M. (1986) Microbial metabolism of D- and L-phenylglycine by *Pseudomonas putida* LW-4. Arch. Microbiol. **144** 169 - 174
- Van den Tweel, W.J.J., Smits, J.P., De Bont, J.A.M. (1988) Catabolism of DL-phenylhydracrylic, phenylacetic and 3- and 4-hydroxyphenylacetic acid via homogentisic acid in a *Flavobacterium* sp. Arch. Microbiol. **149** 207 - 213
- Van den Tweel, W.J.J., Smits, J.P., Ogg, R.L.H.P., De Bont, J.A.M. (1988) The involvement of an enantioselective transaminase in the metabolism of D-3- and D-4-hydroxyphenylglycine in *Pseudomonas putida* LW-4. Appl. Microbiol. Biotechnol. **29** 224 - 230
- Hartmans, S., Smits, J.P., Van der Werf, M.J., Volkering, F., De Bont, J.A.M. (1989) Metabolism of styrene oxide and 2-phenylethanol in the styrene-degrading *Xanthobacter* strain 124X. Appl. Env. Microbiol. **55** 2850 - 2855
- Smits, J.P., Knol, W., Bol, J. (1993) Glucosinolate degradation by *Aspergillus clavatus* and *Fusarium oxysporum* in liquid and solid-state fermentation. Appl. Microbiol. Biotechnol. **38** 696 - 701
- Smits, J.P., Janssens, R.J.J., Knol, W., Bol, J. (1994) Modelling of the glucosinolate content in solid-state fermentation of rapeseed meal with fuzzy logic. J. Ferment. Bioeng. **77** 579 - 581
- Zhu, Y., Smits, J.P., Knol, W., Bol, J. (1994) A novel solid-state fermentation system using polyurethane foam as inert carrier. Biotechnol. Lett. **16** (6) 643 - 648
- Llanos Palop, M., Smits, J.P., Ten Brink, B. (1995) Degradation of sinigrin by *Lactobacillus agilis* strain R16 Int. J. Food Microbiol. **26** 219 - 229
- Zhu Y., Knol W., Smits, J.P., Bol J. (1996) Medium optimization for nuclease P1 production by *Penicillium citrinum* in solid-state fermentation using polyurethane foam as inert carrier. Enzyme Microbial Technol. **18** 108-112
- Smits, J.P., Rinzema, A., Tramper, J., Schlösser, E.E., Knol, W. (1996) Accurate determination of process variables in solid-state fermentation system. Process Biochem **31** 669-678
- Smits, J.P., Rinzema, A., Tramper, J., Sonsbeek, H.M. van, Knol, W. (1996) Substrate composition changes, C-balance, enzyme production, growth and kinetics of *Trichoderma reesei* QM9414 in solid-state fermentation of wheat bran. Appl. Microbiol. Biotechnol. **46** 489-496
- Nout, M.J.R., Rinzema, A., Smits, J.P. Biomass and Productivity Estimates in Solid Substrate Fermentations. In: The Mycota IV, Wicklow and Söderström (Eds.), Springer Verlag Berlin Heidelberg 1997
- Smits, J.P., Rinzema, A., Tramper, J., Sonsbeek, H.M., van, Hage, J.C., Kaynak, A., Knol, W., (1997) The influence of temperature on kinetics in solid-state fermentation. In press Enzyme Microb. Technol.